Erreur ! Signet non défini.الجمهورية الجزائرية الديمقراطية الشعبية

République Algérienne Démocratique et Populaire

Ministère de L'Enseignement Supérieur et de la Recherche Scientifique

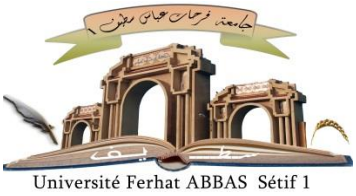

UNIVERSITÉ FERHAT ABBAS - SETIF1

FACULTÉ DE TECHNOLOGIE

THÈSE

Présentée au Département d'Électrotechniquee

Pour l'obtention du diplômede

DOCTORAT

Domaine : Sciences et Technologie

Filière: Automatique **ption: Automatique etinformatique industrielle**

Par

KANOUNI Badreddine

THÈME

Contribution to the control and energy management of multi-source system connected to the network

Soutenue le 15/02/2024 devant le Jury:

RAHMANI Lazhar	**Professeur**	**Univ. Ferhat Abbas Sétif 1**	**Président**
BADOUD Abd Essalam	**Professeur**	**Univ. Ferhat Abbas Sétif 1**	**Directeur de thèse**
MEKHILEF Saad	**Professeur**	**Université de technologie de Swinburne - Australie**	**Co-Directeur**
OULD BOUAMAMA Belkacem	**Professeur**	**Ecole polytechnique de Lille - France**	**Examinateur**
MOKEDDEM Diab	**Professeur**	**Univ. Ferhat Abbas Sétif 1**	**Examinateur**

Erreur ! Signet non défini.الجمهورية الجزائرية الديمقراطية الشعبية

République Algérienne Démocratique et Populaire

Ministère de L'Enseignement Supérieur et de la Recherche Scientifique

Université Ferhat ABBAS Sétif 1

UNIVERSITÉ FERHAT ABBAS - SETIF1

FACULTÉ DE TECHNOLOGIE

THESIS

Presented to the Department of Electrical Engineering

To obtain the degree of

Ph.D

Domaine : Sciences and Technology

Filière: Automatic

Option: Automatic and industrial computing

By

Badreddine KANOUNI

Contribution to the control and energy management of multi-source system connected to the network

Defended on 02/15/2024 before the Jury:

Lazhar RAHMANI	**Professor**	**Univ. Ferhat Abbas Sétif 1**	**President**
Abd Essalam BADOUD	**Professor**	**Univ. Ferhat Abbas Sétif 1**	**Supervisor**
Saad MEKHILEF	**Professor**	**University of Swinburne of Technology - Australia**	**Co-Supervisor**
Belkacem OULD BOUAMAMA	**Professor**	**Ecole polytechnique de Lille - France**	**Examiner**
Diab MOKEDDEM	**Professor**	**Univ. Ferhat Abbas Sétif 1**	**Examiner**

DEDICATION

I dedicate my dissertation to my family and my friends.

A special feeling of gratitude to my parents,

Kanouni Badreddine

Acknowledgement

*In the name of **ALLAH**, the Most Gracious and the Most Merciful. Thanks to **ALLAH** who is the source of all the knowledge in this world, for the strengths and guidance in completing this thesis.*

*I express my deep sense of gratitude and heart-felt thanks to my supervisor, Prof. **Abd Essalem BADOUD** ,and Prof. **Saad MEKHILEF** for invaluable guidance, patience, kindness and consistent encouragementthroughout the course of this work. I am very glad that I have pursued my doctoral studiesunderexcellent supervision.*

I would like to express my appreciation to my thesis committee members: Prof. **Lazhar RAHMANI**, *Prof.* **Belkacem OULD BOUAMAMA***andProf.* **Diab MOKEDDEM ,** *for their discussions, suggestions, and feedbacks to improve my thesis.*

*I would like to thank **Dr. Abdelbaset LAIB, and Dr.bellel Talbi**forhelp and support*

Badreddine KANOUNI

Table of Contents

List of Figures

List of Tables

List of Acronyms

RESRenewable energy sources

AC	Alternating Current
ANN	Artificial neural network
AI	Artificial intelligence
CHB	Cascaded H-Bridge
DC	Direct Current
FCS-MPC	Finite control set model predictive control
FCS-MPCC	Finite control set model predictive Current control
FCS-MPCTS	Finite control set model predictive control tow step
FLC	Fuzzy logic control (controller)
GA	Genetic algorithm
IGBT	Insulated Gate Bipolar Transistor
INC	Incremental conductance
IncCon	Incremental conductance
MPC	Model Predictive Control
MPP	Maximum Power Point
MPPT	Maximum Power Point Tracking
NPC	Neutral-Point Clamped
P&O	Perturb and observe
PI	Proportional-Integral
PID	Proportional-integral-derivative
V-DPC	Direct power control
VFOC	Voltage flux-oriented control
PLL	Phase Locked Loop
VS-INC	Variable step-size incremental conductance
PSO	Particle swarm optimization
PV	Photovoltaic
PEMFC	Proton Exchanege Membren Fule Cell
P-V	Power-voltage
I-V	Current-voltage
P-I	Power -Current
V-I	Voltage - Current
PWM	Pulse Width Modulation
SVM	Space Vector Modulation
THD	Total harmonic distortion
V-DPC	Voltage based direct power control
VOC	Voltage oriented control
VSI	Voltage Source Inverter

List of Symbols

I_{pv} $I_{pv}(k)$ Output current of PV Array

i_{ph} Photocurrent of the cell.

i_{sd} Reverse saturation current of the diode.

q Electronic charge

V_{pv} $V_{pv}(k)$ Output voltage PV.

I_{fc} $I_{fc}(k)$ Output current of PEMFC.

p_{pv} $\mathrm{p}_{pv}(k)$ Output power of PV

p_{fc} $\mathrm{p}_{fc}(k)$ Output current of PEMFC

N_{fc}	Number of PEMF Cconnected in searies
V_{fc} $V_{fc}(k)$	Output current of PEMFC.
$\Delta v_{pv}(k)$	PV voltage variation
$\Delta i_{pv}(k)$	PV current variation
$\Delta v_{fc}(k)$	PEMFC voltage variation
$\Delta i_{fc}(k)$	PEMFC current variation

T_{fc} PMEFC temperture

E_{nernst}	Reversible open-circuit voltage
V_{act}	Activation loos.

V_{conc} Concentration loos.

V_{ohmic}	Represent the ohmic loos.
P_{o2}	Oxygen pressure
P_{H2}	Hydrogen pressure

P_A Anod Pressure

P_C Cathod pressure

ρ_m,	Resistivity of the membrane.
λ	Membrane water content
$\delta_{1,2,3,4}$	Empirical Coefficients

V_{dc}, V_{dc-ref} Measured DC link voltage &DC link Voltage reference

abc	Natural Frame quantities
$\alpha\beta$	Stationary frame quantities
dq	Sychronous frame quantities
θ	Grid voltage angle
T_S	Simpling Time
S	Control action of DC-DC converter
$S_{x,i}$	Switching state of phase $x = a,b,c$ $i = 1,2,...$
$i_{g\alpha.\beta-ref}(k+2)$	Predicted grid reference Current
v_g	Grid Voltage

g	Cost function
SW_x	Number of switching change in inverter phase $x = a, b, c$
λ_{dc}	Weighting factor for DC-link capacitor
λ_s	Weighting factor for switching frequency
$\frac{d}{dt}$	Derivative operator
p_{net}	Net power (W)
V_{dc-bus}	DC bus voltage
SOC	State of charge (%).

Chapter 1 : Introduction

1.1 Introduction

Energy, similar to water, is an essential component of life for all organisms. There are five primary categories of energy, namely mechanical, chemical, thermal, nuclear, and electrical. The previous one, which is widely regarded as the primary and most crucial factor, currently serves as the predominant impetus for human existence. Its indispensability stems from its exceptional portability and storability. The utilization of electrical energy has significantly improved the quality of human life and facilitated the advancement of economic and social activities at a consistent rate. The global consumption of electrical energy has experienced a gradual increase, particularly in light of the industrialization of the world, resulting in a doubling of consumption in recent years. Despite the passage of the first few decades of the 21st century, it is noteworthy that fossil fuel sources, namely coal, oil, and natural gas, continue to serve as the primary means of generating total electrical energy. Traditional sources of electrical energy have played a significant role in facilitating growth in the population, advances in technology, and economic growth. Nevertheless, the utilization of this technology has resulted in significant environmental and health implications, including but not limited to environmental decline, exacerbation of global warming, biodiversity loss, and the proliferation of diseases due to the emission of carbon dioxide gas[1].Notwithstanding, this policy has resulted in an escalation in the cost of electricity and has engendered a certain degree of asymmetry, given that the reduction of these emissions is intricately linked to energy generation and its swiftly mounting consumption.

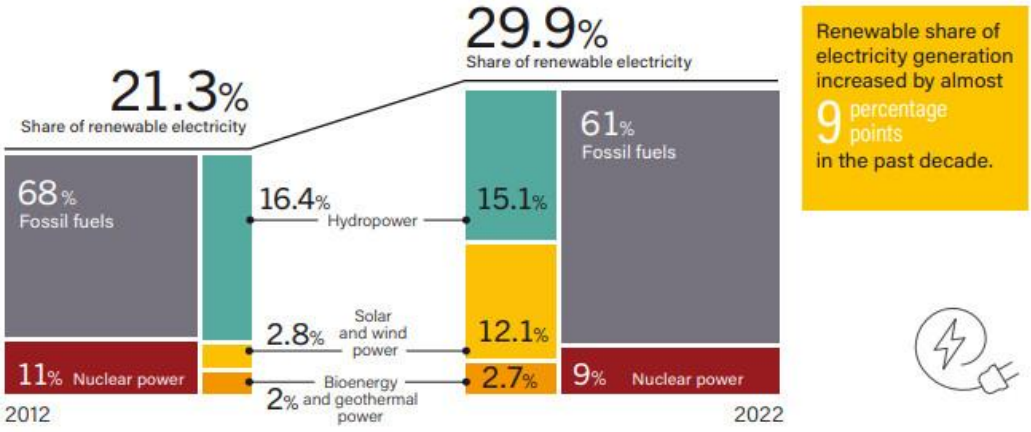

Figure 1. 1 Estimated renewable energy share of total final energy consumption[2].

The consistent rise in demand for clean, economical, and renewable energy has been observed over the past few decades, primarily due to the energy crisis and environmental concerns such as global warming and pollution. Considerable advancements have been made in the realm of sustainable energy sources, including but not limited to biomass, hydropower, solar photovoltaic energy, and wind energy. Renewable energy sources (RES) account for approximately 29.9% of the global electricity production derived from renewable sources, as reported in reference[2]. Figure 1.1 illustrates the various subdivisions of RES percentages.

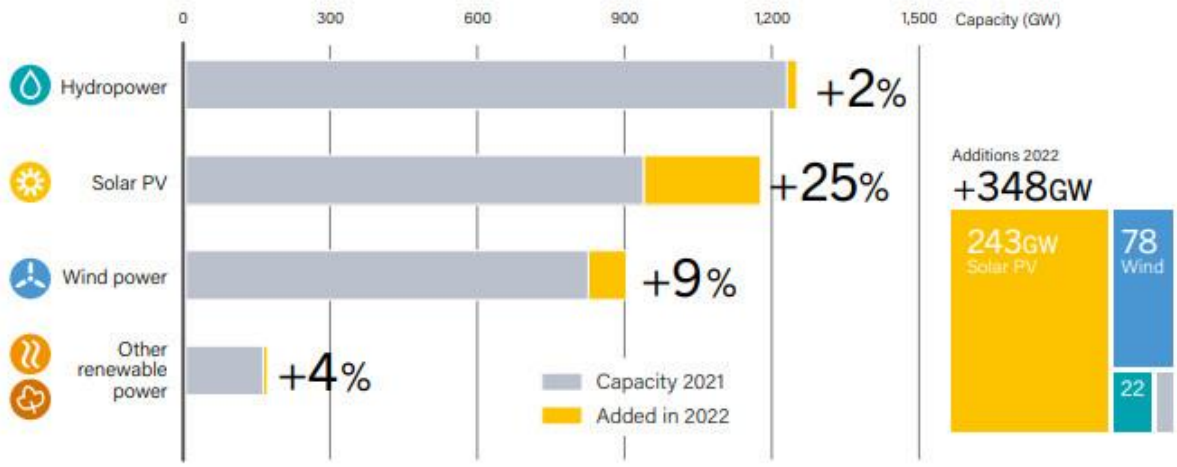

Figure 1. 2Renewable Power Total Installed Capacity and Annual Additions[2].

The energy transition has directed its attention not solely towards power, but also select technologies within the power sector. As of 2022, most renewable power capacity comprised solar photovoltaic and wind power, accounting for 92% of the total. in total, 348 GW of renewable power capacity was added in 2022 (up 13% from the 306 GW added in 2021), as illustrated in figure 1.2[2].

1.2 Hybrid Renewable Energy Systems

In contemporary times, solar energy has emerged as a highly favored renewable energy source owing to its non-depletable and non-polluting nature. The process involves the utilization of photovoltaic (PV) modules to generate electricity. Photovoltaic (PV) power plays a significant role in fulfilling a substantial proportion of the global electricity demand.The photovoltaic (PV) energy sector encounters significant obstacles due to the variability of energy production in response to weather fluctuations, including solar radiation and temperature changes. This variability can result in a discrepancy between the output of PV energy and the temporal distribution of load, posing a significant challenge to the industry[3].Renewable energy sources, as a standalone energy source, are unable to ensure uninterrupted load supply due to their low reliability and high investment cost[4]. An

effective approach to address this challenge involves integrating renewable energy sources, conventional energy sources, and energy storage systems to ensure uninterrupted provision of electricity throughout the day. The nomenclature assigned to this particular configuration is Hybrid Renewable Energy Systems (HRESs) as documented in reference[5]. Hybrid Renewable Energy Systems (HRESs) are utilized in both off-grid and grid-connected settings. In remote and rural areas, HRESs are employed in a standalone mode, while in certain locations such as factories, hospitals, universities, and cities, they are used in a grid-connected mode. Aside from mitigating greenhouse gas emissions, Hybrid Renewable Energy Systems (HRESs) offer significant advantages, including reduced energy expenses, enhanced power quality and dependability, the potential for electricity in remote and rural regions, and improved services[6].The hybrid system satisfies the three fundamental dimensions of sustainable development, namely economic, environmental, and social considerations.(HRESs) encompass a diverse array of renewable energy sources, including solar, wind, and hydrogen energy, which are among the most commonly employed technologies for generating energy.The growth of photovoltaic and wind energy has exceeded initial projections due to their rapid development. Concurrently, fuel cells (FCs) have emerged as a viable option for clean energy production, owing to their numerous benefits, including but not limited to high efficiency, minimal environmental impact, and absence of noise[7].Furthermore, the management of individual sources comprising the hybrid system facilitates the enhancement of the overall system's efficiency and energy. The objective of this procedure is to obtain the utmost amount of power that can be harnessed from sources of renewable energy. The optimization of power extraction from photovoltaic and wind sources has been addressed in various academic publications. Fuel cells have emerged as a viable solution for both mobile and stationary applications in the future. However, the challenge of extracting maximum power and optimizing fuel consumption presents a significant obstacle, rendering fuel cells a potential component of hybrid energy systems.

1.3 Motivation and objectives of a dissertation

The selection of a suitable hybrid system and the design of effective control schemes are considered great challenges. It is necessary to select a suitable renewable source and control depending on the quantity of power injected into the grid in addition to energy management control of the hybrid storage system (photovoltaic,fuel cell and batteries).On the other hand, the development of effective controllers is crucial due to the effect of different operating conditions on the overall selected system. So, this dissertation has two research directions which are: to investigate grid-connected PV and PEMFC system control; and to design

effective control schemes. also, design an energy management control for hybrid storage system (PV, fuel cell, and batteries) stand alone.

The challenges associated with power converters interfacing(PV-fuel cell)systems with the electrical grid are characterized by significant limitations that have been identified in simulation studies. These limitations include a substantial overshoot in the steady state, a prolonged response time, poor power quality, and a total harmonic distortion (THD) that exceeds the established standards set by (IEEE) of less than 5%.

In order to inject the power generated by the PV / fuel cell system into the grid, a secondary conversion stage (DC-AC converter) is required. It is necessary to ensure that the total harmonic distortions (THD%) in the grid currents remain at a minimum level, even under varying conditions. The objective of this control measure is to attain effective DC link regulation and superior power control performance, resulting in rapid transient response, precise current control, and reduced total harmonic distortion (THD).In addition to utilizing the three-level inverters as a secondary conversion stage, various Neutral Point Clamped (NPC) multilevel and F-type inverters are employed for the same purpose of injecting a significant amount of generated power into the grid. Multilevel NPC and F-type inverters are subject to issues such as the potential unbalancing of capacitor voltage in the DC-Link, as well as the intricate design and challenging implementation of the control scheme[8].The common control strategies utilized for the second stage involved the implementation of cascaded linear proportional-integral (PI) regulators and either pulse width modulation or space vector modulation (PWM/SVM) and they suffer from drawbacks such as :

- The degradation of grid current quality is caused by inaccurate power control and the presence of significant lower-order harmonics, as stated in[9].
- The slow regulation of PI regulators coupled with the low-bandwidth modulation stage results in a tardy transient response, as noted in reference[9].
- The performance degradation is caused by the harmonics in the grid voltage and the delay in control[9].

The objective of this dissertation,

The first one is in order to comprehensively investigate the subject of photovoltaics (PV) and proton exchange membrane fuel cells (PEMFC) for grid-connected applications, it is necessary to thoroughly examine their operating principles, modeling approaches, design considerations, as well as the currently available modulation and control methods.

The second objective is to develop FCS-MPCTS systems that are capable of achieving optimal control performance, effectively managing the DC-Link capacitor-regulated operation of a three-level NPC inverter, and injection of the current with high quality.

The third objective of this study is to the development of FCS-MPCC with the aim of regulating the F-Type inverter. This control system is designed to achieve optimal performance and ensure precise regulation of the DC link and injection of the current with high quality.

The last objective is to design an energy management strategy for the proposed hybrid storage (PV, fuel cell, and batteries) stand-alone system.

1.4 Dissertation organization

The present dissertation is structured into six chapters. Each chapter's work is succinctly summarized as follows:

Chapter 2 :

the objective of this chapter is to describe the components model of the proposed photovoltaic-PEMFC connected to the grid that will be used in the following chapters of the control system and simulation. First, photovoltaic modeling (cell, module) and their P-V, and I-V characteristic curves have been described. Next, a fuel cell type PEMFC (Stack) after that we had been also described as the characteristic P-I V-I, after that The power converters were utilized in the proposed Grid-connected system: DC-DC converter and DC-AC inverter.

Chapter 3 :

The present chapter provides an overview of the control strategies that are commonly utilized in dual-stage grid-connected photovoltaic and proton exchange membrane fuel cell systems. where we presented maximum power point algorithms, also, present a brief exposition on DC-link voltage regulation techniques and control strategies for three-phase grid-connected systems, delineating each topic separately.

Chapter 4 :

Chapter four proposes simple and effective controllers for PV systems and PEMFC using NPC multilevel and F-type based on finite control set model predictive control tow step(FCS-MPCTS) and finite control set model predictive current control (FCS-MPCC) strategies

- The studied system is composed of two conversion stages, the first stage contains PV arrays, connected to a DC-DC converter (buck-boost converter). In the second stage, a three-level NPC inverter tied to the grid is employed. Each DC-Link capacitor input of the NPC inverter is connected to the output of the DC-DC buck-boost converter. A fuzzy logic maximum power point tracking is applied for the buck-boost converter to reach the maximum power point of the PV array. In addition, an FCS-MPCTS controller is proposed to control the three-level NPC inverter connected to the grid.
- A Two conversion stages, the first stage contains PEMFC, connected to a DC-DC converter (boost converter). In the second stage, a three-level NPC inverter tied to the

grid is employed. Each DC-Link capacitor input of the NPC inverter is connected to the output of the DC-DC boost converter. A fuzzy logic maximum power point tracking is applied for the boost converter to reach the maximum power point from PEMFC. In addition, an FCS-MPCTS is proposed to control the three-level NPC inverter connected to the grid.

- two conversion stages, the first stage contains PEMFC, connected to a DC-DC converter (boost converter). In the second stage, a three-level single-phase F-Type inverter tied to the grid is employed. Each DC-Link capacitor's input of the F-Type inverter is connected to the output of the DC-DC boost converter. A fuzzy logic maximum power point tracking is applied for each boost converter to draw the maximum power point from PEMFC. In addition, an FCS-MPCC is proposed to control the F-type inverter connected to the grid.

Chapter 5 :

Chapter five proposes a simple and effective controller for multisource stand-alone storage systems(PV, PEMFC, Batteries) based on a state machine control (SMC) strategy.

The stand-alone studied system is composed of contains PV arrays, connected to a DC-DC converter (buck-boost converter), a PEFMC connected to the DC-DC boost converter, and a peak of batteries connected to the DC-DC bidirectional converter, the output of the DCDC converted connected in parallel with DC-Link capacitor, and also parallel with the load A fuzzy logic maximum power point tracking is applied for the buck-boost converter to reach the maximum power point of the PV array. in addition, SMC is proposed to control the boost converter that is connected to PEMFC.

Chapter 6:

This chapter provides a summary of the author's contributions and the general conclusion of the thesis. Furthermore, potential avenues for further research pertaining to the findings presented in this dissertation are proposed.

Chapter 2 Modeling of photovoltaic panel and PEMFC

2.1 Introduction:

Due to the obvious significant rise in population and energy consumption, the direction is toward new and renewable energy sources such as solar, wind, and hydrogen. This is due to the numerous benefits they provide to individuals and the environment [10]. Resemble other conventional energy sources such as heavy oil, coal, and natural gas, these alternatives are more endurable and emit less carbon dioxide (CO2) [11]. Recently, the GPV and fuel cell system has become an increasingly important resource for electrical supply and also an integral element of the electrical grid. Researchers face significant difficulties when working with single-phase and three-phase GPV systems as the same with fuel cell [12].A typical configuration of a dual-stage photovoltaic (PV) and PEMFC connected to the grid, shown in Figure 2.1.The global system consists of a photovoltaic system which is consist of series and parallels connected PV array, first, a capacitor is added to the input of the DC-DC converter (passive filter) to hence the power, after that a DC-DC Buck-Boost converter is used to achieve the maximum power point of the photovoltaic system, and for PEMFC first DC-DC Boost converter is connected to achive the maximum power generated by the PEMFC,next a DC-link capacitor tie up a DC-DC (Buck-Boost) and Boost with AC-DC inverter the least one is used to convert the power from DC to AC and injected the power to the grid through an L filter. In this chapter modeling of a PV system connected to the grid is modeling. The mathematical modeling of PV, the buck-boost controller and the multi-level inverter is developed.

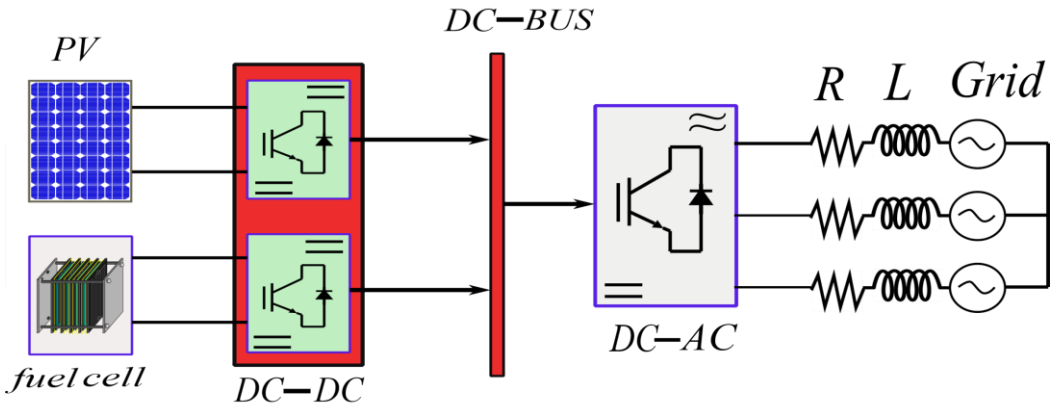

Figure 2. 1the proposed hybrid (PV+PEMFC) grid connected system

2.2 Mathematical formulation of solar PV module:

2.2.1 Soler Cell:

A solar cell is a basic technology for converting photon energy into free power. When these cells are joined in series and parallel, a PV module is produced. In order to construct PV arrays, these modules are connected in series and parallel, generating clean and green power[13].The following figure2.1 represents how forming the PV array starting from cell.A single solar cell may also be modeled as an electrical circuit component. It has a p–n junction known as a diode, a photocurrent producer that generates current from light, and two resistors.

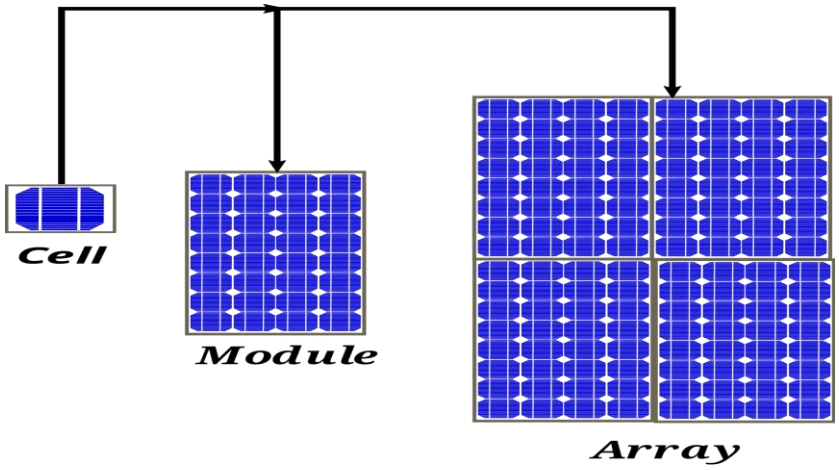

Figure 2. 2forming of soler array.

A single solar cell may also be modeled as an electrical circuit component. It has a p–n junction known as a diode, a photocurrent producer that generates current from light. Solar cell properties are nonlinear and are affected by irradiance and temperature, its exists three type of solar cell single diode model, two diode model and 3 diode model[13], the PV module consists of solar cells that are placed in series or in parallel to make the PV panel. The model of these solar cells is usually considered SDM (single diode model)[14,15].the model use in our work is single diode model the next figure represent the electrical model of PVcell.

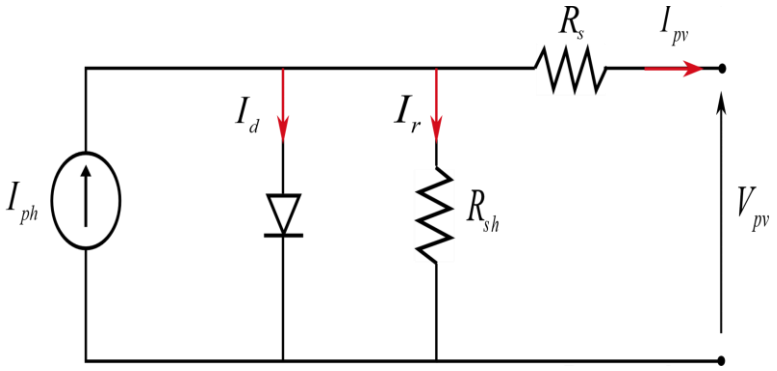

Figure 2. 3equivalent single diode model of solar cell

The output current (Ipv) may be represented as follows using the circuit mentioned in figure 2.3:

$$I_{pv} = I_{ph} - I_d - I_{sh} \quad (2.1)$$

$$I_{pv} = I_{ph} - I_{sd}\left[\exp(\frac{q(V_{pv} - I_{pv}R_s)}{nkT}) - 1\right] - \frac{V_{pv} + I_{PV}R_s}{R_{sh}} \quad (2.2)$$

where :

I_{pv}: the output current of the cell.

I_{ph}: the photocurrent of the cell.

I_{sd}: the reverse saturation current of the diode.

q: the electronic charge its equal to $1.6\times10^{-19}C$.

$V_{pv/c}$: the output voltage of cell.

n: the ideality factor of diode.

k: the Boltzmann factor, its equal to $1.38\times10^{-23}\ j/k$

T: the temperature.

Rs: the searis resistance of the cell.

R_{sh}: the parallel resistance of the cell.

2.2.2 PV module:

The establishment of a PV cell module is the essential part of analyzing the output characteristics, to form it we have to put the cells in series and parallel, due to the low power produced by the cell[16].

The output is related to the standard set at 1000w/m^2 and 25^{o}C and is modeled by the following equation:

$$I_{pv} = N_p I_{ph} - N_p I_{sd}\left(\exp(\frac{N_s V_{pv} + (N_s / N_p) R_s I_{pv}}{nN_s KT}) - 1\right) - \left(\frac{N_s V_{pv} + (N_s / N_p) R_s I_{pv}}{(N_s / N_P) R_{sh}}\right). \quad (2.3)$$

Where:

I_{pv} : represent the PV module current

V_{pv} :the pv module voltage

N_s :number of series cells connected.

N_p number of parallel cells connected.

The MSX 60 W PV panel was chosen and represented to construct the modeling and simulation of a solar panel module in this thises. The parameter specifications of the MSX 60 W PV panel are shown in table.1.1. The maximum power produced by a solar panel is known

as the operation point or maximum power point, and it can be found in the (P-V) and (I-V) curves. The impact of changing the intensity of irradiance from 600 W/m2 to 1000 W/m2 at a constant temperature of 25°C on the solar Photovoltaic model I–V and P–V characteristics curves shown in figures.2.4 and 2.5. Irradiation has a significant impact on short-circuit values but has minimal impact on open-circuit voltage. However, temperature has little influence on short-circuit current but has a large effect on open-circuit voltage.

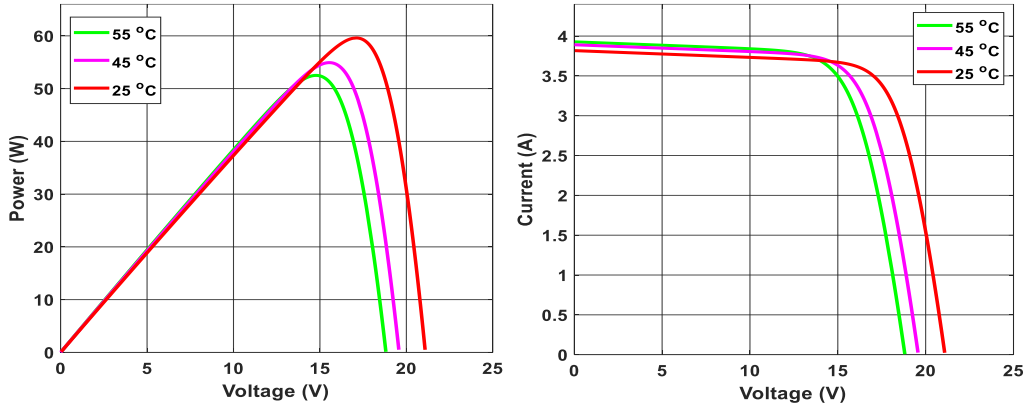

Figure 2. 4The MSX 60 W module (P-V), (I-V) characteristics (variation in irradiation).

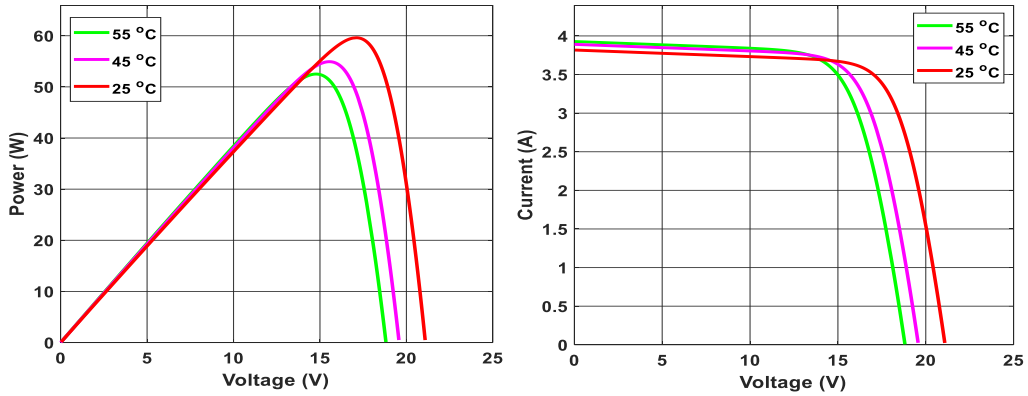

Figure 2. 5The MSX 60 W module (P-V), (I-V) characteristics (variation in irradiation)

Table 2. 1The MSX 60 W module parameter[17]

Parameter specification	Values
Peak power P_{mpp}	60W
Peak voltage V_{mpp}	17.1V
Peak current I_{mpp}	3.5A
Short-circuit currant I_{sc}	3.8A
Open-circuit voltage V_{oc}	21.1V
Temperature co-coefficient of currant	0.003 (mA/°C)
Temperature co-coefficient of voltage	-0.08 (mV/°C)

2.3 Fuel cells:

Fuel cells are an environmental sustainable energy source that produce electricity via an electrochemical process. Further, Fuel cells have received increased interest from academics and manufacturers in recent years because to its high energy density, high efficiency, and low noise[18].

2.3.1 Types of fuel cells:

Several fuel cell models are based on similar fundamental concepts. However, these cells vary depending on the fuel type, operating temperature, and chemical properties of the electrolyte[19,20]. Six different type of fuel cells are used to create electrical power based on these characteristics[21,22]:proton exchange membrane fuel cell (PEMFC), solid-oxide fuel cell (SOFC), alkaline fuel cell (AFC), direct methanol fuel cell (DMFC), phosphoric acid fuel cell (PAFC) and molten carbonate fuel cell (MCFC). Fuel cell types to power ratings and advantages are introduced in figure.2.6.

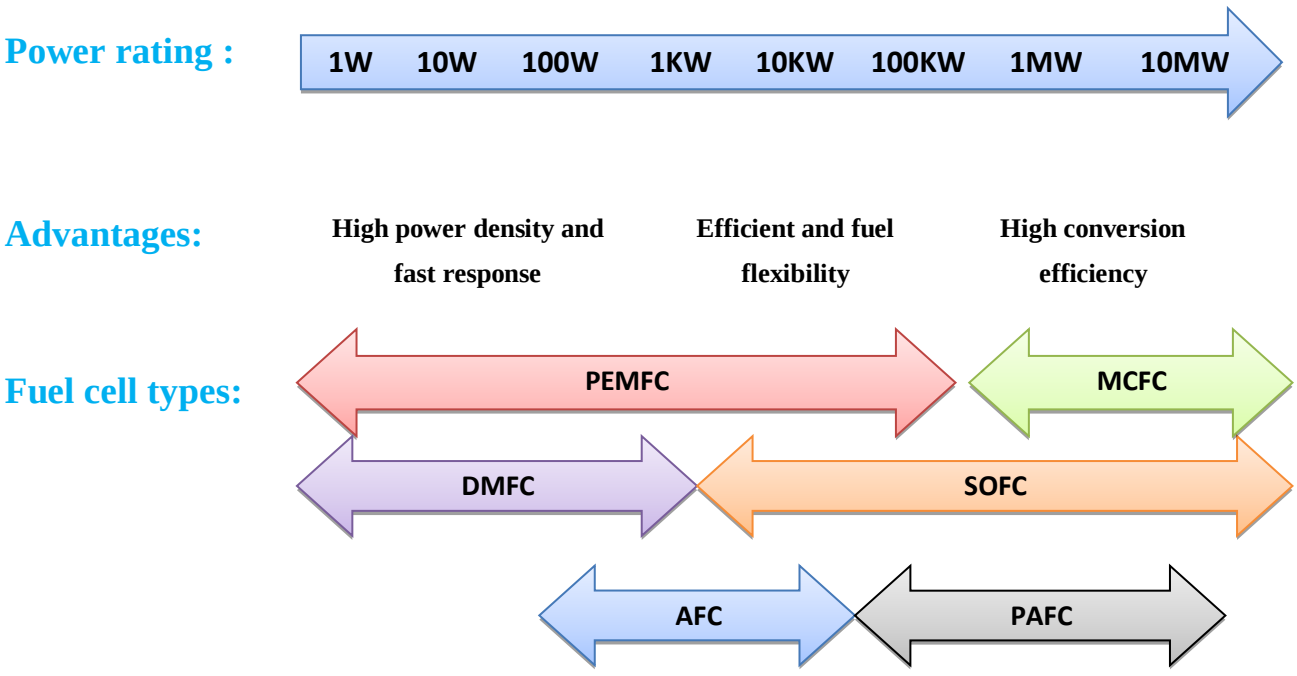

Figure 2. 6fuel cell classification based on power rating and fuel cell type[23].

Furthermore the following table 2.2 we are going to give a detail comparison of fuel cells.The most popular and widespread type of fuel cell is PEMFC compared to other types.

Table 2. 2properties of different fuel cell[23]

	PEMFC[24]	*SOFC*[25]	*AFC*[26]	*DMFC*[27]	*PAFC*[28]	*MCFC*[29]
Electrolyte	**Proton Exchange Membrane (solid)**	**Ceramic (solid)**	**KOH (liquid)**	**Proton Exchange Membrane (solid)**	**H3PO4 (liquid)**	**Molten Carbonates (liquids)**
Efficiency with cogeneration	**70%-90%**	**<90%**	**>80%**	**80%**	**>85%**	**>80%**
Power range	**1 W-100 kW**	**1 kW - 2 MW**	**1kW-100kW**	**1 W-100 kW**	**200kW-10MW**	**500kW-10MW**

2.3.2 PEM Fuel Cell Modeling :

A PEMFC is an electrochemical energy conversion device that transforms fuel's chemical energy into electric energy. It is composed of a cathode, an anode, and an electrolyte formed of polymer electrolyte membrane. [30].the reason why we chose this type due to heir high power densities, lightweight, low operatingtemperature (quick start-up), long cycle life, as well as zero pollution[31]. The electrical circuit model use in our work described in the following figure[18]:

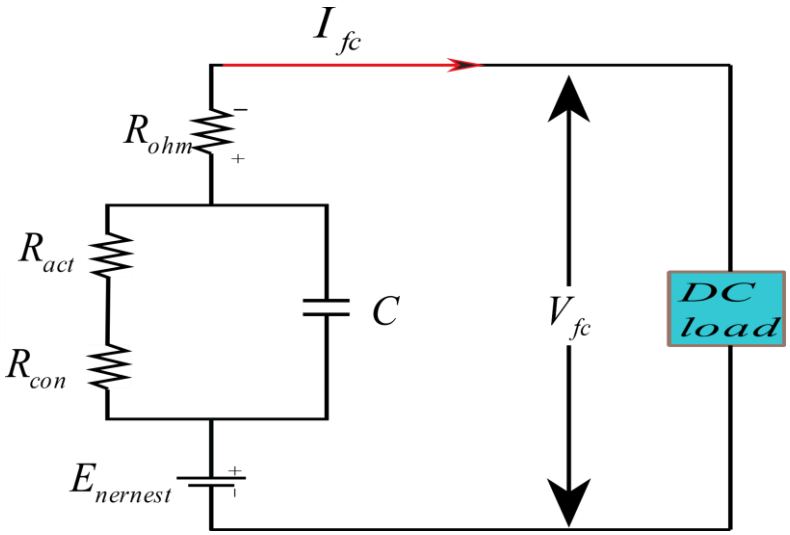

Figure 2. 7PEMFC electrical circuit.

The PEMFC output voltage is represented as:

$$V_{fc} = E_{nernst} - V_{act} - V_{conc} - V_{ohmic} \qquad (2.4)$$

E_{nernst} : represent the reversible open-circuit voltage

V_{act} : represent the activation loos.

V_{conc} : concentration loos.

V_{ohmic} : represent the ohmic loos.

Each term mentioned above represent in the following equations[32]:

$$\begin{cases} E_{nernst} = 1.229 - (0.85\times10^{-3})\times T_{FC} - 298.15) + (4.31\times10^{-5}\times T_{FC}\times(\ln(p_{H_2}) + 0.5\times\ln(p_{O_2}))) \\ V_{act} = -\left[\delta_1 + \delta_2 T_{FC} + \delta_3 T_{FC}\ln(C_{O_2}) + \delta_4 T_{FC}\ln(I_{FC})\right] \\ V_{ohm} = I_{FC}(R_M + R_C) \\ V_{con} = -\beta\ln\left(1 - \frac{j}{j_{\max}}\right) \end{cases} \quad (2.5)$$

where P_{H2} represents the hydrogen partial pressure (atm), P_{O2} represents the oxygen partial pressure (atm),as shown in equation (2.5) and T_{fc} represents the absolute temperature (K).

$$\begin{cases} P_{O_2} = R_{HC}\times P_{H_2O}\left[\left(\frac{R_{HC}\times P_{H_2O}}{P_C}\times e^{\left(\frac{1.635 I_{FC}/A}{T_{FC}^{1.1334}}\right)}\right)^{-1} - 1\right] \\ P_{H_2} = 0.5\times R_{HA}\times P_{H_2O}\left[\left(\frac{R_{HA}\times P_{H_2O}}{P_A}\times e^{\left(\frac{1.635 I_{FC}/A}{T_{FC}^{1.1334}}\right)}\right)^{-1} - 1\right] \end{cases} \quad (2.6)$$

Where P_C, P_A are the inlet pressure of cathode and anode respectively, I_{FC} the PEMFC current, R_{HC}, R_{HA} are the relative humidity of vapor in cathode and anode respectively, A is the membrane surface (cm^2).Where Each cell's empirical coefficients are indicated by $\delta_{1,2,3,4}$, and the oxygen concentration is represented by C_{O_2}.

$$C_{O_2} = \frac{P_{O_2}}{5.08\times e^{(-4.98/T_{FC})}} \quad (2.7)$$

Where R_M indicates electron flow resistance and $R_C$indicates proton resistance. So R_M $R_M$is written as follow:

$$R_M = (\rho_m \times 0.0128)/A \quad (2.8)$$

$$\rho_m = \frac{1.81.6\left[0.062\left(\frac{T_{FC}}{303}\right)^2\left(\frac{I_{FC}}{A}\right)^{2.5} + 0.03\left(\frac{I_{FC}}{A}\right) + 1\right]}{\left[\lambda - 0.634 - 3\left(\frac{I_{FC}}{A}\right)\right]\times e^{4.18\times(T_{FC}-303)/T_{FC}}} \quad (2.9)$$

ρ_m, λ are specific resistivity of the membrane and membrane water content respectively.Where J, J_{max}, β are maximum current, maximum current density and concentration loss constant respectively.

The present dissertation employs the PEMFC model as the basis for constructing a simulation of a PEMFC stack.The parameters of the Proton Exchange Membrane (PEM) fuel cell are presented in the table.2.3. The point at which a Proton Exchange Membrane Fuel Cell

(PEMFC) generates the highest amount of power is commonly referred to as the maximum power point.The Figure (2.8) presenteddepicts the polarization V-I curve of an ideal fuel cell, which illustrates the efficiency of a singular cell under typical temperatures and pressures..It is observed that the voltage declines at first, then acts linearly, and eventually, a precipitous fall occurs at a larger current density. This voltage differential is caused by three types of polarization losses: activation, ohmic, and concentration[31].

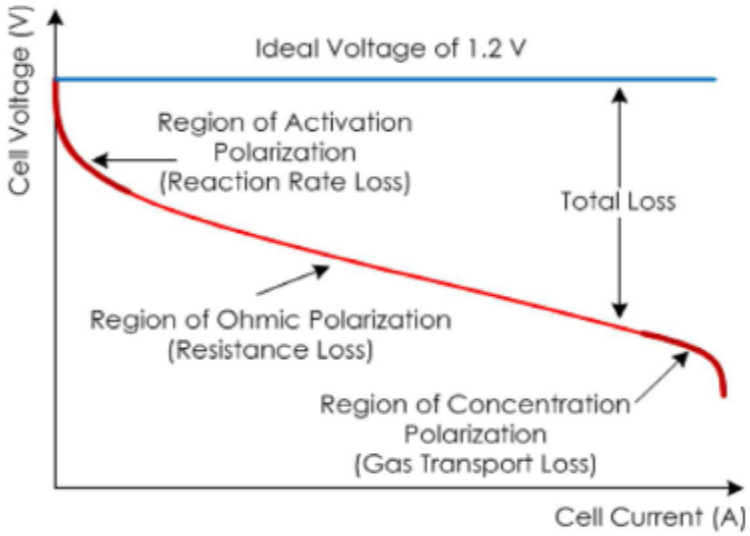

Figure 2. 8polarization V-I curve[33].

To formulate a PEMFC stack, the output voltage must constitute by (N_{fc})fuel cell connected in series is given by the following equation:

$$V_{st} = V_{fc} N_{fc} \quad (2.10)$$

The impact of changing the intensity of temperature from 298.15K to 340K at a constant pressure(Pa,Pc) of 1 atm on PEMFC stack. I–V and P–V characteristics curves shown in Figure 2.9, figure 2.10 temperature has a impact on voltage values but has minimal impact on current. However, when we fix the temperature at constant value equal to 340.5k at a variation of pressure (Pa,Pc) from 1 atm to 5 atm has little influence on stack current and also on voltage.

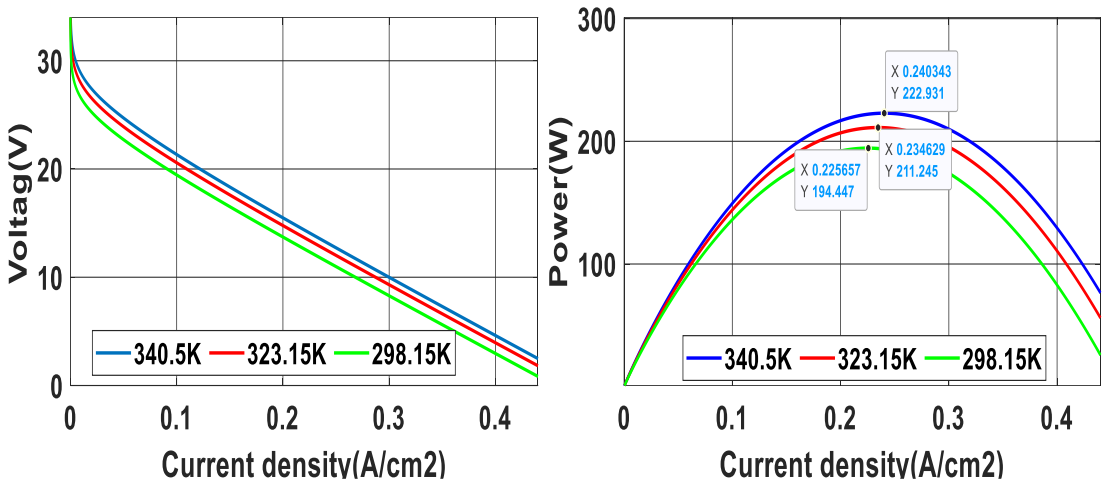

Figure 2. 9PEMFC stack (P-V), (I-V) characteristics (variation in temperature).

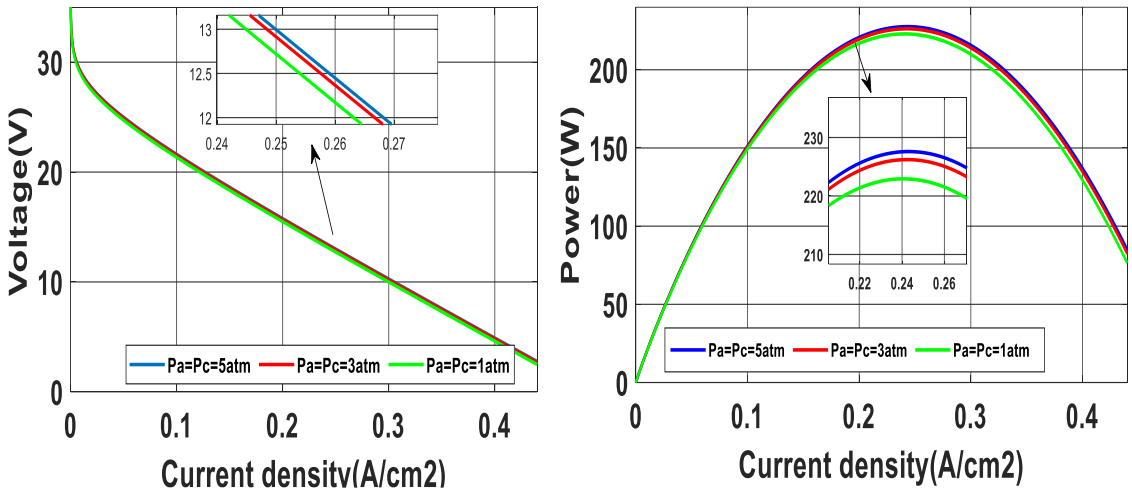

Figure 2. 10PEMFC stack (P-V), (I-V) characteristics (variation in temperature)

Table 2. 3PEMFC stuck parameter

Parameter	**Values**
$\mathbf{N_{fc}}$	20
A	70 cm2
ξ_1	-0.994
ξ_2	0.00354
ξ_3	$7.8e^{-8}$
ξ_4	1.96×10^{-4}
R_c	15×10^{-4}
B	0.0165
$\mathbf{J_{max}}$	1.7cm

2.4 power converter:

Power converters are typically used to control the input voltage to meet the needs of the application. Since centuries, power converters have played a prominent role in power distribution systems and drives[34]. For photovoltaic or PMFC the output power are variables and depends on the climatic conditions for the photovoltaic array and (temperature, pressure) for PEMFC, we can't be connected directly to AC inverter first must be connected to DC-DC converter to maximized the power and then converted to AC using inverters. To convert the power, the system uses two-stage: the first stage is DC-DC and the second one is DC-AC as shown above in figure 2.1.

2.4.1 DC-DC converters:

Many DC-DC converters now used to control the input voltage dependent on the application requirements. DC-DC converters are divided into two main types: isolated ig : Push-Pull, Flaybck,Forward, Multiport [35]and non-isolated converters ig : conventional DC-DC, interleaved DC-DC, Multi Device/port[36]. The DC-DC converter is responsible for maintaining the renewable sources' work at the maximum power point (MPP). In this these for our hybrid global system we used buck-boost with PV array and Boost with PEMFC.The DC-DC converters, including the Buck Boost and Boost c topologies, are modeled using a state space modeling technique. First and foremost, state-space modeling is primarily represented in equation (2-11) and (2), where A, B, C, D are the system matrix, χ is the state variable, $x^{'}$ isthe state variable derivative, u is the input, and y is the output.

$$\begin{cases} x^{'} = Ax + Bu \\ y = Cx + Du \end{cases} \quad (2.11)$$

2.4.1.1 Buck-Boost converter:

The buck-boost converter topology combines two separate converter topologies.The buck converter and the boost converter, where the buck converter lowers the output voltage level and the boost converter enhances it. Nevertheless, buck-boost converter architecture is still being researched in order to improve the efficiency of photovoltaic (PV) energy generating systems. This hybrid converter architecture is utilized in a wide variety of applications, including driving applications, stand-alone and grid-connected photovoltaic (PV) energy generating systems[37]. The buck-boost is implemented with an capacitor, inductor , power switch (IGBT), a diode. the equivalent circuit switch in the both state ON(figure2.11) and OF (figure2.12) are shown in the figure bellow:

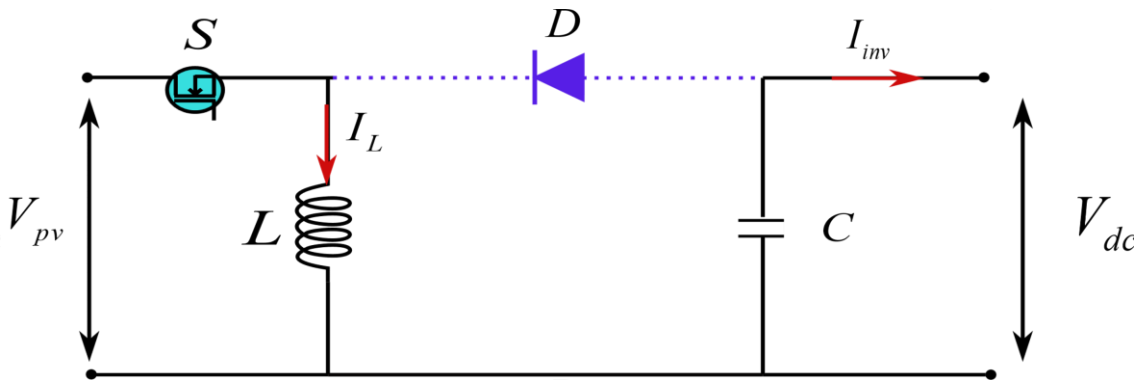

Figure 2. 11closed switch.

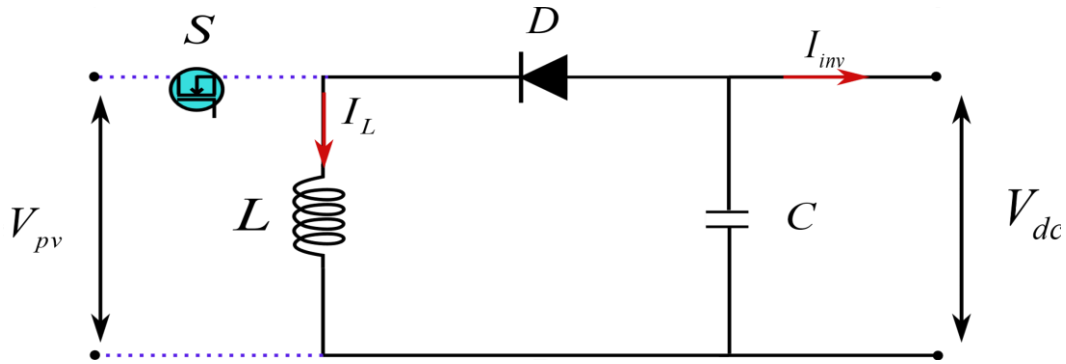

Figure 2. 12opened switch.

Mode one when the switch is closed (ON) as represented in figure2.11.the state represent in equation

$$\begin{bmatrix} x_1' \\ x_2' \end{bmatrix} = \begin{bmatrix} 0 & 0 \\ 0 & -\frac{1}{C} \end{bmatrix} \begin{bmatrix} x_1 \\ x_2 \end{bmatrix} + \begin{bmatrix} \frac{1}{L} \\ 0 \end{bmatrix} u_1 \qquad (2.12)$$

Mode 2 when the switch is opened (OFF) as represented in figure2.12we can described the equation as follow:

$$\begin{bmatrix} x_1' \\ x_2' \end{bmatrix} = \begin{bmatrix} 0 & \frac{1}{L} \\ -\frac{1}{C} & -\frac{1}{C} \end{bmatrix} \begin{bmatrix} x_1 \\ x_2 \end{bmatrix} + \begin{bmatrix} 0 \\ 0 \end{bmatrix} u_1 \qquad (2.13)$$

Where the state variables are, $I_L = x_1$ $V_{dc} = x_2$

2.4.1.2 Boost converter :

In certain RE (renewable energy system)systems, the amplitude of the load side voltage must be larger than the size of the output voltage[38].Among numerous choices, the boost converter was picked to connected with PEMFC. The construction of this converter is basic and the case, also can control the MPPT. An inductor, a power electronic switch (IGBT), a

diode, and a capacitor are commonly used in boost converters. The equivalent circuit switch in the both state ON (figure2.13) and OFF (figure 2.14) are shown in the figures bellow:

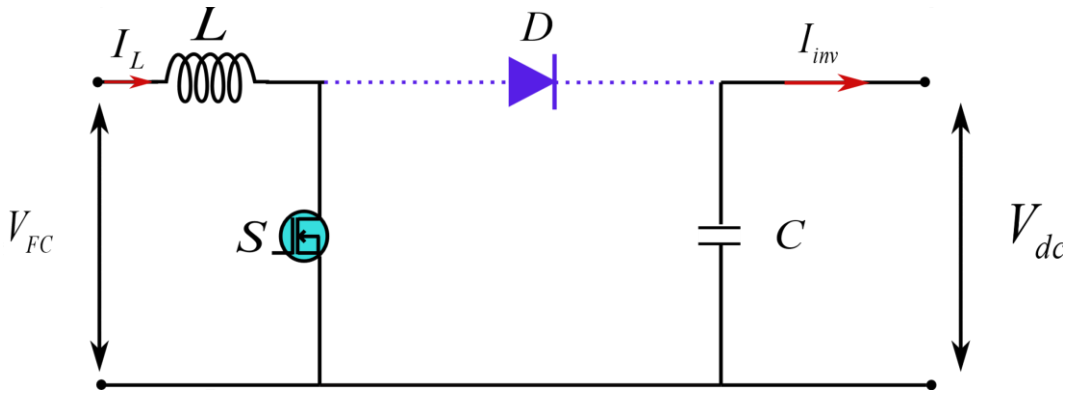

Figure 2. 13mode one : closed switch

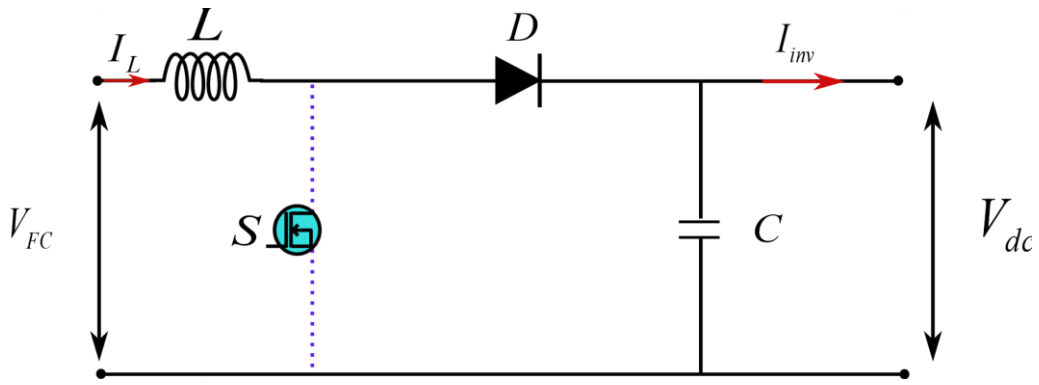

Figure 2. 14mode tow open switch

Mode 1 when the switch is closed (ON) as represented in figure2.13,we can described the equation as follow :

$$\begin{bmatrix} x_1' \\ x_2' \end{bmatrix} = \begin{bmatrix} 0 & 0 \\ 0 & -\frac{1}{C} \end{bmatrix} \begin{bmatrix} x_1 \\ x_2 \end{bmatrix} + \begin{bmatrix} \frac{1}{L} \\ 0 \end{bmatrix} u_1 \qquad (2.14)$$

Mode 2 when the switch is opened (OFF) as represented in figure2.14 we can described the equation as follow:

$$\begin{bmatrix} x_1' \\ x_2' \end{bmatrix} = \begin{bmatrix} 0 & -\frac{1}{L} \\ \frac{1}{C} & -\frac{1}{C} \end{bmatrix} \begin{bmatrix} x_1 \\ x_2 \end{bmatrix} + \begin{bmatrix} \frac{1}{L} \\ 0 \end{bmatrix} u_1 \qquad 2.15)($$

Where the state variables are: $I_L = x_1$, $V_{dc} = x_2$, $u_1 = V_{fc}$

2.5 DC-AC inverters topology:

Renewable energy sources generate electricity, which is sent to the distribution station. However, the DC power generated at the (RS) cannot be directly fed into the electrical

system. As a result, power electronic converters and electrical components are used to connect renewable energy sources to the grid [39]. Typically, utility-scale renewable energy systems are made up of four components: 1- DC-DC converter with MPPT 2- DC-AC inverter, 3- output filter at inverter-side and 4- grid. Inverters are DC-AC inverter that convert DC power to alternating current, voltage in order to give electric power to the grid[40]. Fundamentally, The voltage source inverter has two types : 2-level voltage source inverter and multi-level inverters.As seen in Figure 2.15.

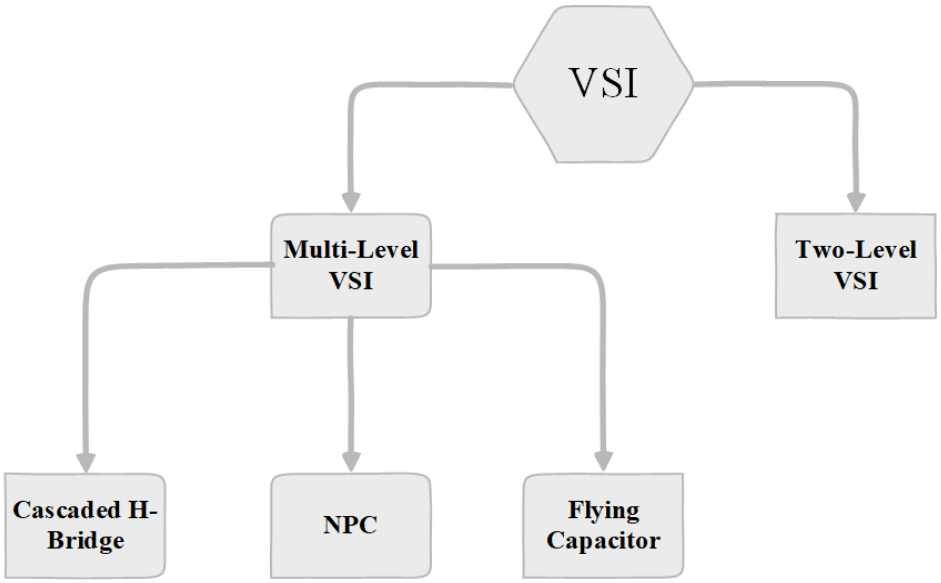

Figure 2. 15 Voltage source classifications

Voltage source inverter (VSI).In general, VSI refers to an inverter that uses the input voltage to produce a regulated output voltage.the use of VSI is gaining wide acceptance day by day.Thus, the high efficiency of these inverters is the main constraint andcritical parameter for their effective utilization in such application[39],The 2-Level VSI has found use in a variety of typical industrial machinery. While multi-level VSI (MLVSI) are more newer and well-established in industry because to their benefits, particularly the ability to create multilayer stepped-waveform with lower harmonic distortion, higher voltage operation, and increased flexibility[41].

2.5.1 Voltage source inverter :

The DC voltage source is at the input side of the Voltage Source Inverter (VSI), therefore the polarity of the input voltage remains constant. However, the direction of average power flow through the inverter is determined by the polarity of the incoming DC current[38]. An AC voltage waveform with variable width and constant amplitude can be generated at the output side. This section describes many VSI topologies that are typically used in Renewable energy sources , emphasizing the description and characteristics of each. Two-level and multi-level

VSI topologies are studied. MLVSI topologies are classified into three types: cascaded H-bridge (CHB), diode-clamped, and flying capacitor.

2.5.1.1 Tow-level Voltage source inverter:

Two-level converters are commonly utilized in the grid connection of renewable energy sources for low power applications. However, the reliable sources are occasionally linked to medium voltage for high power applications, making the use of two-level inverters challenging due to the high voltages that the switching devices can block[42]. We take a look at this inverter generally the component of two-level-VSI six switches with a free-wheeling diode in parallel with each switch[43]. , The usage of multilevel inverters solves the disadvantage of two-level VSI. These converters' main feature is their smaller and many voltage levels, which give higher power performance improvement, reduced overall harmonic distortion, and reduced switching device losses[23].

2.5.1.2 Multi-level voltage source inverter (MlVSI):

2.5.1.2.1 **Natural point champed inverter:**

The clamping diodes and cascaded DC capacitors used in the diode-clamped multilevel inverter create AC voltage waveforms with several levels. This inverter has a three level or more configuration is called Natural point champed (NPC) ,however is commonly used for medium voltage power applications[44].Furthermore, the major advantages are classified as follows[45]

- Good dynamic response
- Simple design
- Low const and compact in 3-level structure
- No floating capacitors
- Low THD in AC voltage side, also reduces the dv/dt stresses.

2.6 Conclusion:

The objective of this chapter is to describing the components model of the proposed photovoltaic-PEMFC connected to the grid that which will be used the following chapters of the control system and simulation. First a photovoltaic modeling (cell, module) and their P-V, I-V characteristic curves have been described. Next a fuel cell type PEMFC (Stack) we had been also described the characteristic P-I V-I, after that The power converters utilized in the proposed Grid-connected system ig; DC-DC converter were shown to demonstrate their power circuits and model them finely a DC-AC inverter described the voltage source inverter ig; a two-level and three-level natural pointed champ inverter.

Chapter 3 Literature review of control techniques for dual stage grid-connected PV and PEMFC system

3.1 Introduction

Grid-connected renewable energy systems have been utilized to inject power generated by the renewable energy in our case PV array or PEMFC into the public grid. The challenges of this systems are to extractant the maximum power from renewable sources and injected into grid with high current quality under different inputs climatic conditions (irradiation, temperature) for PV array and pressure, temperature for PEMFC. There are significant advantages to two-stage grid-connected renewable energy systems. That means improving MPP tracking and raising the DC-link voltage value above the grid peak voltage value whatever the PV or PEMFC produce.

In the last decade many researchers have proposed many controls algorithms witches can be employed for dual stage that mean forthe first stage or the second stage as well. These controls are divided into three essential steps: Maximum power point trucking (MPPT), DC-link voltage control and regulation and of the injected power onto the grid.

In this chapter, an overview of the most control approaches have been proposed for the dual stage grid-connected PV and PEMFC system.First Maximum power point trucking and analysis for the first stage, after that, a brief review of DC-Link regulation and control, finally, a control strategy for three-phase systems are described respectively.

3.2 Maximum Power Point trucking strategies:

Few years ago, researchers started to develop strategies to extract as possible power from renewable energy sources and specially the PV array and recently the FC's .The PV array and Fuel cell suffer from problems; efficiency, weather-dependency and intermittency for PV array and pressure, temperature for Fuel cell of the generated electric power[46,47]. Furthermore, there is a unique point on the nonlinear P-V curve of the solar array and P-I curve for fuel cell called Maximum Power Point (MPP), at which the entire PV system and fuel cell operates with maximum efficiency[48,49]. Therefor it is essential to build a controller capable of forcing PV systems to continuously track and fast extract maximum power [50].this approaches called Maximum Power Point Truck (MPPT) controller, this controller t is required to predict and to track the MPP at all circumstances and then force the PV system and Fuel cell to run at that MPP point[48,51,52]. They are employed in the DC-DC converter (In the first stage),The most commonly used MPPT algorithms are presented and compared in this section. This overview includes a lot of MPPT techniques for PV array and for Fuel cell.

3.3 MPPT techniques for Photovoltaic system:

3.3.1 Classique MPPT techniques:

3.3.1.1 ***Perturb And Observe (P&O):***

This approach is based on the behavior of PV arrays.From the According to the literature, several researchers prioritized Perturb and Observe-based MPPT algorithms. To be near to the Maximum power point[53], If the operational power point is on the left side of the MPP, the algorithm transfers it to the right by raising the power converter duty cycle of the first conversion stage (DC-DC converter), and vice versa if it is on the right side of the MPP[54][55][56]. The P&O algorithm is shown in figure.3.1.

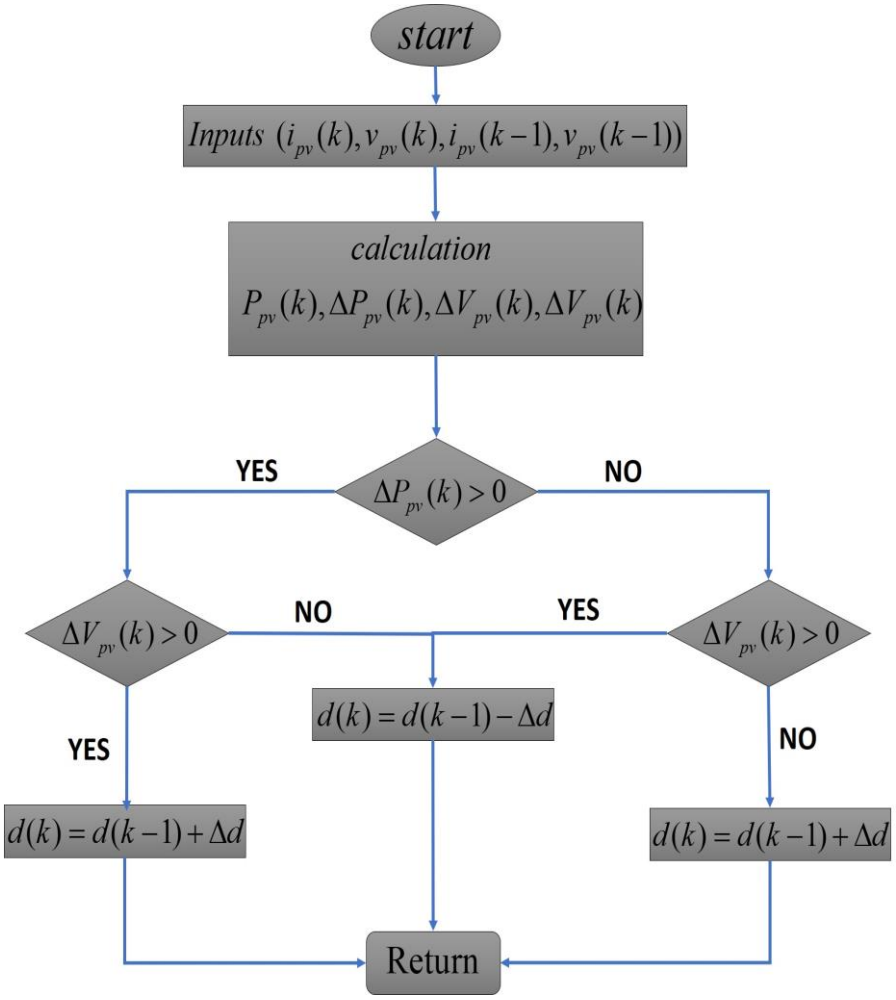

Figure 3. 1Flowchart of the P&O algorithm.

3.3.1.2 ***Incremental conductance algorithm:***

The incremental conductance algorithm (INC) represented in figure (3.2) is also built as a P&O algorithm based on the PV array's behavior.To track MPP, Incremental Conductance (IC) method utilizes theratio of incremental conductance to instantaneous conductancevalue of the PV array. Based on this value, The slope of the P-V characteristics changes[57]. The duty cycle for the converter is determined by the change in slope[58][59][60][61]. This algorithm's basic equations are as follows:

$$\begin{cases} \dfrac{dp_{pv}}{dv_{pv}} = 0 \quad at\ MPP \\ \dfrac{dp_{pv}}{dv_{pv}} > 0 \quad left\ of\ MPP \\ \dfrac{dp_{pv}}{dv_{pv}} < 0 \quad right\ of\ MPP \end{cases} \tag{3.1}$$

Since the equation (3.1) expressed as follow :

$$\frac{\Delta p_{pv}}{\Delta v_{pv}} = \frac{\Delta(i_{pv}.v_{pv})}{\Delta v_{pv}} = i_{pv} + v_{pv}\frac{\Delta i_{pv}}{\Delta v_{pv}} \tag{3.2}$$

Comparing the equation (3.1) & (3.2), we can find the equation (3-3):

$$\begin{cases} \dfrac{\Delta i_{pv}}{\Delta v_{pv}} = -\dfrac{i_{pv}}{v_{pv}} \quad at\ MPP \\ \dfrac{\Delta i_{pv}}{\Delta v_{pv}} > -\dfrac{i_{pv}}{v_{pv}} \quad left\ of\ MPP \\ \dfrac{\Delta i_{pv}}{\Delta v_{pv}} < -\dfrac{i_{pv}}{v_{pv}} \quad right\ of\ MPP \end{cases} \tag{3.3}$$

MPP is tracked by the operational point by comparing the immediate conductance (I/V) to the incremental conductance (I/V)[48].

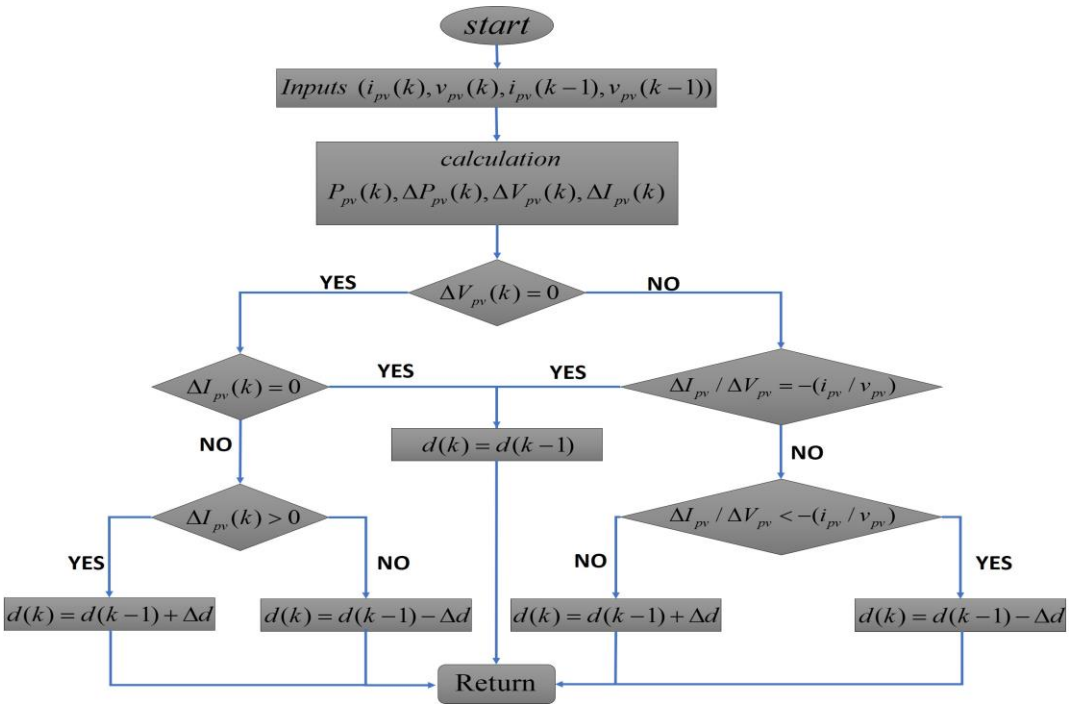

Figure 3. 2Flowchart of the INC algorithm[62].

3.3.2 Advanced MPPT approaches based on artificial intelligence:

Several new research works[63–69] have been examined to apply artificial intelligence (AI) to solve the disadvantages of P&O and INC algorithms.Furthermore, these techniques track the MPP with fast response and reduced fluctuation.The approaches are discussed below:

3.3.2.1 ***Fuzzy Logic Control based MPPT:***

Fuzzy Logic Control (FLC) is a rule-based technique that solves non-linear optimization problems with robustness. Because of benefits such as (1) flexible operation, (2) user interface convenience, (3) ease of implementation, and (4) qualified validation.Without requiring parameter estimates, the FLC parameters may be modified fast in response to changes in system dynamics.When environmental circumstances shift, the performance of a fuzzy-based MPPT algorithm is strong; nevertheless, the strength of the method is highly dependent on the controller design. The FLC is preferred for MPPT implementation. Therefore, it is less common to see FLC applied on its own, However, it is highly valued when combined with other techniques such as artificial neural networks [70], Genetic algorithm and other conventional methods[71].In FLC design, the main control variables must be identified, as well as the sets that define the values of each linguistic variable, and there are three steps: Fuzzification, inference fuzzy rules and defuzzification for its MPP tracking.During fuzzification, the input variables are translated into linguistic variables using the membership function of choice.The linguistic variables are changed at the inference stage depending on the rule base that determines the controller's behavior. The FLC result is transformed to a numerical variable from the linguistic variable during the defuzzification stage by using membership function [63,71].For instance the triangular membership functions are used in this case with seven fuzzy variables, i.e., NB (Negative Big), NM (Negative Medium), NS (Negative Small), ZE (Zero), PS (Positive Small), PM (Positive Medium) and PB (Positive Big), as shown in table (3-1) similar in figure (3.3).The FLC usually the inputs are tracking error (E) and change in error (DE), as given below in equation (3.4) :

$$\begin{cases} E(k) = \dfrac{P_{pv}(k) - P_{pv}(k-1)}{I_{pv}(k) - I_{pv}(k-1)} \\ CE(k) = E(k) - E(k-1) \end{cases} \quad (3.4)$$

Where k refers to sampling time, ‘ P’ is the powerand ‘ I’ is the current of the PV array.Uselly the output variable is the change in duty cycle Dd of the DC-DC converter. Table 3-1 explains the principles for calculating the error and the change in error. The changing duty cycle is taken into account in Fuzzy implemented MPPT for appropriate duty cycle adjustment[72].

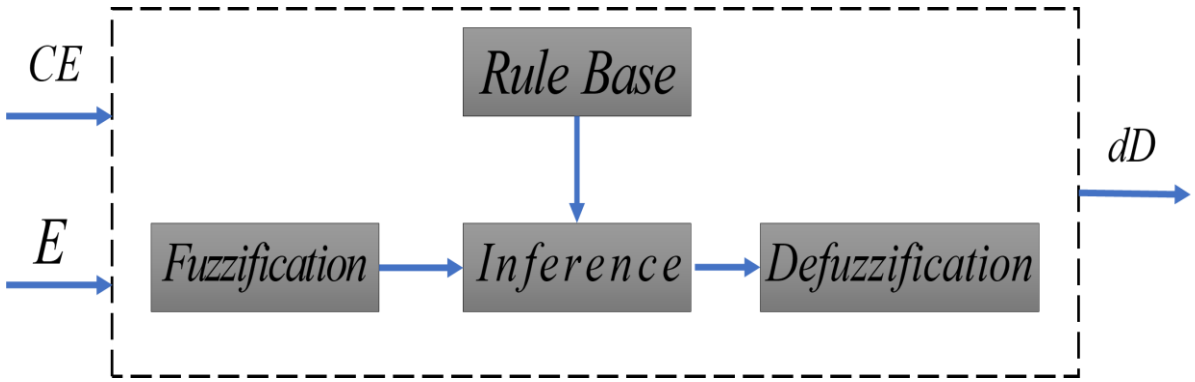

Figure 3. 3Schematic of a fuzzy controller[72].

Table 3. 1the fuzzy rules of FLC MPPT

E/DE	NB	NM	NS	ZE	PS	PM	PB
NB	ZE	ZE	ZE	NB	NB	NB	NB
NM	ZE	ZE	ZE	NM	NM	NM	NM
NS	NS	ZE	ZE	NS	NS	NS	NS
ZE	NM	NS	ZE	ZE	ZE	PS	PM
PS	¨PM	PS	PS	PS	ZE	ZE	ZE
PM	PM	PM	PM	ZE	ZE	ZE	ZE
PB	PB	PB	PB	ZE	ZE	ZE	ZE

3.3.2.2 ***Artificial Neural Network:***

The term "Artificial Neural Network" refers to a technique that is based on the behavior of neurons.The ANNhave become popular and expanded in MPP tracking for PV systems Because it is can think for itself. However, substantial knowledge is required to train the neurons present in the algorithm[73–78], According to the report, ANN incorporates three levels in MPPT installation.A typical three layer ANN model is shown in figure.3.4. As a result, the input layer consists of two neurons that are supplied by the PV system's voltage and current, PV array parameters such as open-circuit voltage V_{OC} and short-circuit current I_{SC}, as well as climatic data such as temperature and irradiance, or any combination of these elements[68].The output is a duty cycle that is utilized to power the converters that are operating at or around the MPP. The hidden layer is used to propagate the input signals to the output layer based on the transfer function applied on it, furthermore The link between nodes I and J is considered as having a weight of W_{ij} as illustrated in figure.2.4.The ANN approach works by weighting the links between nodes based on a training procedure in which the PV parameters are evaluated and recorded over months or years to determine the appropriate weight for each node.According to the previous discussion, ANN has a greater priority in solving nonlinear issues; nevertheless, this approach has a larger computation and takes a big memory. Furthermore, ANN requires training in order to construct an MPPT controller. to overcome the drawbacks the ANN is preferred to implement in combination with other conventional MPPT techniques for instance with Fuzzy and other algorithm to extract maximum power from a PV array[78,79].

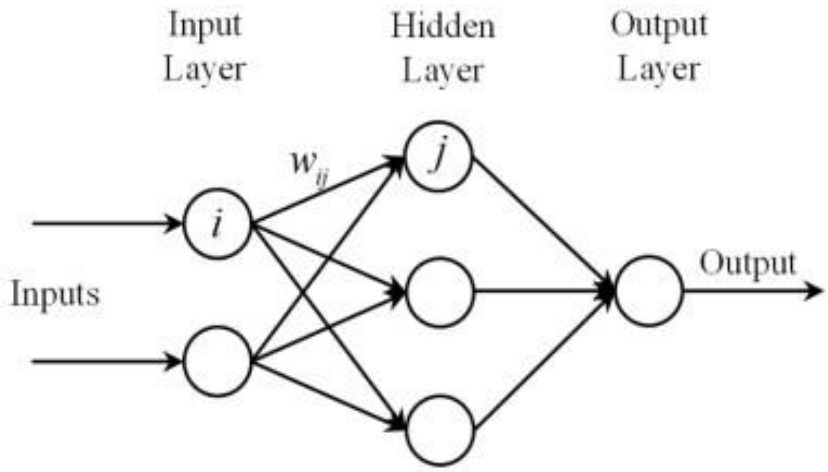

Figure 3. 4A diagram of a neural network[80].

3.3.2.3 Other MPPT Approaches:

Other MPPT controllers[81–88] that have been discased in the literature included; They employ various control strategies in terms of complexity, efficiency, and implementation costs. For instance, these approaches included once based on firefly algorithm (FA)[82],particle swarm optimization (PSO) [88] andDifferential Evolutionary (DE)[89].When compared to traditional techniques, these techniques are capable of boosting tracking performance even when the PV system is partially shaded. Unfortunately, numerous factors in these systems are chosen by trial and error, primarily based on the designer's expertise. Furthermore, because they need expensive hardware resources, most of these approaches have a narrow range of practical use. Table (2.2) summarizes a comparison of the existing MPPT strategies based on the research results presented in the literature and other approaches.

Table 3. 2performance comparison between MPPT strategies

MPPT techniques	**Implemented Capacity**	**Convergence speed**	**accuracy**	**Power oscillation**	**Complexity**
P&O[54–56]	Lower	Low	low	Larg	Low
INC[58,61,63]	Lower	Low	low	Larg	Low
FLC[69,71,72,90]	Hight	Fast	Hight	Very small	Hight
ANN[73–75,78,79]	Hight	Fast	Hight	Very small	Hight
FA[58,81,82]	Medium	Fast	Hight	Very small	Medium–high
PSO[87,88]	Hight	Fast	Hight	Very small	Hight
DE[89]	Lower	Fast	Medium–high	Very small	Medium

3.4 MPPT techniques for PEMFC system:

3.4.1 Conventional techniques :

Traditional MPPT methods are the simplest methods and have been used for a long time. Due to their simplicity, these approaches come at a low cost.

3.4.1.1 Perturb And Observe (P&O):

The Perturb and Observe (P&O) control approach and recent advancements are briefly discussed in this sub-section, with the strategy being provided first and the developments coming after.The P&O method perturbs an appropriate parameter to follow the optimal value of any variable in the time function. With the use of this approach, the operating point of FC is shifted closer to MPP by changing the current or voltage. Figure(3.5) shows a flowchart of MPPT utilizing the P&O method[91].Multiple optimal points will provide inaccurate results, therefore this method only works if there is one maximum power point. P&O's simplicity and ease of use are two of its primary features. On the other hand, because of the fixed step size of the perturbation, the residual constant state fluctuations are the main drawback.Although it is a less complicated approach, due to its slow convergence as well as elevated output power fluctuations, investigators do not often employ it.Additionally, this approach was used in multiple papers as a comparative study[92][49][93].Additionally, to provide a consistent comparison platform, P&O was utilized in these publications using DC/DC converters, and the duty cycle was adjusted appropriately.

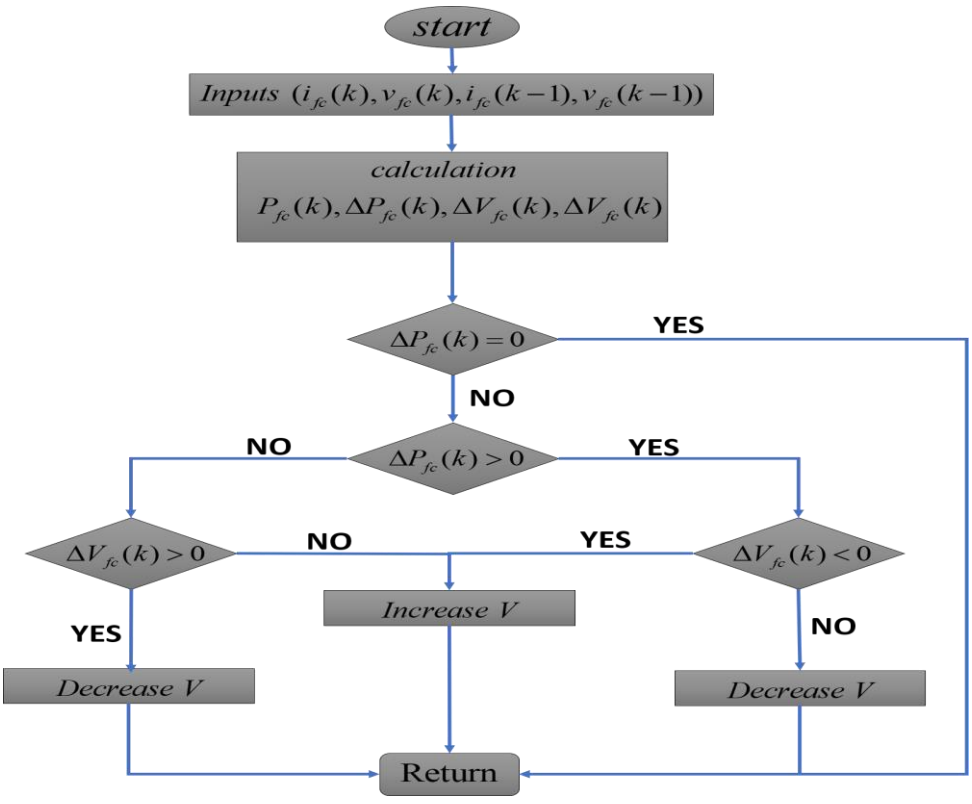

Figure 3. 5flowchart of P&O[91].

3.4.1.2 Incremental conductance algorithm:

The sections go into further detail on the control scheme and most recent developments in the Incremental Conductance (IC) control approach for MPPT of PEMFC.The IC approach includes computing the slope of the P-I characteristic of the PEMFC, as illustrated in figure(3-6).By locating the location where the slope is close to zero, it may calculate the MPP of the FC. Additionally, perturbations are performed with the MPP set to dPFC/dIFC = 0. Other ways to define the MPP include:

$$V_{fc} + I_{fc}\frac{\Delta V_{fc}}{\Delta I_{fc}} = 0$$
$$\frac{V_{fc}}{I_{fc}} = -\frac{\Delta V_{fc}}{\Delta I_{fc}} \quad . \tag{3.5}$$

Using the previously mentioned reasoning, perturbations are put into practice to determine if the present working point is to the left of, to the right of, or at the MPP. The formula that follows is used to calculated it:

$$\begin{cases} \frac{V_{fc}}{I_{fc}} = -\frac{\Delta V_{fc}}{\Delta I_{fc}} \ at\ MPP \\ \frac{V_{fc}}{I_{fc}} > -\frac{\Delta V_{fc}}{\Delta I_{fc}} left\ of\ MPP \\ \frac{V_{fc}}{I_{fc}} < -\frac{\Delta V_{fc}}{\Delta I_{fc}} \ right\ of\ MPP \end{cases} \tag{3.6}$$

Despite being comparatively more sophisticated than P&O, IC delivers more efficiency and less fluctuation around MPP. Figure(3.6) displays the IC algorithm's flowchart. Additionally, this approach was used and developed by resercher : For the MPPT of the PEMFC, incremental was used with various Fixed Step Sizes (FSS) at the perturbations of 0.02, 0.05, 0.07, and 0.09[94].The FSS itself is a significant disadvantage of this method. Variable Step Size (VSS) incremental resistance was used and compared to FSS incremental resistance, and it was found that VSS incremental resistance follows MPP more accurately and quickly.A thorough comparison of VSS IC and FSS IC revealed that VSS IC was better with regard to ripple, reaction time, and overshoot[95].

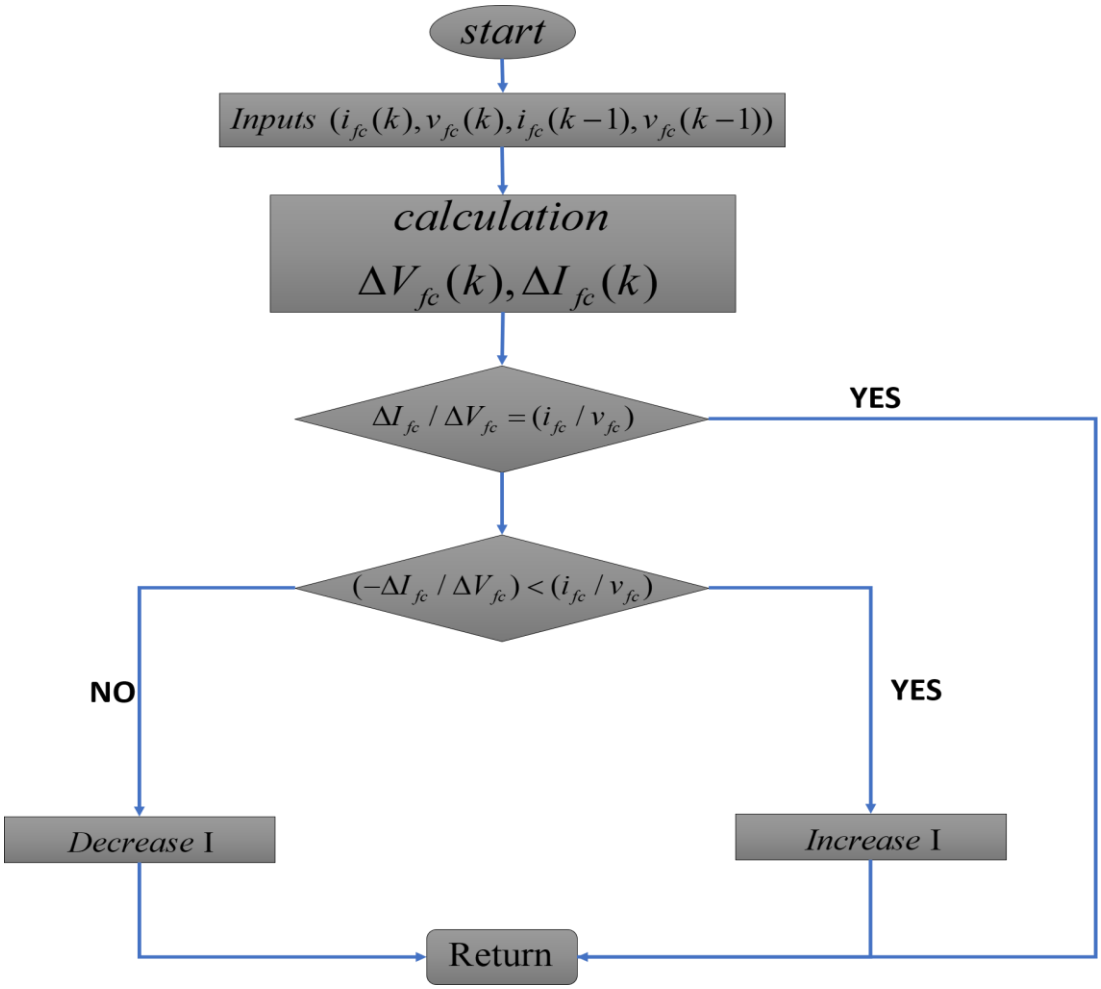

Figure 3. 6flowchart of INC[91].

3.4.2 Advanced MPPT approaches based on artificial intelligence:

the methods that self-correct while being used to account for changes in operating circumstances and ensure the plant or process operates as efficiently as possible.These are more challenging to put into practice, yet they provide superior outcomes over the conventional methods.

3.4.2.1 ***NN predictive control technique:***

Even though NN Predictive Controller (NNPC) is a very valuable approach, it hasn't been well studied.One of the most significant and efficient control methods for non-linear systems is NNPC. NN is employed in this control strategy to forecast the plant's future output utilizing historical plant inputs and outputs over a certain time horizon.This feed-forward method only uses one hidden layer, and the network was trained offline in batch mode. Because of its precise training, the levenberg Marquardt technique is utilized. Depending on the receding horizon approach[96].the block diagram of the NNPC is described below in figure (3.7).

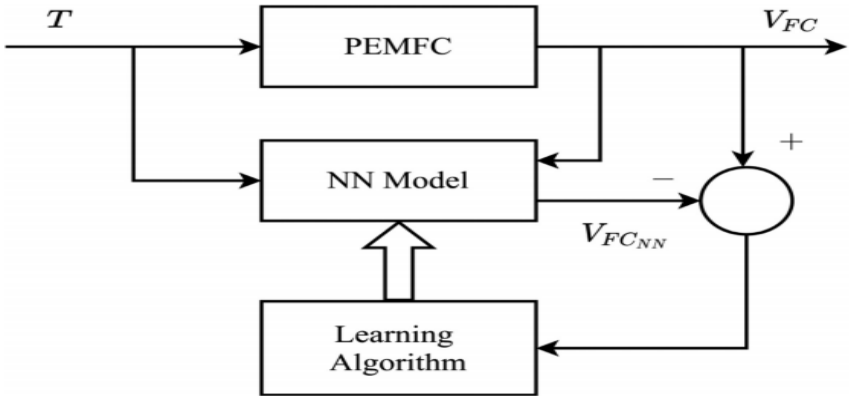

Figure 3. 7diagram of NNPC[91].

3.4.2.2 Fuzzy logic contror*:*

In order to build controllers that have shown their efficacy in following the MPPT of FC, fuzzy logic is employed. The three main stages of FLC design are as follows: One) Fuzzification (3), two) Rule Evaluation.and three) Defuzzificationand These stages are depicted figure (3.8). To work successfully, an FLC-MPPT strategy requires two inputs, particularly the error e and the change in error De. The can specify as follow[97]:

$$\begin{cases} E(k) = \dfrac{P_{fc}(k) - P_{fc}(k-1)}{V_{fc}(k) - V_{fc}(k-1)} \\ dE(k) = e(k) - e(k-1) \end{cases} \quad (3.7)$$

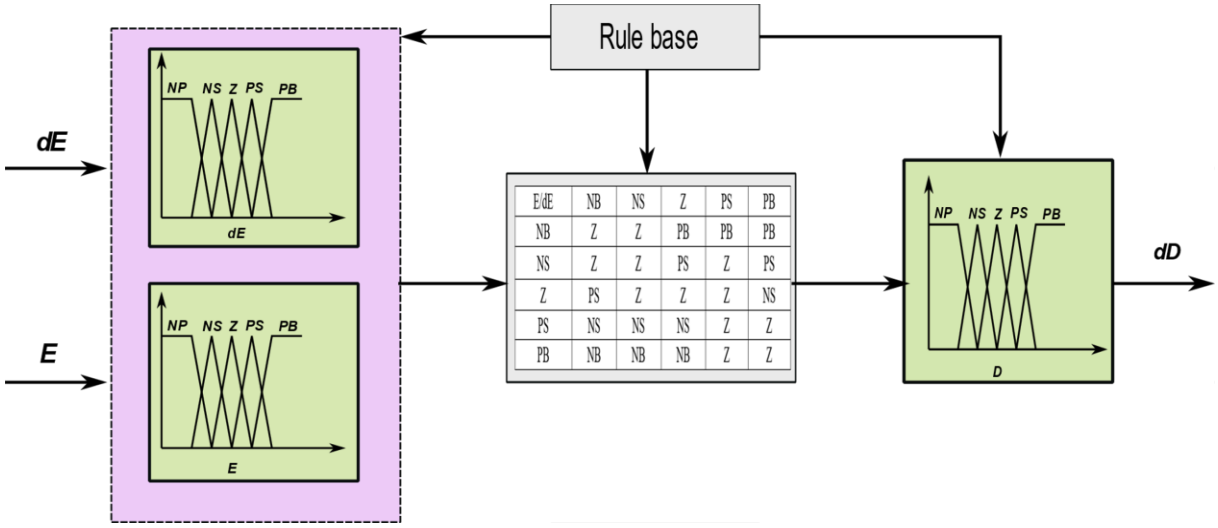

Figure 3. 8block diagram of FLC[72].

3.4.2.3 Other MPPT technique:

There have also been discussions of other MPPT controllers in the literature, like as Tracking the MPPT using P-V characteristics has been done using Particle Swarm Optimizer (PSO)[98].The PID controller's performance has been tuned using Grey Wolf Optimizer

(GWO)[99].and hybrid algorithm.The comparative evaluation of the performance of the several MPPT approaches is shown in the table (3.3) below:

Table 3. 3performance comparison between MPPT strategies for PEM fuel cell.

MPPT techniques	**Robustness**	**Convergence speed**	**accuracy**	**Power oscillation**	**Complexity**
P&O[91]	lowe	Very Low	Medium	Hight	Very Low
INC[95]	Lower	Very Low	Medium	Hight	Very Low
SMC[91]	Medium	Hight	Low	hight	Low
FLC[100]	Hight	Hight	Hight	Low	Medium
NN[96]	Hight	Hight	Hight	Low	Hight
PSO[98]	Hight	Hight	Hight	Very low	Hight
GWO-PID[98]	Very Hight	Very hight	Very Hight	Very low	Hight

3.5 Dc link control :

Solar, fuel cell, or wind energy is extracted during the first conversion stage and used to feed the DC link. At this level, regulating the DC-link voltage to the designated reference value and determining the amplitude of grid currents are the objectives .The DC-link voltage reference value must be at least greater than the grid maximum voltage in order to enable effective power injection regulation.Figure (3.9) shows the DC link voltage regulation block diagram. Furthermore any variations in voltage across the DC-link result in total harmonic distortion (THD) in grid current, which lowers the system's power quality.

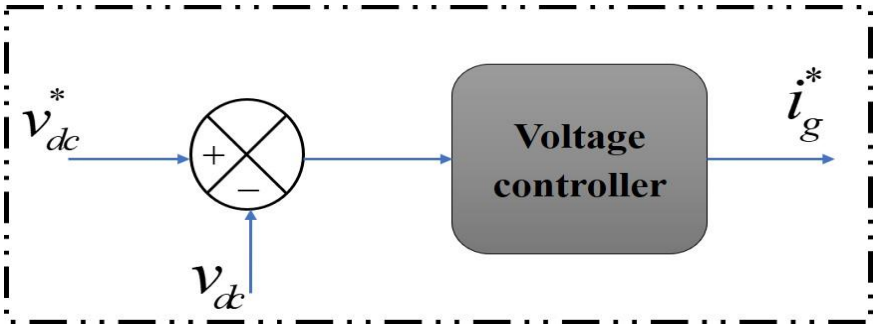

Figure 3. 9voltage regulater of DC-LINK voltage

Multiple studies have created a DC-link controller that uses traditional controllers like P, PI, and PID.[101,102][103].however the conventional methods have drawbacks, they show a slow reaction time, an overshoot, and voltage ripples.To overcome these drawbacks several research works have employed intelligent technics,tocreate an accurate DC-link controller, researchers have used techniques including fuzzy logic control (FLC) [104], neuro-fuzzy networks[105], and particle swarm optimization (PSO)[106].However, the implementation of

these intelligent AI technics necessitates big a sizable memory capacity, As a result, the applicability of these regulators is limited, particularly in complex systems.

3.5.1 Other DC-link voltage controllers

Other DC link regulators have been investigated to control the DC link voltage for instance : sliding mode (SMC)[107,108], feed-Forwerd.[109,110].Under varying conditions, these controllers are able to provide powerful operations. Furthermore, the hardware design for this type of controller is simple. As a result, the implementation of these control theories is regarded as a current study area.

3.6 Summary Grid current control techniques

This section evaluates the control difficulties that are observed while using grid-connected voltage source converters (VSI) in renewable energy systems.Different mechanisms for control have been introduced and analyzed, including direct power control (DPC), voltage-oriented control (VOC) in the stationary frame, and model predictive control. Furthermore, the descriptions of these control structures are summarized to allow for a quick comparison.

3.6.1 DIRECT POWER CONTROL BASED ON SWITCHING TABLE (DPC)

The DPC operates on the basis of direct control of active power that is estimated from DC-link voltage regulate and reactive power given by the grid operator, and the achieves low THD[111].This control scheme's operation relies on selecting a switching state that minimizes the error between the measured powers and their references.Using switshing table shown in table (3.4).the error Sd and Sq between the references and the actual values of the active and reactive powers, acquired by two comparators with hysteresis band[111][112].The scheme of DPC based on switching table ispresented in figure 3.10.

Table 3. 4DPC switshing table[113]

S_d	S_q	S_1	S_2	S_3	S_4	S_5	S_6	S_7	S_8	S_9	S_{10}	S_{11}	S_{12}
1	0	V_6	V_7	V_1	V_0	V_2	V_7	V_3	V_0	V4	V_7	V_5	V_0
	1	V_7	V_7	V_0	V_0	V_7	V_7	V_0	V_0	V_7	V_7	V_0	V_0
0	0	V_6	V_1	V_1	V_2	V_2	V_3	V_3	V_4	V_4	V_5	V_5	V_6
	1	V_1	V_2	V_2	V_3	V_3	V_4	V_4	V_5	V_5	V_6	V_6	V_1

V_0(0,0,0) V_1 (100)V_2(110) V_3 (010) V_4 (011) V_5 (001) V_6 (101) V_7 (111)

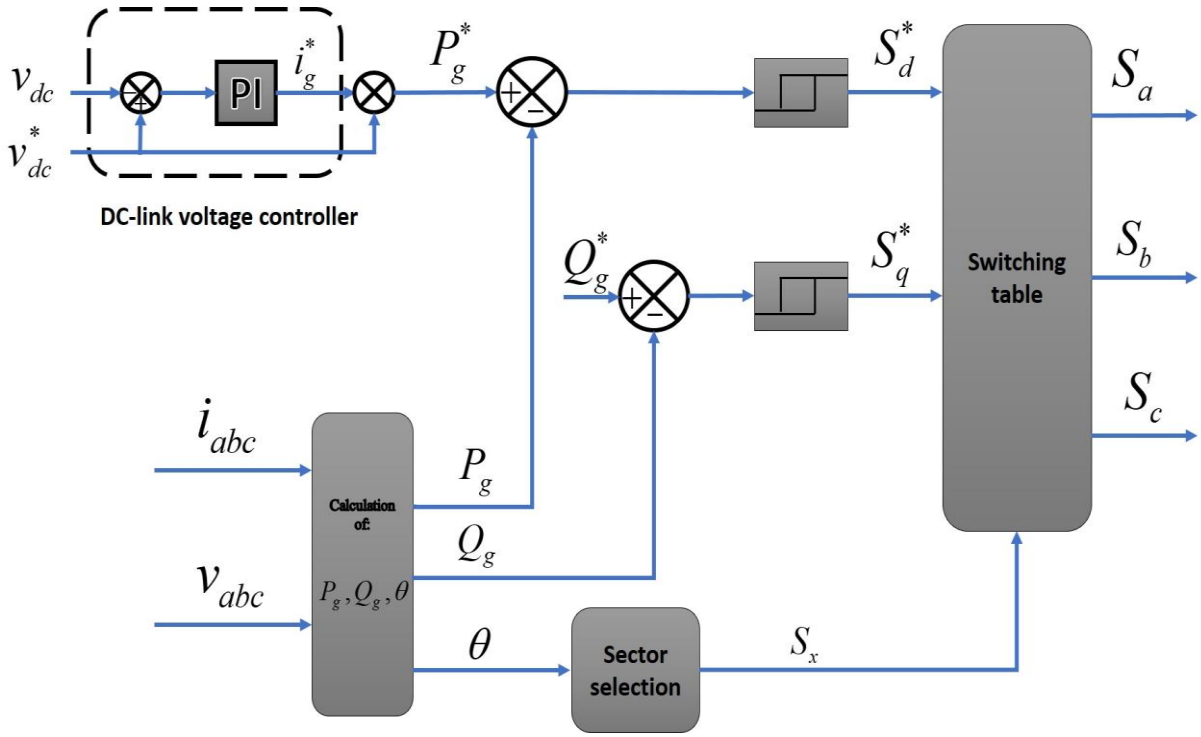

Figure 3. 10DPC(dIrect power control) scheme[114].

The DPC method is simple to apply in practice. It does, however, have a poor reaction time and substantial lower-order harmonics. In addition, it has a changeable switching frequency.

3.6.2 Stationary Frame Voltage oriented control (*VOC)*:

The scheme of classique VOC presented in figure (3.11). The main objectives of this Classique control are to achieve the sinusoidal form of the grid current and low THD value. The peak of the grid current reference i_g^* is estimated by the DC-link voltage controller.The PLL keeps being used for resonant controller frequency adaptation and obtaining the first harmonic of grid voltages needed for computing unitary waveforms.[115].Next in order to produce three-phase grid current references, the current i_g^* is multiplied by grid unitary waveforms and translated into αβ frame. After that The grid currents are measured and transported to the stationary frame, where they are compared to reference values.Finely two PI regulators are utilized to create the reference voltage for the modulation stage[116].

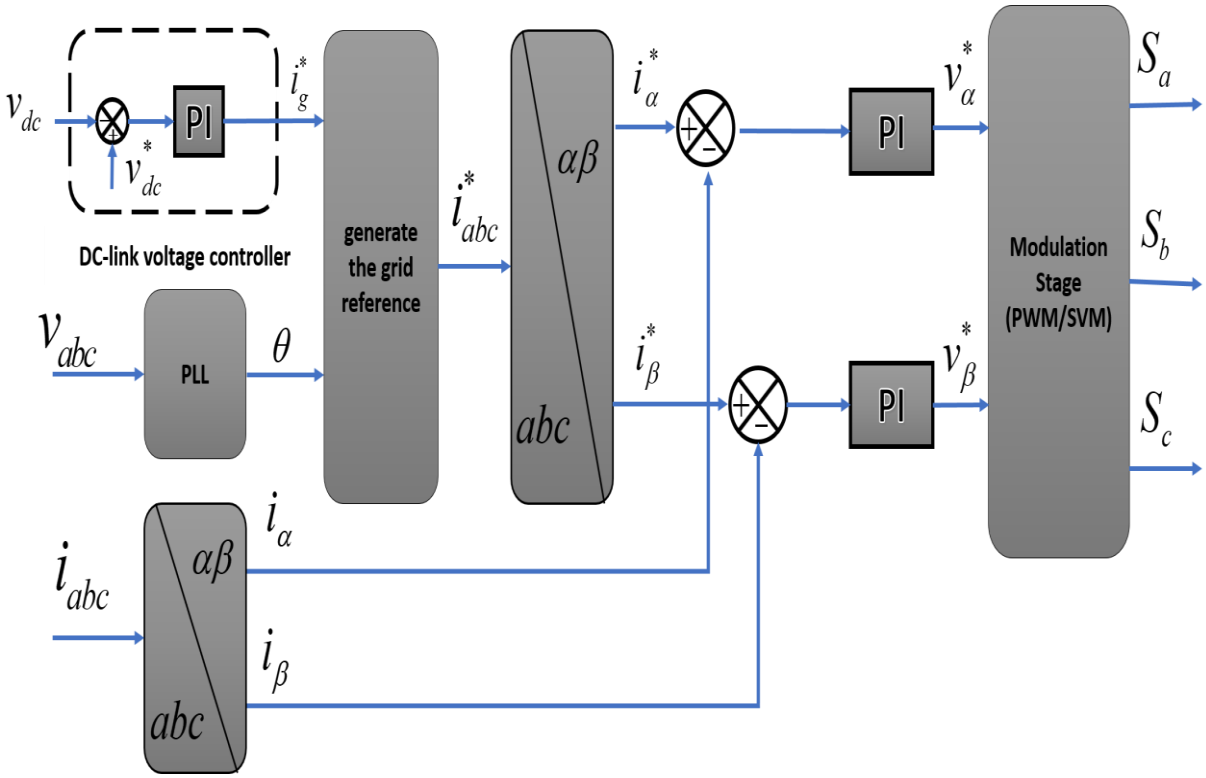

Figure 3. 11Voltage oriented control (VOC) scheme

The stationary frame VOC method ensures operation at a constant switching frequency. It is very simple to put into practice. It does, however, have a poor reaction time and much lower-order harmonics.

3.6.3 FSC-MPC FOR VOLTAGE SOURCE CONVERTER:

The finite-control set model predictive control (FCS-MPC) has recently been used in several power electronic applications in a recent study[117][118],this is because the power electronic converter has a limited number of switching states.for instance we have eight switching states for two-level voltage source inverters.The FCS-MPC approach has been used for a variety of control applications, including synchronous grid current control [118]and power control[119].The performance of FCS-MPC depends on a prediction of the upcoming behavior of variables related to state for all potential switching states compare them using a cost function depending on the references and measured variables as well as applying the discrete-time model of VSI linked to the network.Figures (3.12) and (3.13) show a scheme and flowchart that explain the capabilities of FCSMPC. FCS-MPC removes the requirement for linear PI regulators and modulation stages compared to traditional control approaches. It also offers high-performance operations. The major aspects and problems of the FCS-MPC are outlined below[120].

- **Advantages of FSC-MPC :**

- instandable and easy concept for FSC-MPC.
- It takes use of the VSI's inherent discrete character when linked to the grid, making it simple to install using industry-standard digital management platforms.
- The ability to include nonlinearities and limitations in controller design
- Optimizations are substantially simplified because to the finite number of switching states provided by VSI.

- **Drawbacks of FSC-MPC:**
  - Variable switching frequency is used.
  - Weighting factor value estimation is neither analytical nor numerical.
  - Control performance will be affected if the system concept and prediction horizon are not adequately established.

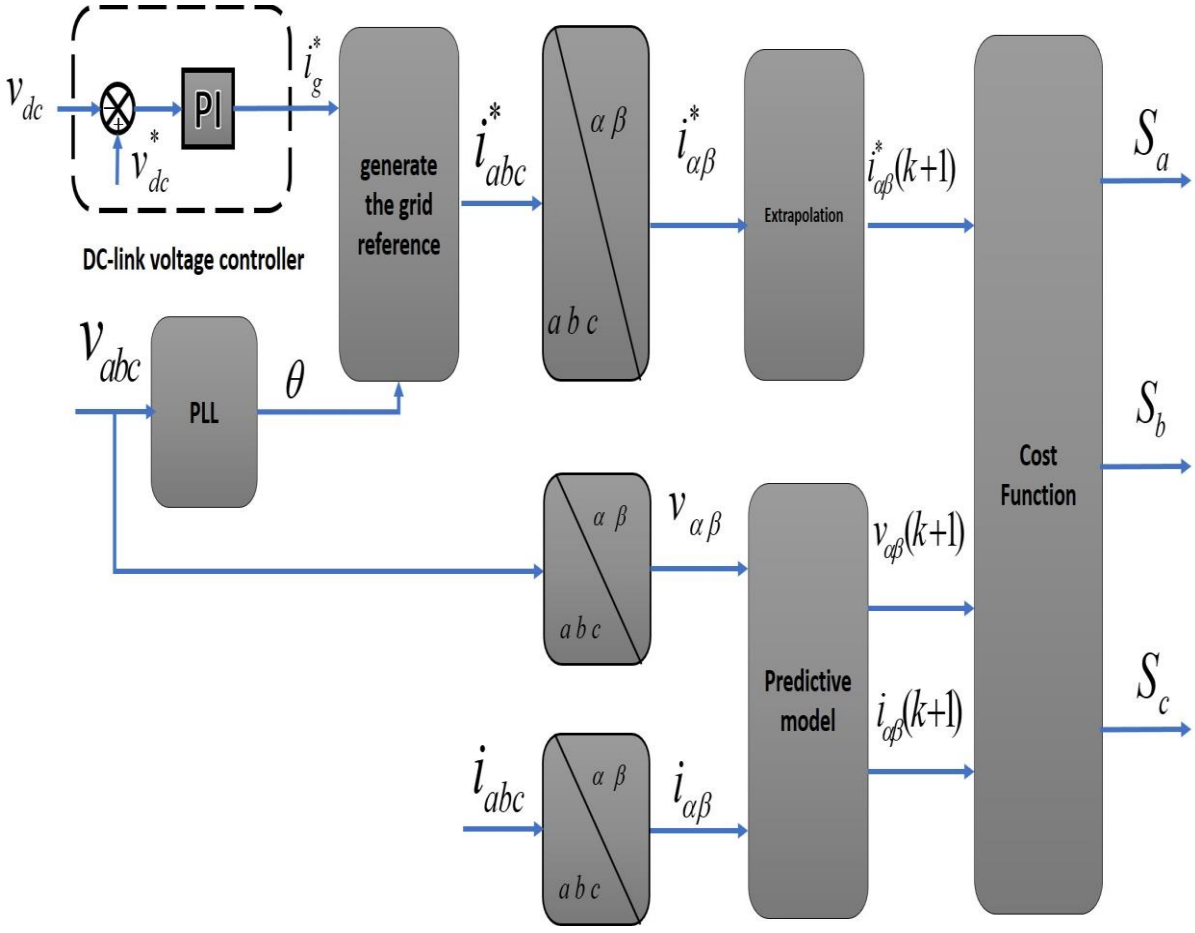

Figure 3. 12FSC-MPC scheme.

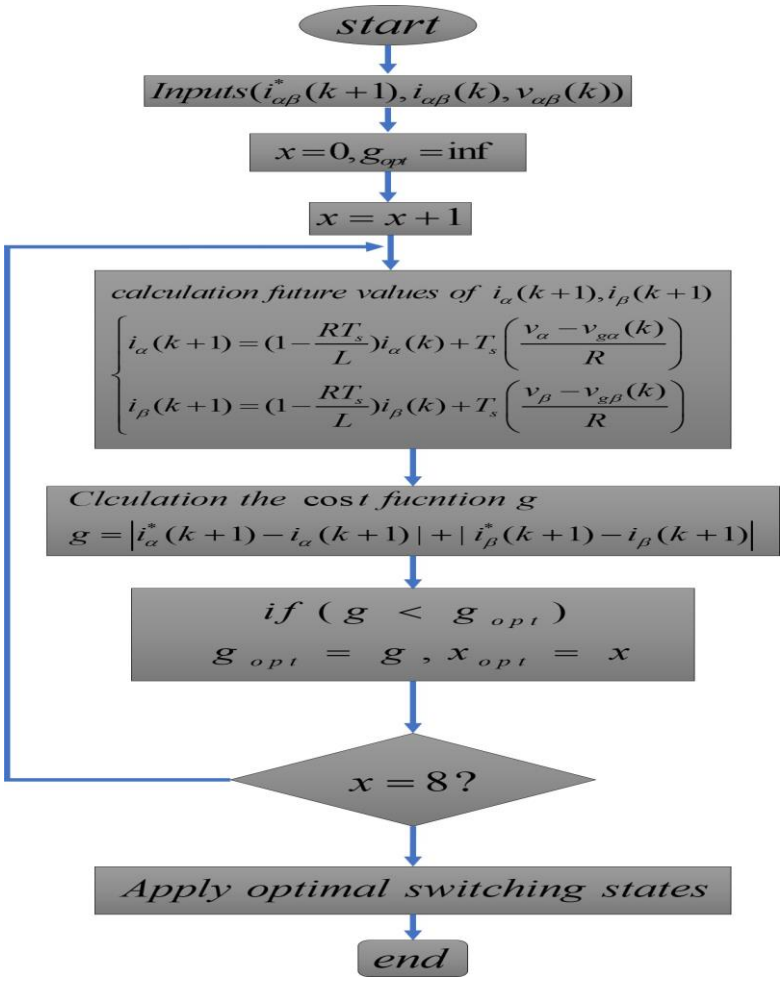

Figure 3. 13FSC-MPC flowchart[121]

3.6.4 Comparison between FSC-MPC and other techniques

In this part, we will compare the FSC-MPC to other approaches based on literature research.

The table (3.5) below summarizes this comparison.

Table 3. 5comparison between conventional control and FSC-MPC

	linear control based on PI/modulator[116]	DPC based on switching table[122]	FCS-MPC[121]
Diagram	/		
Control design	PI adjustment + Modulatordesign	Design of lookup table	Cost function definition
The controller's nature	Linear	Nonlinear	Nonlinear
Modulation	PWM/SVM/SHE	Not required	Not required
Switching frequency	Fixed	Variable	Variable(butcontrollable)
Complexity of concept	High with SVM	Simple and intuitive	Simple and intuitive
Steady-state performance	Good in dq frame	Bad	Good in abc, αβ anddq frames
Transientperformance	Medium	Medium	Good
Robustness ofcontroller	bad	bad	Excellent
Stability of controller	reasonable	reasonable	Excellent

In comparison to other traditional methodologies, the research suggests that the FCS-MPC strategy is a simple yet powerful tool for controlling grid-connected VSI systems. However, the FCS-MPC technique has numerous limitations, including variable switching frequency.

3.7 Conclution:

This chapter provides an overview of the most extensively used control approaches for dual-stage grid-connected PV and PEMFC systems.The first half of this chapter presents and compares different maximum power point methods (conventional and advanced) for solar power plants and PEMFC. The benefits and drawbacks of various MPPT algorithms in terms of reaction time, tracking accuracy, and power oscillations are discussed for various renewable sources (PV and PEMFC).Furthermore, the state-of-the-art of DC-linked voltage regulators is examined and compared in terms of performance operating quality, and ease of design.The final section of this chapter describes specifically regulated strategies for three-phase VSI grid-connected systems.The study given in this chapter recommends the Fuzzy MPPT and the FCS-MPC approach as the future command tool for grid-connected renewable sources (PV and PEMFC).

Chapter 4 Control of Grid-Tied PV System/ PEMFC system using FCS-MPC

4.1 Introduction

Currently, the investigation of grid-connected dual stage renewable systems (GRES) represents a crucial field of study. The proliferation of these systems can be attributed to several factors, including heightened energy consumption, the ecological advantages of sustainable energy, and advancements in power electronics converters[123,124]. The primary performance indicators for a Grid-Connected Renewable Energy System (GRES) are the peak power output of the Photovoltaic (PV) and Proton Exchange Membrane Fuel Cell (PEMFC) components, as well as the level of Total Harmonic Distortion (THD) present in the current that is fed back into the electrical grid. The efficacy of a Grid-Connected Renewable Energy System (GRES) is significantly influenced by the selection of the power converter and the control methodology. Nowadays , power converters have gained widespread usage across various applications owing to their enhanced performance and efficiency[125][126]. The implementation of two-level inverters in grid-connected renewable energy system is associated with several drawbacks, including significant ripple, high switching frequency, elevated grid-side filter values, heightened semiconductor switch stress, and a hight of harmonic in the output voltage and current. therefore to overcome the drawbacks mentioned before,many researchers used Multilevel inverters MLI because they represent a highly promising category of power converters, sutch as Neutral point clamped (NPC), cascaded H-bridge, flying capacitor (FC) and F- Type multilevel inverters [127][128].the most comonley stiued is NPC and this topology utilized in the system under consideration has been designed for medium to high power and for the F-Type inverter this topology utilized for the low and medium voltage application. However the primary limitations of said inverters pertain to the imbalanced voltage of the DC-link capacitor and the complicated nature of the control architecture.[129].

In this chapter three-level NPC inverters in grid-connected PV and PEMFC systems to effectively inject the power generated by PV and PEMFC into the grid while maintaining high grid current quality.Also, a 3-level F-type is employed in grid-connected PEMFC systems in order to inject hight produced PEMFC power into the grid with hight current quality.A Fuzzy logic Maximum Power Point Tracking (MPPT) was implemented to control the initial stage with the objective of enhancing the system's efficiency in relation to the accuracy of Maximum Power Point (MPP) tracking, the speed of dynamic response, and the reduction of oscillation at the MPP.The focus of this chapter pertains to the control of the second stage.A finite set control MPC strategy for two steps prediction is introduced containing three

objectives included in one cost function proposed for grid connected PV system NPC and grid connected PEMFCsystem using NPC, a finite Set control MPC also proposed for PEMFC grid connected PEMFC system using F-type , that premite to injected a hight quality current into the grid, ensure the balance of DC-link capacitor voltages and minimize the switching frequency.The effectiveness of the proposed FSC-MPC for two steps (FSC-MPCTS) for 3L-NPC is tested under sudden irradiation for PV grid-connected and pressure change and temperature for PEMFC grid-connected. the proposed FSC-MPC for 3-L F-Type is tested under pressure change and temperature for PEMFC grid-connected through Matlab/Simulink and Simpower packages simulation.

4.2 State of art of grid connected renewable energy systems:

Numerous conventional Maximum Power Point Tracking (MPPT) techniques can be utilized to enhance the energy harvesting capability. These techniques may include: perturbation and observation (P&O)[130], incremental conduction[131] and fractional short-circuit current and current[132].Nonetheless, these tracking techniques exhibit unfavorable limitations such as inadequate precision in Maximum Power Point (MPP) tracking, slow response, and significant fluctuations at the MPP.In recent times, various alterations have been implemented to the traditional Maximum Power Point Tracking (MPPT) algorithms through the utilization of artificial intelligence methodologies, including :Fuzzy logic[71,133], neural networks[134,135], and neuro-fuzzy[18,70] techniques are utilized to deal with those issues. However, the practical implementation of these techniques in extensive systems may pose challenges to the effective implementation of global system control. Additionally, there exist other academic investigations that concentrate on the advancement of Maximum Power Point Tracking (MPPT) algorithms that do not employ artificial intelligence methodologies, such as Voltage-Oriented Loop (VO-MPPT)[136] and Current-Oriented Loop (CO-MPPT)[137].The previously mentioned methodology is executed through the utilization of various current control techniques, including but not limited to conventional PI[138], predictive[136][139], and sliding mode[32] current controllers.

In the second stage, the conventional control classifications are proposed and documented in the literature pertaining to grid-connected NPC inverters.The previous studies explore the utilization of switching tables in the implementation of Virtual flux-oriented DPC (VF-DPC)[140] and direct power control (DPC)[141,142].The complexity of the switching table will increase for inverter cases with higher levels (three or more). Moreover, these techniques fail to produce higher power control efficacy, and voltage-based direct power control (V-DPC)[143].

The finite-control set model predictive control (FCS-MPC) has been the subject of significant study in power Converter control in the past few years[144–146].This approach provides the capability of integrating non-linearities and constraints into the controller design, thus removing the requirement for PI controllers and modulation stages.The FCS-MPC approach has been introduced in various renewable energy system implementations, including both autonomous[147–149] and interconnected systems[150–152].The FCS-MPC has demonstrated superior control performance in comparison with traditional techniques, regardless of the specific application for which it has been utilized, this method is considered to be the most effective for regulating complex PV and PEMFC systems, particularly those utilizing advanced NPC inverters and F-Type inverters , in comparison to alternative control techniques.Where it is feasible to be created and practically implemented. Moreover, the integration of DC-link capacitor voltage balancing into the objective control is simple to do.

4.3 grid connected using three level NPC:

4.3.1 Grid connected PV system:

As depicted in Figure 4.1, the analyzed system comprises a photovoltaic (PV) array, a DC-DC converter operating in boost mode, a three-level neutral-point-clamped (NPC) inverter, and an R-L filter connected to the grid.The Photovoltaic arrays produce electrical energy in proportion to the level of solar irradiation. The buck-boost converter is employed to track and maintain the maximum power point (MPP) and its continuous delivery to the DC link. The current sourced from the buck-boost converter is injected into the grid through the three-level NPC inverter.

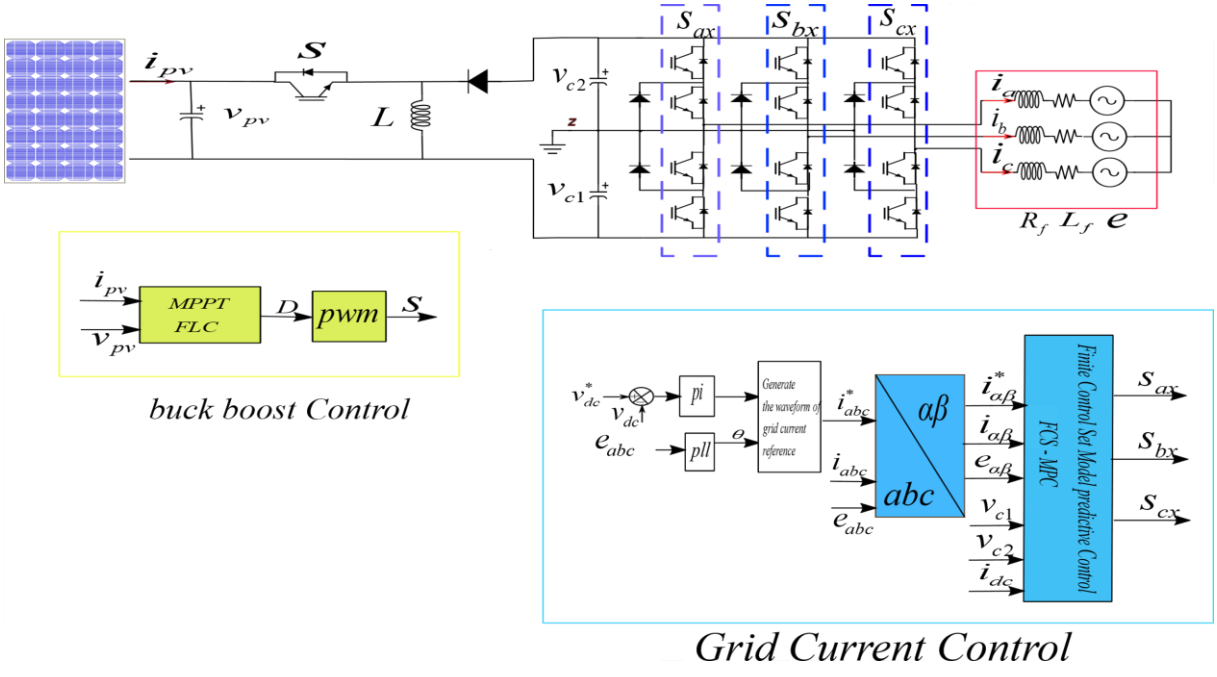

Figure 4. 1globel system of grid connected PV system.

4.3.2 Grid connected PEMFC system:

The provided illustration, indicated in Figure 4.2, depicts a standard fuel cell configuration that is connected to a grid. The fuel cell grid integration system comprises various components, including a Proton Exchange Membrane Fuel Cell (PEMFC), a boost converter equipped with Maximum Power Point Tracking (MPPT) controller, a Direct Current (DC) Link capacitor, a three-phase Neutral Point Clamped (NPC) inverter that is connected to the grid through a Resistor-Inductor (RL) filter.

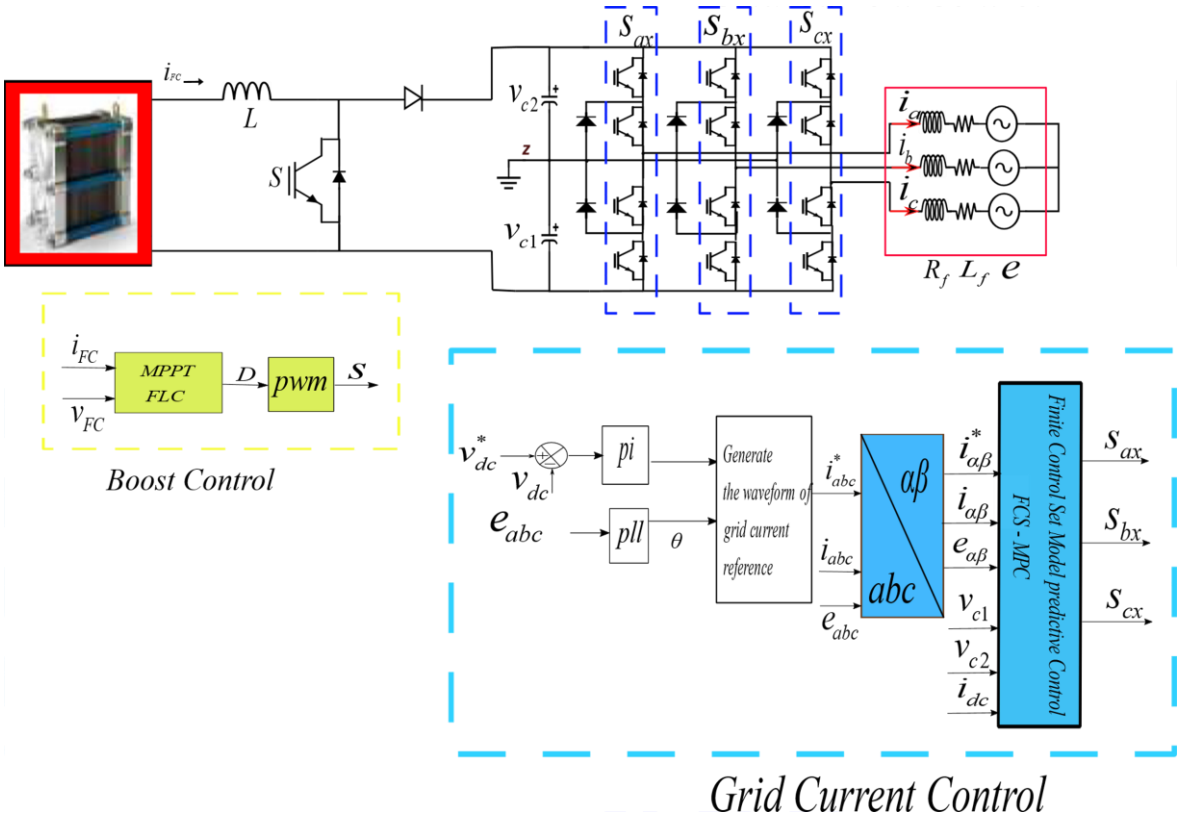

Figure 4. 2globel system of grid connected PV system.

The development of FCS-MPCTS and FCS-MPCC controllers for grid-connected photovoltaic (PV) systems and proton exchange membrane fuel cell (PEMFC) systems utilizing a three-level neutral point clamped (NPC) inverter and F-type inverters depends on the discrete-time representation of power converters. This chapter presents the DC-DC boost converter/buck-boost converter mentioned in Chapter 2,the three-level NPC inverter/F-Type inverters that are connected to the grid.

4.4 Mppt technique and dc link regulator:

The present chapter examines the control approach for grid-tied multilevel inverters. control schemes are utilized to implement the fuzzy logic MPPT technique and conventional DC-link regulator.

- The fuzzy logic Maximum Power Point Tracking (MPPT) technique[150] is utilized to monitor and regulate the maximum power point produced by Photovoltaic (PV) arrays in response to variations in irradiation, as well as Proton Exchange Membrane Fuel Cells (PEMFC) in response to changes in pressure.
- A PI controller, utilizing Ki ,Kp as its parameters, is employed to maintain the DC-link voltage at a stable level and to produce the grid current reference[153] as represented in figure below:

The adjustment of the reference DC link voltage is achieved via the grid voltage amplitude V_{max} :

$$v_{dc}^{*} > \sqrt{3}V_{\max} \tag{4.1}$$

- A FCS-MPC tow step prediction controller is proposed to control the grid-tied three-level NPC inverter.

4.5 Grid tied three level NPC inverter model:

Figure 4.4 depicts the configuration of a three-level inverter NPC that is linked to the grid via an inductive filter *L*f, which includes a parasitic resistor *R*f. therefore The inverter is responsible for controlling the DC-link voltage (Vdc), DC-link capacitor voltages (Vcx), and the Ia, ib, and ic currents. Table 4.1 displays the switching states that produce a three-level voltage at the output of the inverter in a single phase. The three-level Neutral Point Clamped (NPC) inverter produces a total of 27 switching states across three phases, resulting in 19 voltage vectors, as depicted in Figure 4.3.

Table 4. 1switching state for one phase of the three-level NPC inverter.

Voltage level	**Switching state**			
	S_{1x}	**S_{2x}**	**S_{3x}**	**S_{4x}**
V_{dc}	1	1	0	0
$V_{dc/2}$	0	1	1	0
0	0	0	1	1

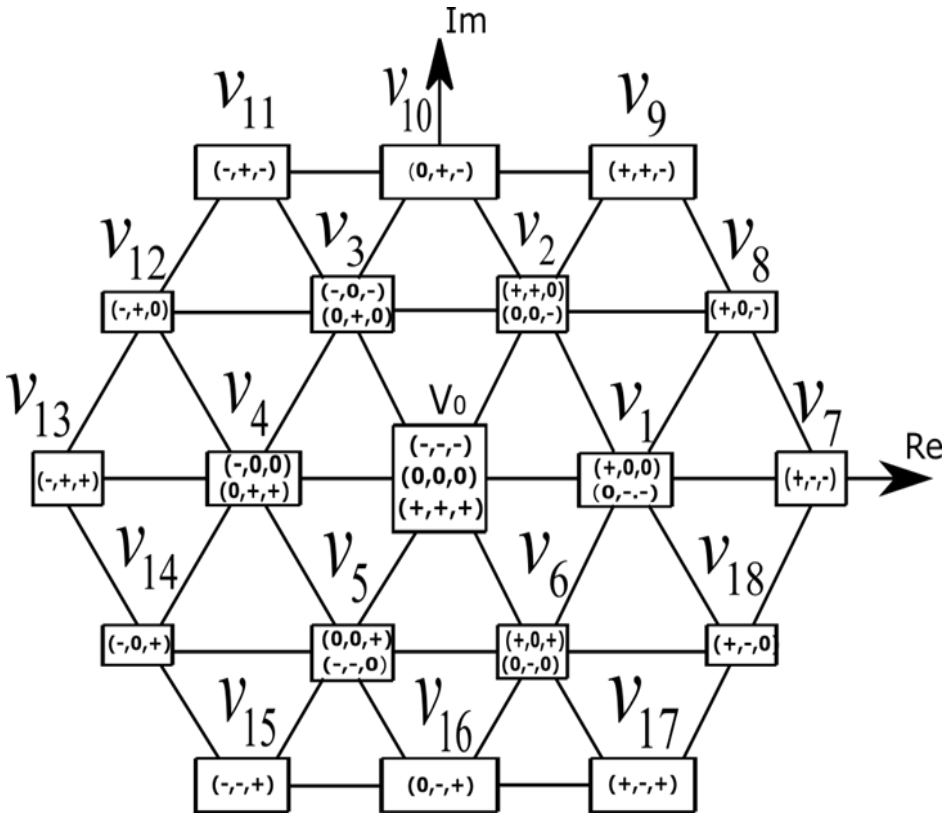

Figure 4. 3voltage vectors of three-level NPC in αβ stasionary[154]

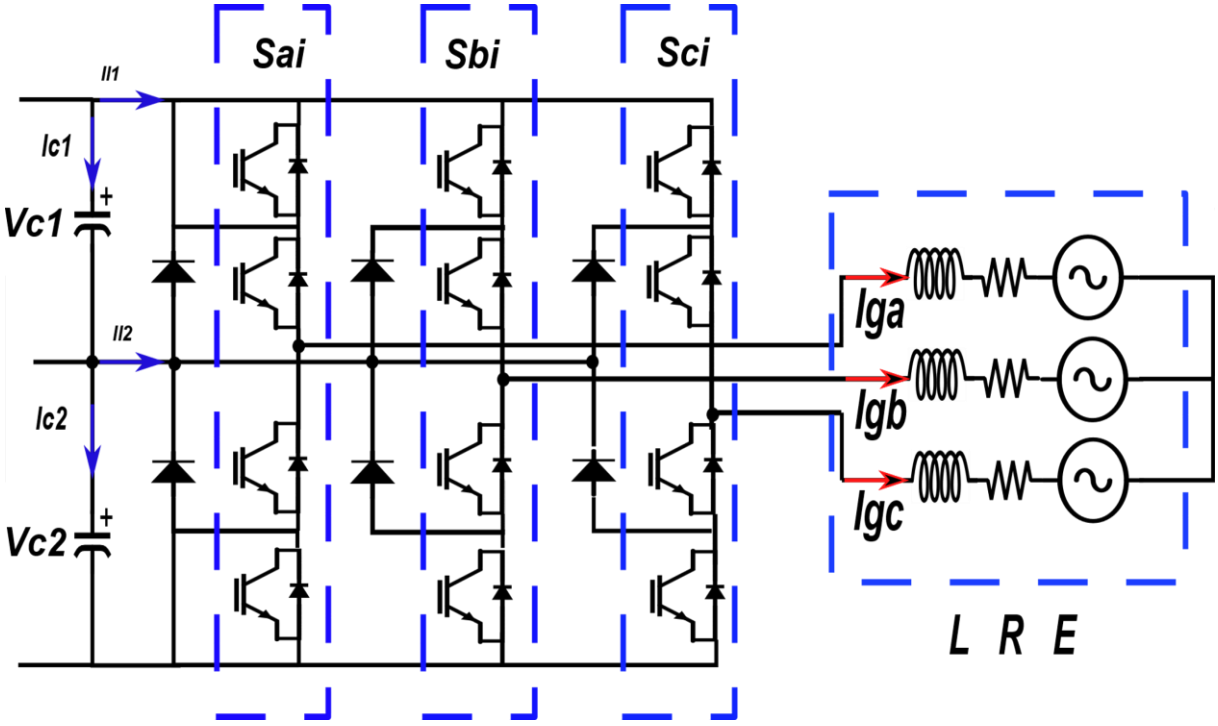

Figure 4. 4topology of three level NPC.

4.5.1 Modeling of grid currents in the synchronous frame:

Regarding Figure 4.4, it is observed that the current in the natural frame abc can be mathematically modeled and represented[155]:

$$\frac{di_g(t)}{dt} = \frac{1}{L}\left[V - v_g - Ri_g\right] \tag{4.2}$$

The equation representing the relationship between the grid current (ig), voltage vectors generated by the three-level NPC inverter (V), grid voltage (vg), and filter value parameters (Rf, Lf).

Form equation 4.2 the grid currents in frame αβ can be write as follow :

$$\begin{cases} \frac{di_{g\alpha}(t)}{dt} = \frac{1}{L}\left[V_\alpha - v_{g\alpha} - Ri_{g\alpha}\right] \\ \frac{di_{g\beta}(t)}{dt} = \frac{1}{L}\left[V_\beta - v_{g\beta} - Ri_{g\beta}\right] \end{cases} \tag{4.3}$$

Where $V\alpha, V_\beta$ are the voltage vectors gererated by the inverter in stationary frame αβ as shwen in figure (4.3).

The discrete-time model of Equation 4.2 can be obtained through the application of the Euler forward method[155] :

$$\frac{di(t)}{dt} \approx \frac{i(k+1) - i(t)}{Ts} \tag{4.4}$$

$$\begin{cases} i_\alpha(k+1) = \frac{T_s}{L}\left[V_\alpha(k) - v_{g\alpha}(k) - Ri_{g\alpha}(k)\right] + i_a(k) \\ i_\beta(k+1) = \frac{T_s}{L}\left[V_\beta(k) - v_{g\beta}(k) - Ri_{g\beta}(k)\right] + i_\beta(k) \end{cases} \tag{4.5}$$

The second prediction horizon for equation (4.5) can be expressed:

$$\begin{cases} i_\alpha(k+2) = \frac{T_s}{L}\left[V_\alpha(k+1) - v_{g\alpha}(k+1) - Ri_{g\alpha}(k+1)\right] + i_a(k+1) \\ i_\beta(k+2) = \frac{T_s}{L}\left[V_\beta(k+1) - v_{g\beta}(k+1) - Ri_{g\beta}(k+1)\right] + i_\beta(k+1) \end{cases} \tag{4.6}$$

4.5.2 Modeling of DC-link capacitor voltages:

The voltage model of DC-link capacitors can be expressed as an equation that relates to the currents of the DC link capacitors, denoted as i_{cx}[156].

$$\frac{dv_{cx}}{dt} = \frac{1}{C} i_{cx} \qquad x = 1, 2 \tag{4.7}$$

Where C is the value of capasitor.

The currents of the capacitors can be mathematically expressed as demonstrated in Figure 4.4. When the capacitors are charged to equal energy levels, the direct current (i_{dc}) flowing through the circuit becomes zero.

$$\begin{cases} i_{c1} = -i_{l1} \\ i_{c2} = i_{c1} - i_{l2} \end{cases} \tag{4.8}$$

From equation 4.7 The discrete-time model for DC-link capacitor voltages can be expressed[154]:

$$v_{cx}(k+1) = v_{cx}(k) + \frac{T_s}{C} i_{cx}(k) \tag{4.9}$$

The second prediction horizon for equation (4.9) can be expressed:

$$v_{cx}(k+2) = v_{cx}(k+1) + \frac{T_s}{C} i_{cx}(k+1) \tag{4.10}$$

4.5.3 Fuzzy logic MPPT technique:

The primary advantages of utilizing a Fuzzy Logic Controller (FLC) for accurately tracking the Maximum Power Point (MPP) are its simplicity and robustness[157]. The FLC comprises three constituent parts, namely the fuzzification module, fuzzy inference engine, and defuzzification module[72], as illustrated in the figure 4.5.

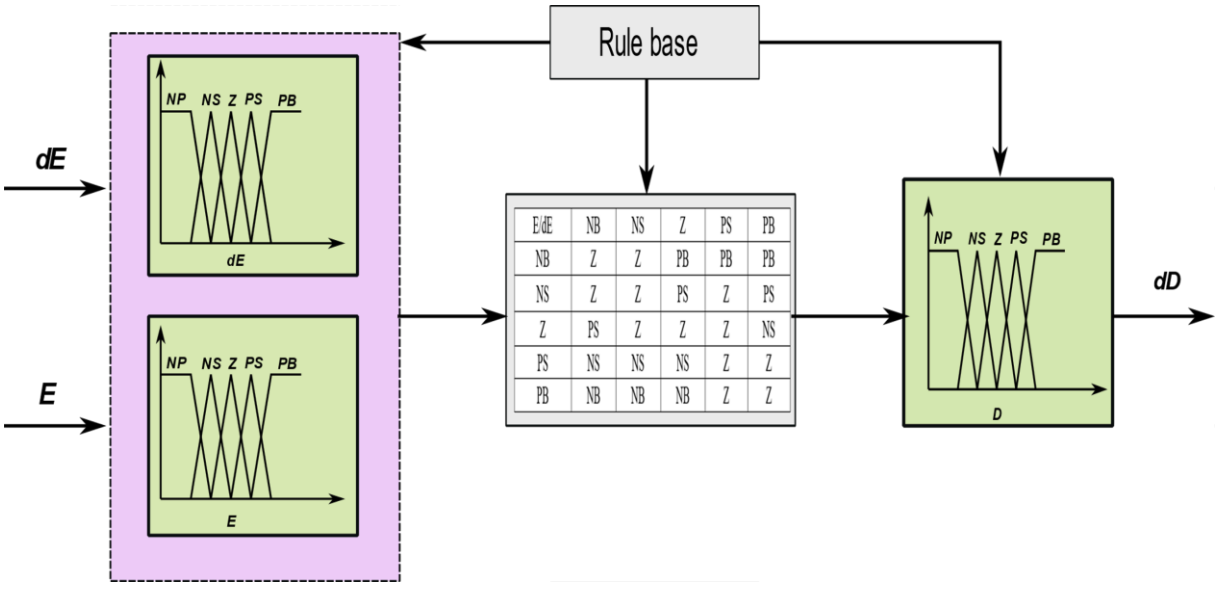

Figure 4. 5fizzy logic membership

Fuzzification involves the conversion of numerical input variables into linguistic variables through the use of membership functions (MFs).To attain the MPP, it is necessary to measure the voltage and current of the photovoltaic (PV) system or the proton exchange membrane

fuel cell (PEMFC) for the purpose of computing the output power[158,159].The proposed controller is implemented using two input control variables, namely the error (E(k)) and the change of error (CE(k)) at the instant samplingk

$$\begin{cases} E(k) = \dfrac{P_{pv/fc}(k) - P_{pv/fc}(k-1)}{I_{pv/fc}(k) - I_{pv/fc}(k-1)} \\ CE(k) = E(k) - E(k-1) \end{cases} \tag{4.11}$$

Regarding the topic of inference. By applying a rule within the inference engine, it is possible to derive a fuzzy output. Prior to the implementation of the rule, it is necessary to fuzzify the actual input value in order to attain an appropriate linguistic value. The attainment of the maximum power point (MPP) is facilitated by the utilization of a rule table containing 49 rules within the structure of the fuzzy controller. Table 2.1 in Chapter 2 illustrates the FLC rule table. The matrix entries in this table comprise E, DE, and ΔD.Through the process of defuzzification, the output of a fuzzy logic controller is converted from a linguistic variable into a numerical variable.

4.6 FCS-MPCTS algorithm for grid tied three-level NPC inverter:

In order to ensure high grid current quality for the produced PV power and PEMFC system, precise control of the three-level NPC inverter is necessary. This control must take into consideration the balancing of DC-link capacitor voltages. The proposed approach involves utilizing the two-step model predictive control for FCS MPCTS. The algorithm proposed in this study is implemented for the purpose of controlling a three-level Neutral Point Clamped (NPC) inverter. The objectives of the proposed algorithm are as follows:

- Ensure that the grid current values, namely $ig\alpha$, and $ig\beta$. track the reference current $ig\alpha\_ref$, and $ig\beta\_ref$, which are provided by the DC link voltage control,
- Maintain the state of balance of the two DC-link capacitor voltages under irradiation changes in the photovoltaic (PV) system and variations in temperature and pressure in the proton exchange membrane fuel cell (PEMFC) system.
- Reduce the switching frequency.

The previously mentioned goals are included within the cost function, which is explicitly defined as:

$$g = \left|(i_{g\alpha-ref} - i_{g\alpha}(k+2)\right| + \left|(i_{g\beta-ref} - i_{g\beta}(k+2)\right| + \lambda_{dc}\left|v_{c1}(k+2) - v_{c2}(k+2)\right| + \lambda_s\left|SW_a + SW_b + SW_c\right| \tag{4.12}$$

The terms of coste function are described as follow [156]:

- The $i_{\alpha\text{-ref}}$and$i_{\beta\text{-ref}}$are the imaginary and the real of the reference grid current generated by the PI controller according to the PV/PEMFC power.

- $ig\alpha(k+2)$ and $ig\beta\ (k+2)$ are the predicted grid currents in the αβ frame. After measuring the instantaneous grid currents, and calculating from Equation (4.6).
- The expression $Vc1(k+2)\ \ Vc2(k+2)$ represents the anticipated voltages of the DC-link capacitors from Equation 4.10 it requires measuring the grid currents measured in a natural frame (abc) to facilitate the computation of forthcoming DC-link capacitor voltage trends.
- The SWxis the difference between the number of three level NPC inverter switch commutations.
- λdc and λs represent the weighting factors utilized for achieving DC-link capacitor voltage balance and minimizing switching frequency, respectively.

The cost function g is evaluated for all 27 possible switching states after computing the future behaviors of $ig\alpha-\beta$ currents and DC-link capacitor voltages based on the measured grid currents and voltages, along with the two DC-link capacitor voltages.The selection and application of the switching state that minimizes the cost function occurs in the subsequent sampling time. Figure 4.6 provides a summary of the functioning of the proposed FCS-MPCTS.

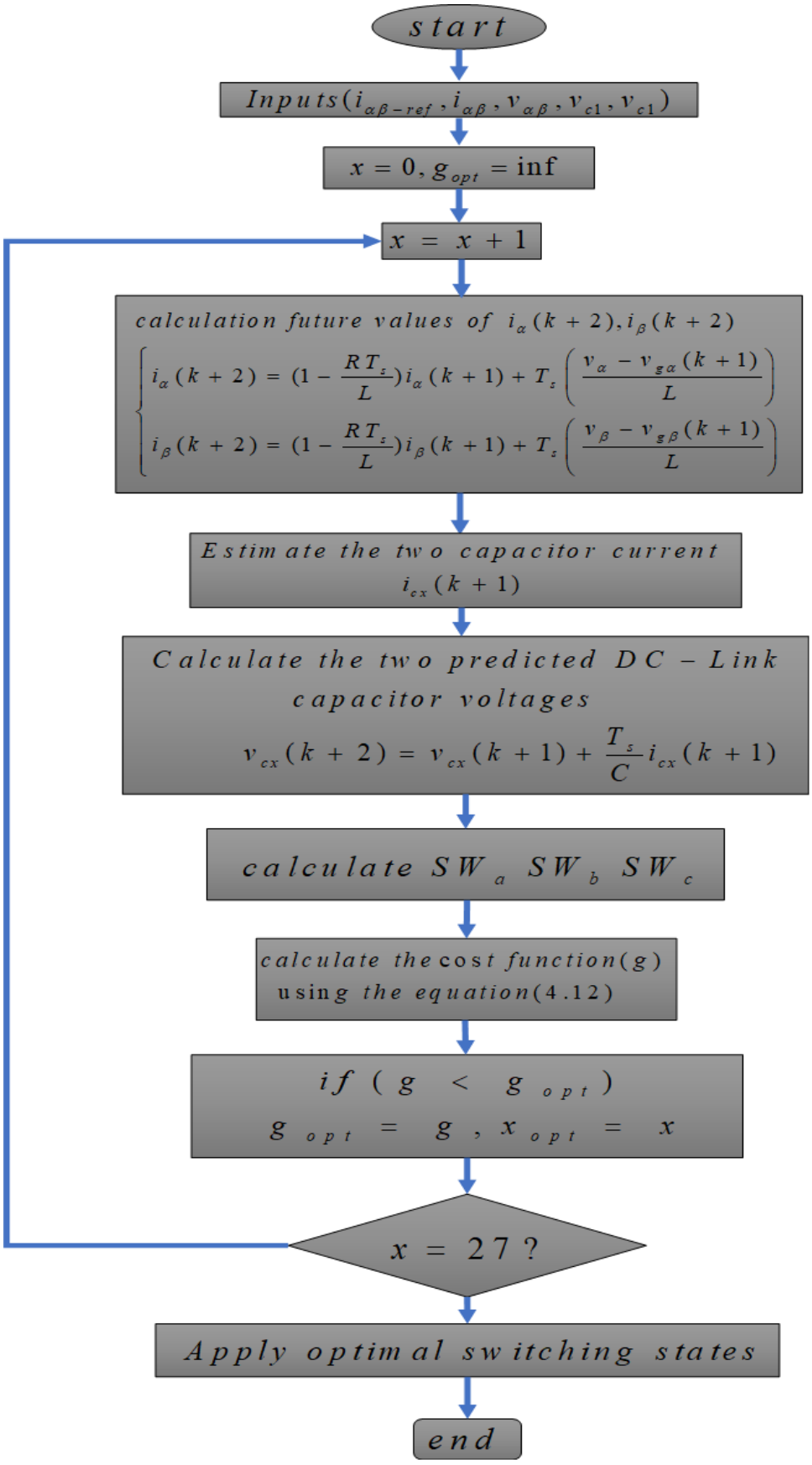

Figure 4. 6 Flowchart of the proposed FSC-MPCTS.

4.7 Grid tied single phase F-Type inverter model:

Figure 4.7 depicts the configuration of a three-level single phase F-Type inverter that is linked to the grid via an inductive filter L_f, which includes a parasitic resistor R_f.therefore The inverter is responsible for controlling the DC-link voltage (V_{dc}), DC-link capacitor voltages (V_{cx}), and the current Ia.Table 4.2 displays the switching states that produce a three-level voltage at the output of the inverter in a single phase.The three-level single phase F-Type inverter produces a total of 9 switching states across single phase.

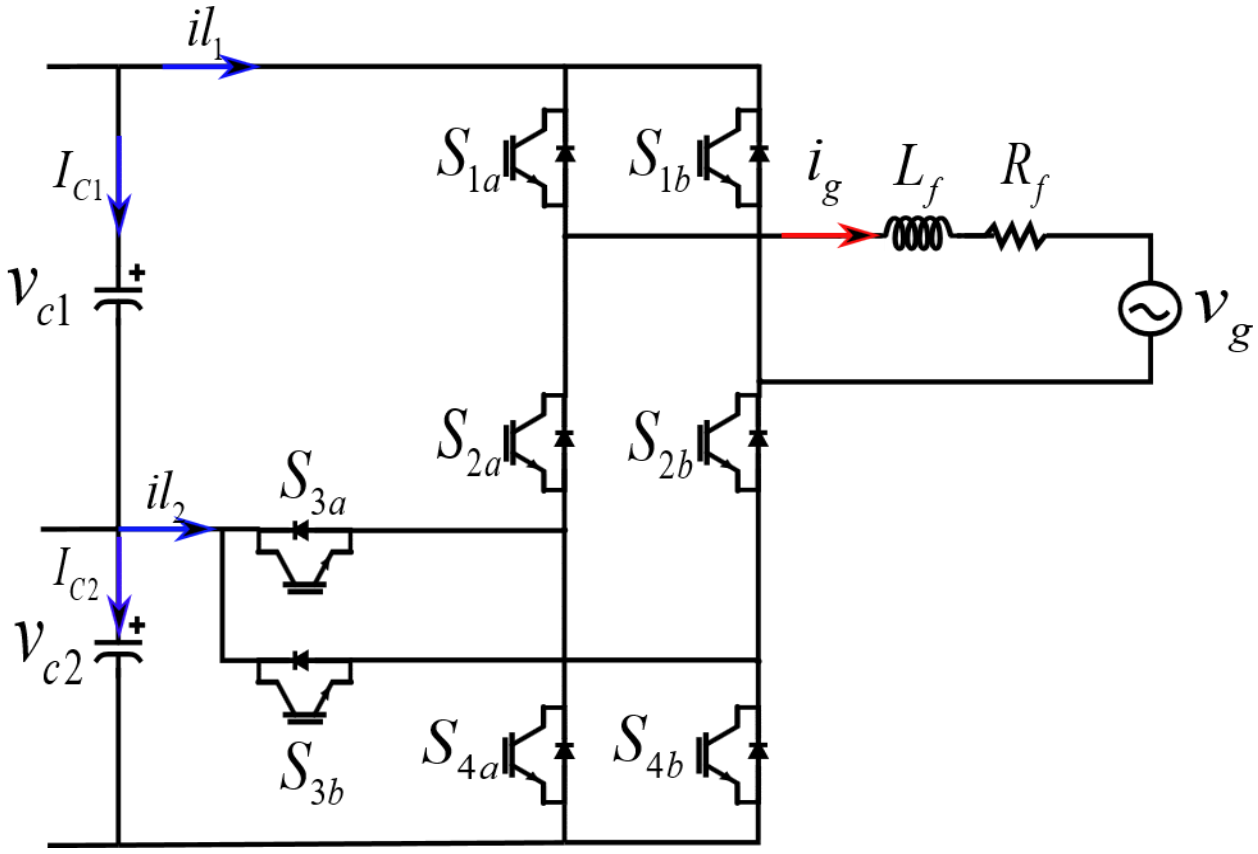

Figure 4. 7configuration of a three-level single phase F-Type inverter.

Table 4. 2The voltage of the inverter's output during switching states.

states	$S_{1a}\ \overline{S_{2a}}$	$S_{3a}\ \overline{S_{4a}}$	$S_{1b}\ \overline{S_{2b}}$	$S_{3b}\ \overline{S_{4b}}$	**V_{ab}**
0	1	1	1	1	0
1	1	1	0	1	Vc1
2	0	1	0	0	Vc2
3	1	1	0	0	Vc1+Vc2)
4	0	1	0	1	0
5	0	1	1	1	0
6	0	0	0	1	-Vc1
7	0	0	1	1	-Vc2
8	0	0	0	0	-(Vc1+Vc2)

4.7.1 Modeling of grid currents in the synchronous frame

Regarding Figure 4.7, it is observed that the current be mathematically modeled and represented:

$$\frac{di_{ga}(t)}{dt} = \frac{1}{L}\left[V - v_{ga} - Ri_{ga}\right] \quad (4.13)$$

The equation representing the relationship between the grid current (ig), voltage vectors generated by the three-level single phase F-Type inverter (V), grid voltage (vg), and filter value parameters (Rf, Lf). The discrete-time model of Equation 4.13 can be obtained through the application of the Euler forward method :

$$i_g(k+1) = i_g(k)(1 - T_s\frac{R}{L}) + \frac{T_s}{L}(V - v_g) \quad (4.14)$$

4.7.2 Modeling of DC-link capacitor voltages

The voltage model of DC-link capacitors can be expressed as an equation that relates to the currents of the DC link capacitors, denoted as i_{cx}:

$$\frac{dv_{cx}}{dt} = \frac{1}{C}i_{cx} \qquad x = 1, 2 \quad (4.15)$$

Where C is the value of capasitor.

The currents of the capacitors can be mathematically expressed as demonstrated in Figure 4.7.When the capacitors are charged to equal energy levels, the direct current (i_{dc}) flowing through the circuit becomes zero.

$$\begin{cases} i_{c1} = -i_{l1} \\ i_{c2} = i_{c1} - i_{l2} \end{cases} \quad (4.16)$$

From equation 4.15 The discrete-time model for DC-link capacitor voltages can be expressed:

$$v_{cx}(k+1) = v_{cx}(k) + \frac{T_s}{C}i_{cx}(k) \quad (4.17)$$

4.8 FCS-MPCC algorithm for grid tied three-level single phase F-Type inverter

In order to ensure high grid current quality for the produced PEMFC system power, precise control of the three-level single phase F-Type inverter is necessary. This control must take into consideration the balancing of DC-link capacitor voltages. The proposed approach involves utilizing model predictive control for FCS MPCC. The algorithm proposed in this study is implemented for the purpose of controlling a three-level single phase F-type inverter. The objectives of the proposed algorithm are as follows:

- Ensure that the grid current values, namely ig track the reference current ig_ref, which are provided by the DC link voltage control,
- Maintain the state of balance of the two DC-link capacitor voltages variations in temperature and pressure in the proton exchange membrane fuel cell (PEMFC) system.

The previously mentioned goals are included within the cost function, which is explicitly defined as:

$$g = \left| i_{g-ref} - i_g(k+1) \right| + \lambda_{dc} \left| V_{C1}(k+1) - V_{C2}(k+1) \right| \quad (4.18)$$

The terms of coste function are described as follow :

- The $i_{g\text{-}ref}$the reference grid current generated by the PI controller according to the PEMFC power.
- $(k + 1)$ is the predicted grid currents. After measuring the instantaneous grid currents, and calculating from Equation (4.14).
- The expression $Vc1(k + 1)$ $Vc2(k + 1)$ represents the anticipated voltages of the DC-link capacitors from Equation 4.17 it requires measuring the grid current measured to facilitate the computation of forthcoming DC-link capacitor voltage trends.
- represent the weighting factors utilized for achieving DC-link capacitor.

The cost function g is evaluated for all 9 possible switching states after computing the future behaviors of ig current and DC-link capacitor voltages based on the measured grid currents and voltages, along with the two DC-link capacitor voltages.The selection and application of the switching state that minimizes the cost function occurs in the subsequent sampling time. Figure 4.8 provides a summary of the functioning of the proposed FCS-MPCC.

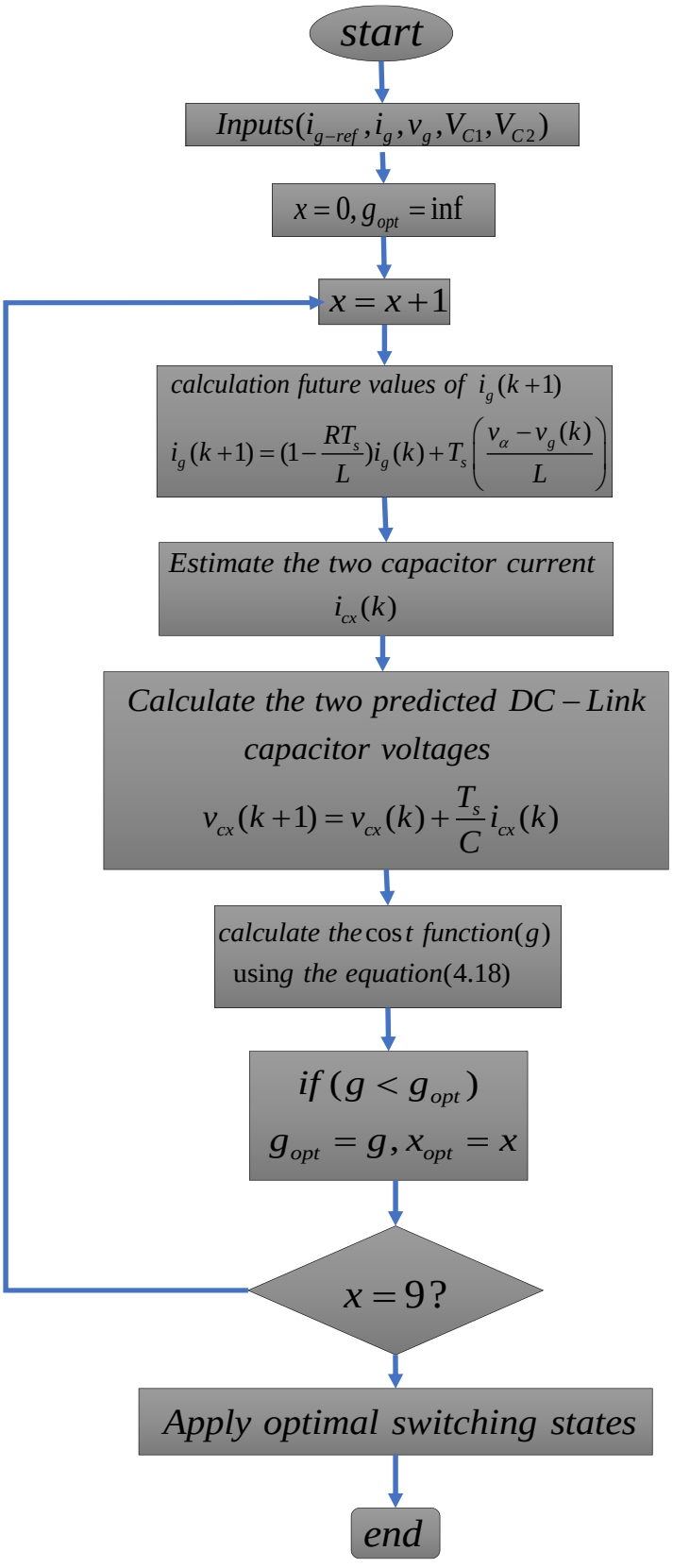

Figure 4. 8flowchart of FSC-MPCC.

4.9 Results and analysis:

4.9.1 FCS-MPCTS for Grid-Connected PV using three-Level NPC-Inverter:

The proposed system was simulated utilizing MATLAB/Simulink and Simpower system packages. The settings for PV, buck-boost converter, and the Rg, Lg filter were presented in

Table 4.3.The evaluation of system performance is conducted under specific conditions, namely a constant temperature of 25°C, sudden shifts, and constant levels of solar irradiation.

Table 4. 3proposed system parematres.

PV prametres	
Power max (P_{MPP})	60 W
Votage (V_{MPP})	17.1 V
Current I_{MPP}	3.5 A
Open circuit voltage V_{oc}	21.1 V
Short circuit current I_{sc}	3.8 A
Parallel Cells	1
Series Cells	36
Parallel Modules	2
series Modules	5
Bock-Boost converter electrical parameters	
Input capasitor C_{in}	
Inductore L	
DC-link capasitors C_1=C_2	2100µF
Grid parameters	
Grid peak voltage	50V
Grid inductance L_f	10mH
Grid resistance R_g	0.1Ω
Grid frequency F_g	50HZ
Simulation parameters	
Sampling time T_s	5µs

In this section, the efficacy of the suggested control scheme will be demonstrated through a demonstration of its improvement. The objective of this study is to demonstrate the efficacy of the suggested control technique utilizing FCS-MPCTS in improving DC-link capacitor voltage balancing, and grid current THD%.

The impact of irradiation on the results depicted in Figures 4.9 to 4.13 were examined through numerical simulations carried out via Matlab/Simulink and Simpower system packages. The grid-connected photovoltaic system was equipped with a three-level NPC inverter and utilized a control scheme based on FCS-MPCTS.

As illustrated in Figures 4.9 a sudden drop in solar irradiation from 800 to 700 W/m² is implemented at a specific moment of 1.5 seconds. The fuzzy logic MPPT achieves the new maximum power point in an immediate way, without any deviation as depicted in figure 4.10. Furthermore, the aforementioned alteration results in an undershoot and a short rise time in

the voltage across the capacitor (Vdc) in relation to its reference, as depicted in Figure 4.11.Figure 4.12 demonstrate a decrease in grid currents and their maintenance in a sinusoidal form.

Subsequently, a sudden rise in solar irradiation, from 700 to 1000 W/m², occurred at time point 3 seconds. The fuzzy logic (MPPT) technique demonstrates quick and precise tracking of the Maximum Power Point (MPP). Despite the presence of overshoot and settling time in the voltage deviation from its reference, as depicted in figure 4.10 and 4.11.also the Figure 4.12 the grid current increase and kept its sinusoidal. form.next a sudden deacrise in sollar irradiation from 1000 to 900 W/m² at 4s in this case fuzzy logic reache the MPPT quikley Despite the presence of undershoot and settling time in the voltage deviation from its reference, as depicted in figures 4.10 and 4.11 also, the Figure 4.12 the grid current increased and is kept sinusoidal.

We utilized the (FFT) to estimate the harmonic magnitude of the three-phase (a, b, c and d) to compute the THD. Figures (4.13,a), (4.13,b), (4.13,c) and (4.13.d) depicts obtained THD results of the PV grid-connected system with 3L-NPC using tow- step current prediction for irradiance ($800W/m^2, 700W/m^2, 1000W/m^2, 900W/m^2$) respectively, the THD is around 2.15% for $800W/m^2$, 2.35% for $700W/m^2$, 2.03% for $1000W/m^2$ and 2.10% for $900W/m^2$ we summary the result in the table 4.4. Analysis between THD result for all irradiance cases show the method of MPC current control for tow-step horizon provide high grid current quality under the irradiation changes cases according to the international standers (THD<5%)

Table 4. 4Obtained THD under irradiation levels

G(w/m2)	$800W/m^2$	$700W/m^2$	$1000W/m^2$	$900W/m^2$
THD %	2.15%	2.35%	2.03%	2.10%

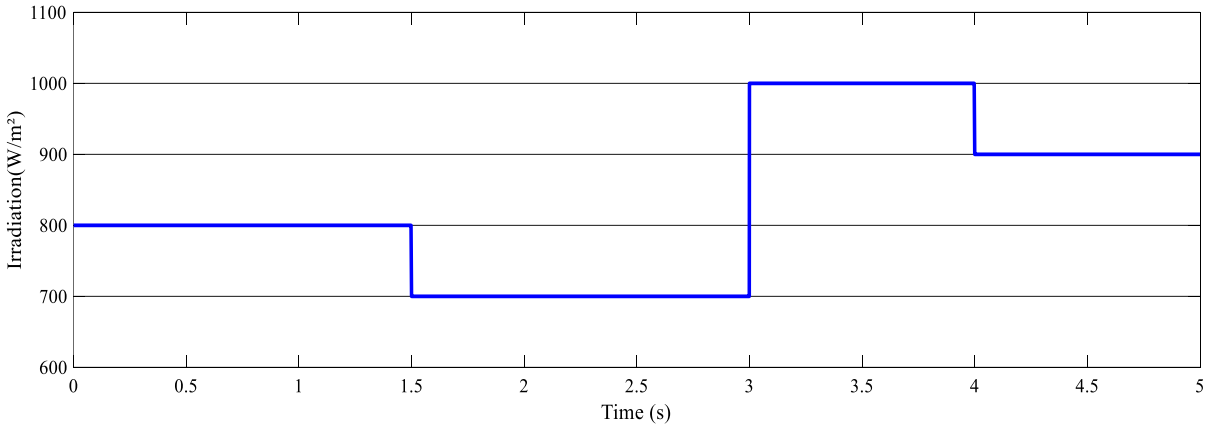

Figure 4. 9Irradiance profile.

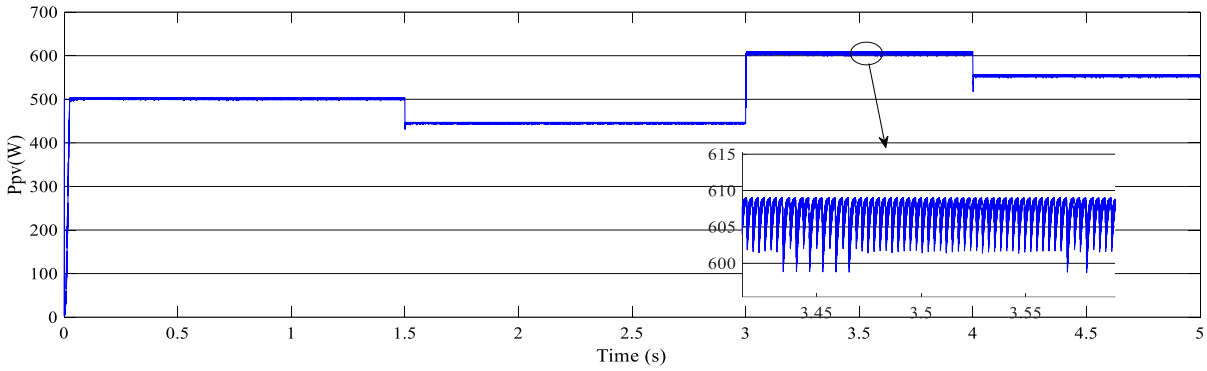

Figure 4. 10 Power of PV system connected to 3L-NPC under irradiance changes.

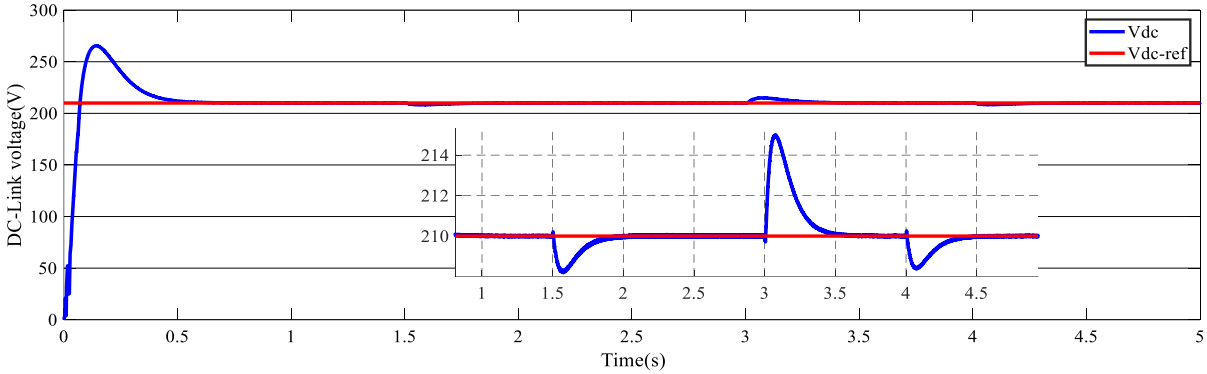

Figure 4. 11DC-link voltage with reference.

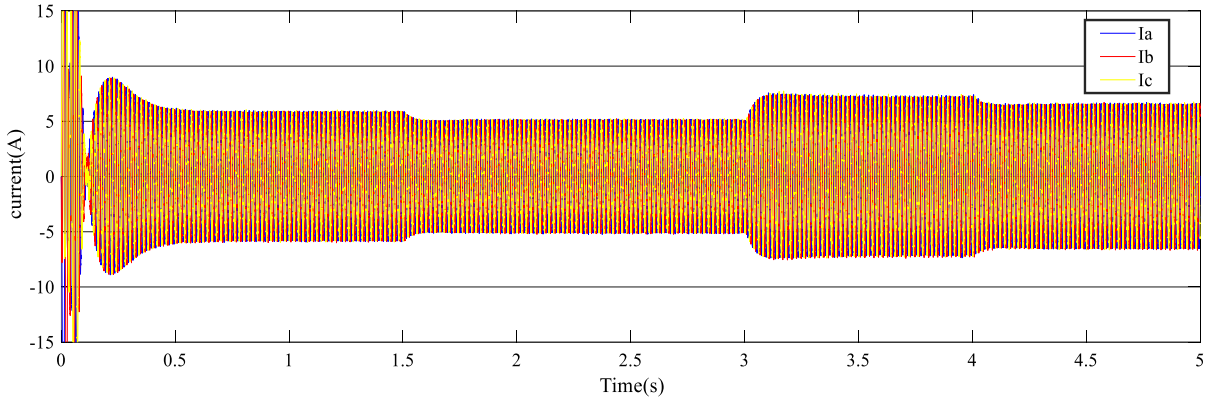

(a)

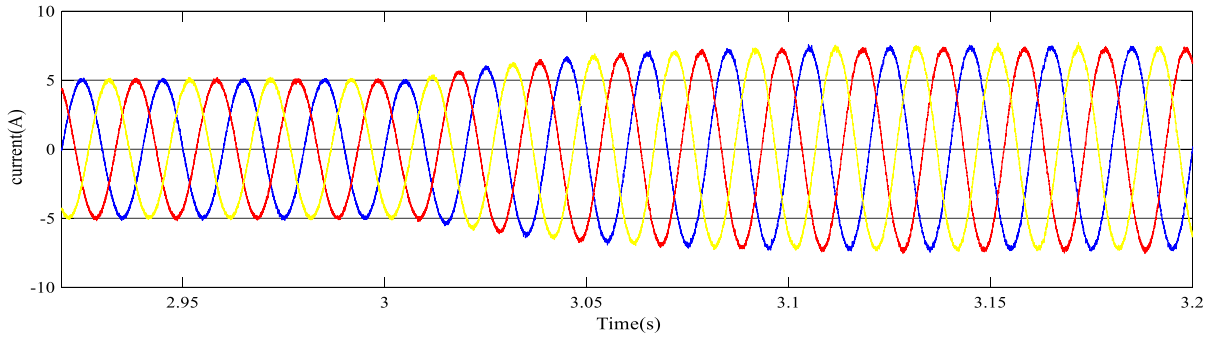

(b)

Figure 4. 12 (a) Grid current injected into the grid (b) zoom of grid current.

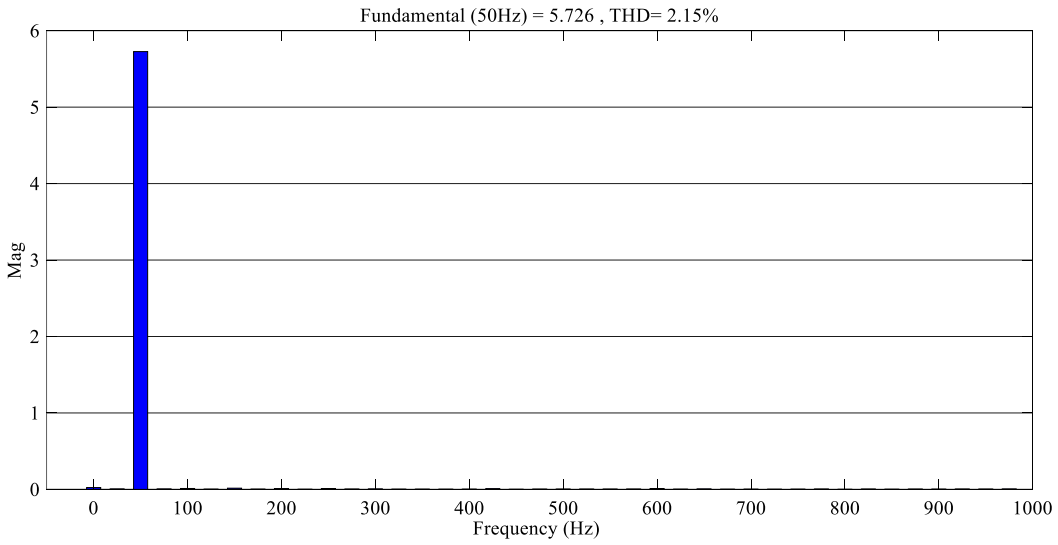
Fundamental (50Hz) = 5.726 , THD= 2.15%
Mag
Frequency (Hz)
0
1
2
3
4
5
6
0
100
200
300
400
500
600
700
800
900
1000

(a)

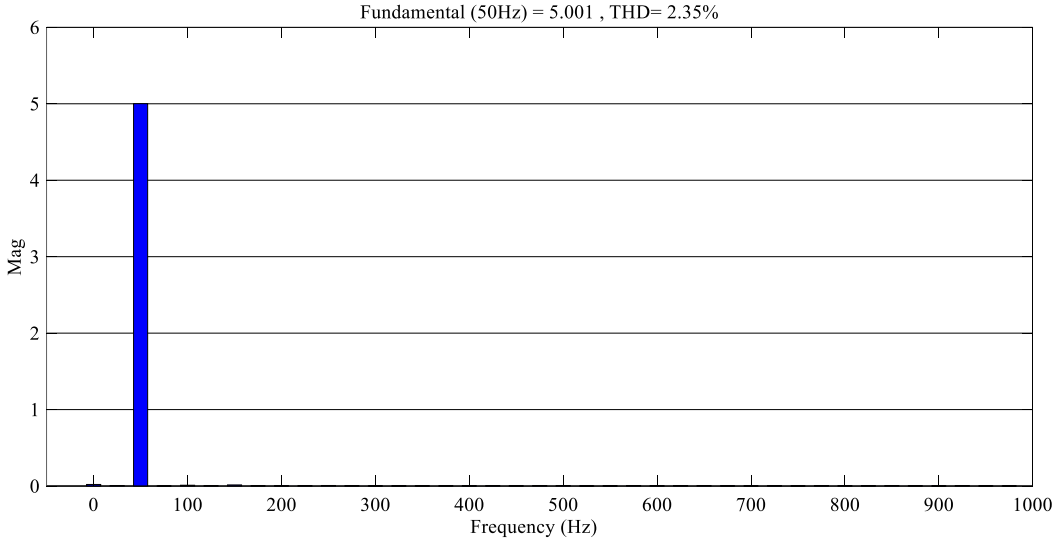
Fundamental (50Hz) = 5.001 , THD= 2.35%
Mag
Frequency (Hz)
0
1
2
3
4
5
6
0
100
200
300
400
500
600
700
800
900
1000

(b)

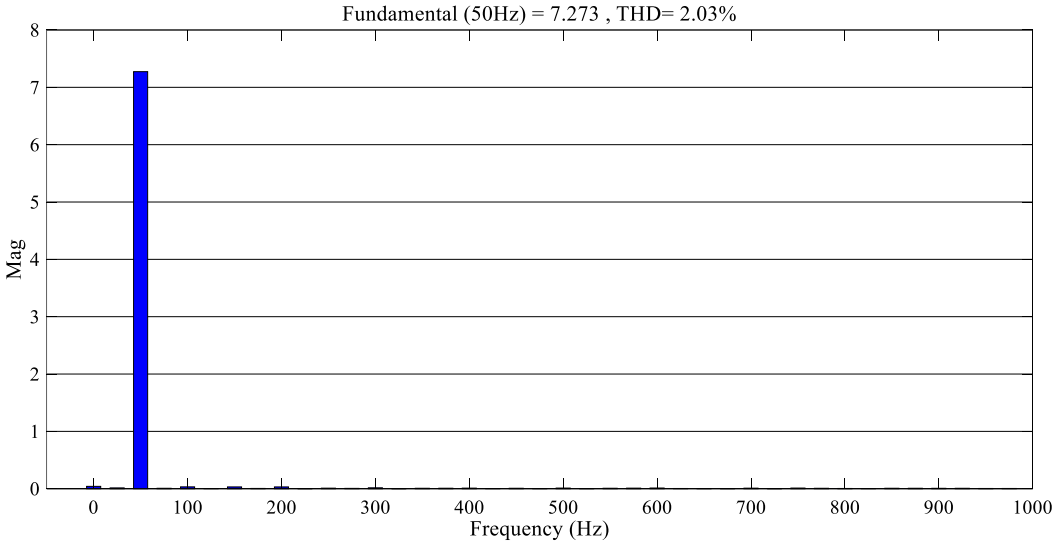
Fundamental (50Hz) = 7.273 , THD= 2.03%
Mag
Frequency (Hz)
0
1
2
3
4
5
6
7
8
0
100
200
300
400
500
600
700
800
900
1000

(c)

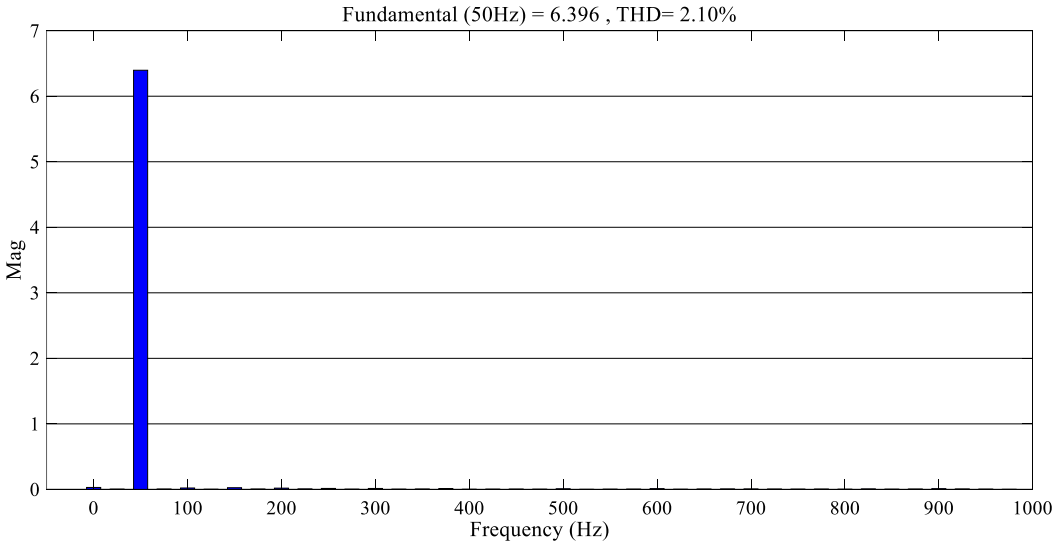

(d)

Figure 4. 13THD of grid current (a)800w/m2 (b)700w/m2 (c)1000w/m2 (d)900w/m2.

4.9.2 FCS-MPCTS for Grid-Connected PEMFC using three-Level NPC-Inverter:

The proposed system was simulated utilizing MATLAB/Simulink and Simpower system packages. The settings for PEMFC, boost converter, and the Rg, Lg filter were presented in Table 4.5.The evaluation of system performance is conducted under specific conditions.

Table 4. 5proposed system parematres

PEMFC prametres	
A	$70cm^2$
S	136
δ_1	0.994
δ_2	0.00354
δ_3	$7x10^{-8}$
δ_4	$1.96x10^{-4}$
λ	12
J_{max}	$1.7cm^{-2}$
Bock-Boost converter electrical parameters	
Inductore L	0.2H
DC-link capasitors C_1=C_2	3800µF
Grid parameters	
Grid peak voltage	50V
Grid inductance L_f	10mH
Grid resistance R_g	0.1Ω
Grid frequency F_g	50HZ
Simulation parameters	
Sampling time T_s	4µs

The efficacy of the suggested control scheme will be demonstrated through a demonstration of its improvement. The objective of this study is to demonstrate the efficacy of the suggested control technique utilizing FCS-MPCTS in improving DC-link capacitor voltage balancing, and grid current THD%. The influence of temperature and pressure on the outcomes illustrated in Figures 4.14 to 4.23 was investigated by means of computational modeling conducted using Matlab/Simulink and Simpower system software. The perfect system that was connected to the grid was equipped with a three-level Neutral Point Clamped (NPC) inverter and implemented a control strategy that relied on Finite Control Set Model Predictive Control with Two-Step (FCS-MPCTS).

We tested the proposed algorithm based on two scenarios:

- **scenario 1:**fast fariation in PEMFC temperature.
- **scenario 2**: fast variation in temperature and pressure.

4.9.2.1 Scenario 1: fast fariation in PEMFC temperature:

In the first scenario, the objective was to evaluate the Fuzzy Logic Control (FLC) and the proposed FCS-MPCTS techniques. The partial pressures of Pa and Pc were kept constant at 2 atm, while the temperature of the Proton Exchange Membrane (PEM) fuel cell was varied.

A suddens changes in the temperature of the fuel cell happens as depicted in Figure (4.14). Initially, the system is observed to operate at a temperature of 305K within the time interval of [0,2s]. Subsequently, the temperature is elevated to 355K within the time interval of [2s,4s], followed by a decrease in temperature to 325K within the time interval of [4s,5s].

As illustrated in Figures 4.14 a sudden rise in PEMFC tempurture from 305k to 355k is implemented at a specific moment of 2 seconds. The fuzzy logic MPPT achieves the new maximum power point in an immediate way and with lass fulctiation, without any deviation. Moreover, the previously mentioned change leads to a deficiency in voltage across the capacitor (Vdc) in comparison to its reference, accompanied by a brief increase in time, as illustrated in Figure 4.15 and 4.16. The graphical representations depicted in Figures 4.17 exhibit a rise in grid currents and their consistent preservation in a sinusoidal form.

next asudden decrease in temperature, from 355 to 325k occurred at the time point of 4 seconds. The fuzzy logic (MPPT) technique demonstrates quick and precise tracking of the Maximum Power Point (MPP). Despite the presence of undershoot and settling time in the voltage deviation from its reference, as depicted in figures 4.15 (c) and 4.16 (c). Furthermore,

in Figure 4.17, it can be observed that the grid current experienced an increment while maintaining its sinusoidal waveform.

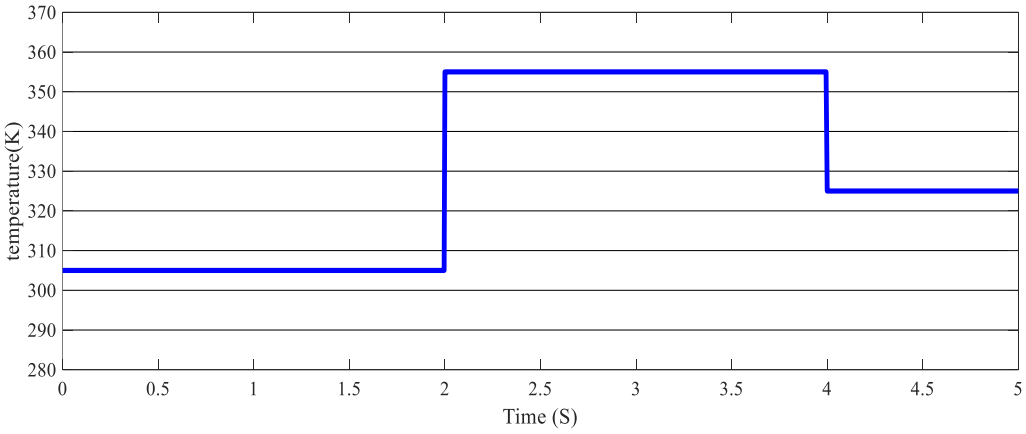

Figure 4. 14Temperature profile.

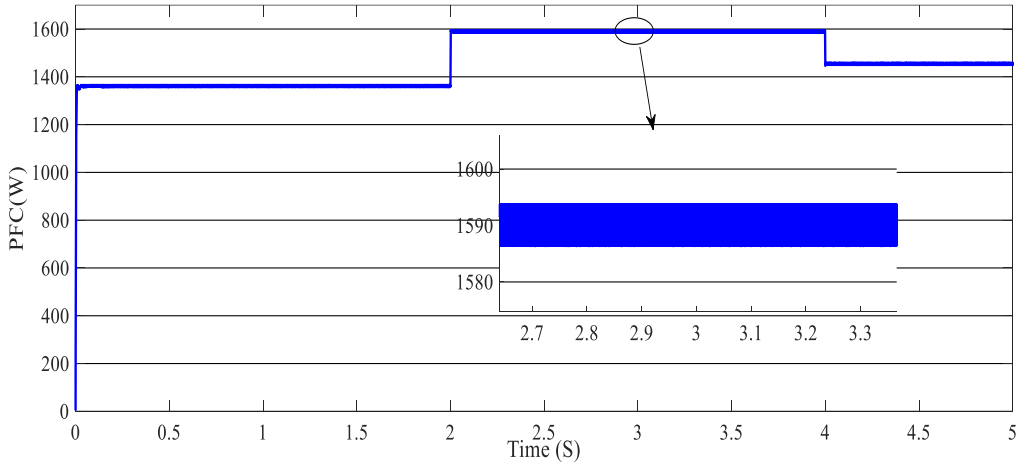

Figure 4. 15 Output power of PEMFC system.

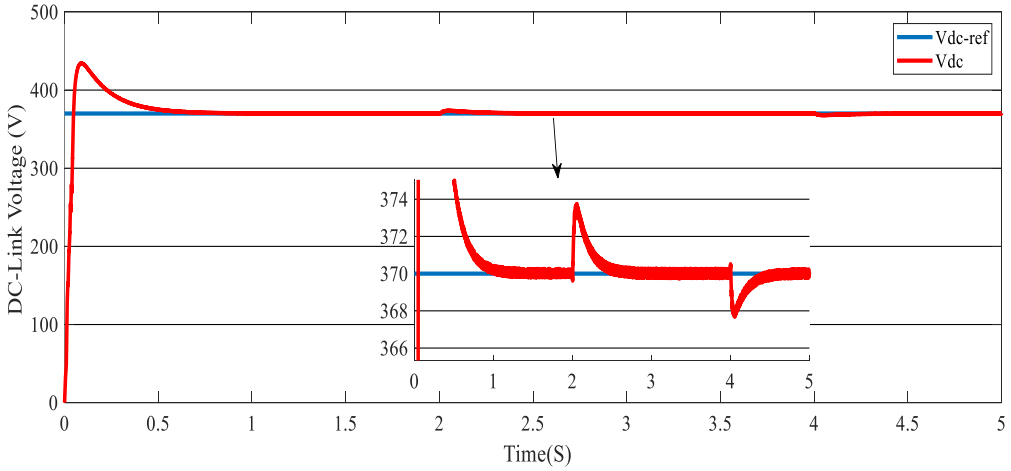

Figure 4. 16DC-link voltage with reference.

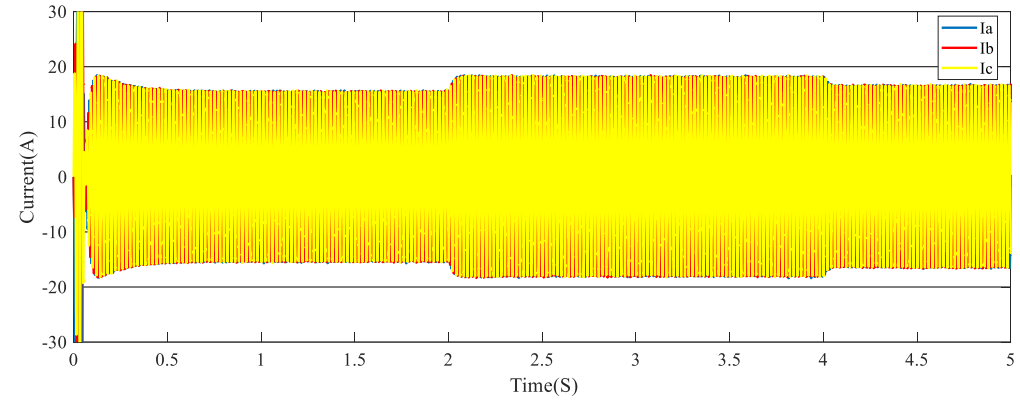

(a)

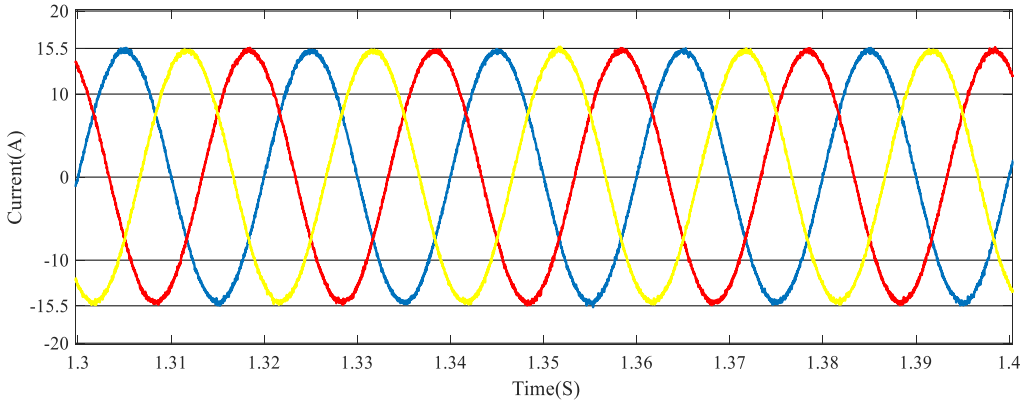

(b)

Figure 4. 17(a) grid current, (b) zoom of grid current.

4.9.2.2 Scenario 2 : fast variation in temperature and pressure:

In the second scenario, the objective was to evaluate the Fuzzy Logic Control (FLC) and the proposed FCS-MPCTS techniques. The partial pressures of Pa and Pc and the temperature of the Proton Exchange Membrane (PEM) fuel cell were varied.

A suddens alterations in temperature and pressure (Pc, Pa) is simultaneously introduced, as depicted in Figures 4.18, 4.19, and 4.20, respectively. Initially, the system functions at a temperature of 315K and a pressure of 2 atm for the duration of the time interval [0,2s], where Pc and Pa are equal. In the second phase, the temperature was elevated to 345K, while maintaining a partial pressure of 3.5 atm for both the cathode and anode. This condition was sustained for the duration of the time interval between 2s and 4s. Subsequently, the temperature was reduced to 305K, while maintaining a partial pressure of 2.5 atm for both the cathode and anode. This condition was sustained for the duration of the time interval between 4s and 5s.

As illustrated in Figure 4.18, 4.19 and 4.20 a sudden rise in PEMFC temperature from 315k to 345k and the pressure (PA,PC) from 2 atm to 3.5 atm are implemented at a specific moment of 2 seconds. The fuzzy logic MPPT achieves the new maximum power point rapidly and

with less fluctuation, without any deviation from the MPP. Moreover, the previously mentioned change leads to a deficiency in voltage across the capacitor (Vdc) in comparison to its reference, accompanied by a brief increase in time, as illustrated in Figures 4.21 and 4.22. figure 4.23(g) demonstrate a rise in grid currents and their kept sinusoidal form.

Next asudden decrease in temperature, from 345 to 305k and pressure of (Pa and Pc) from 3.5 atm to 2.5 atm occurred at the time point of 4 seconds. The fuzzy logic (MPPT) technique demonstrates quick and precise tracking of the Maximum Power Point (MPP). Despite the presence of undershoot and settling time in the voltage deviation from its reference, as depicted in figures 4.21 and 4.22. Furthermore, in Figure 4.23, it can be observed that the grid current experienced an increment while maintaining its sinusoidal waveform.

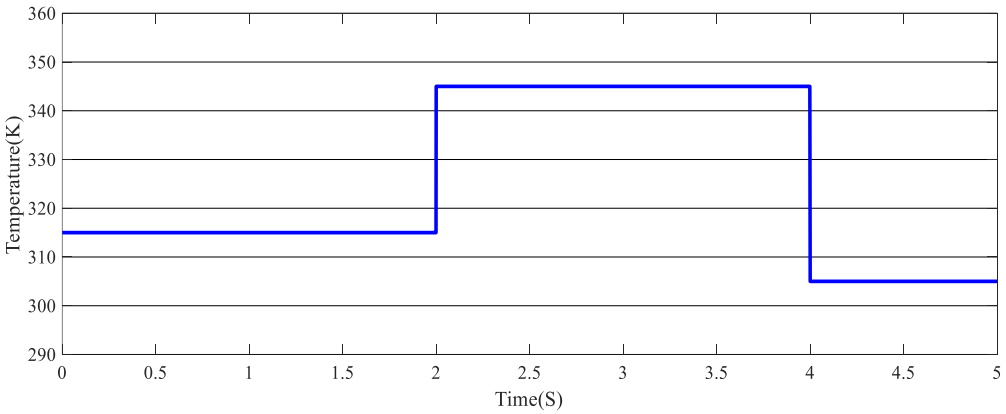

Figure 4. 18Temperature profile.

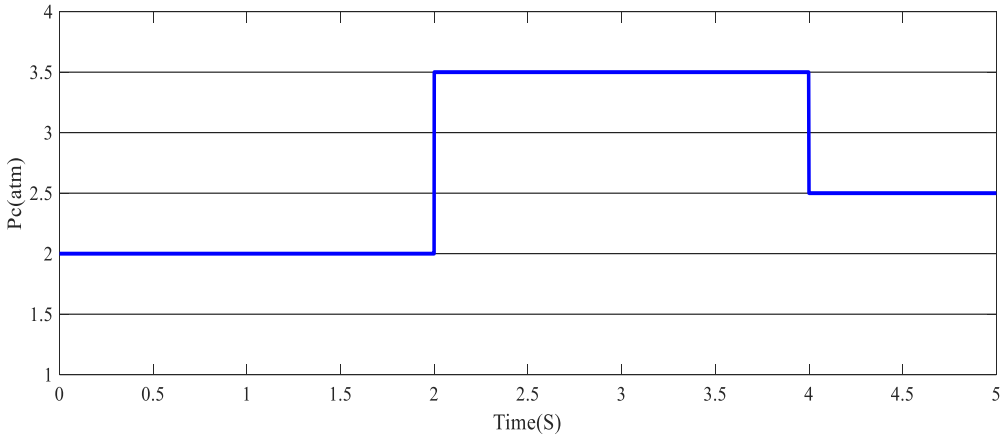

Figure 4. 19Pc pressure profile.

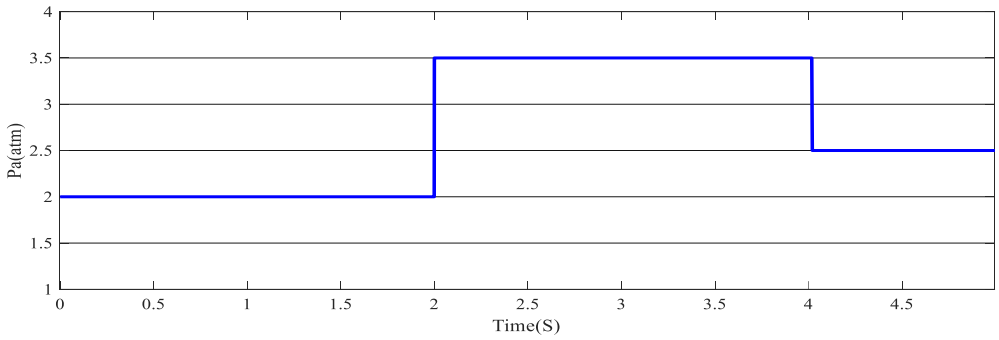

Figure 4. 20Pa pressure profile.

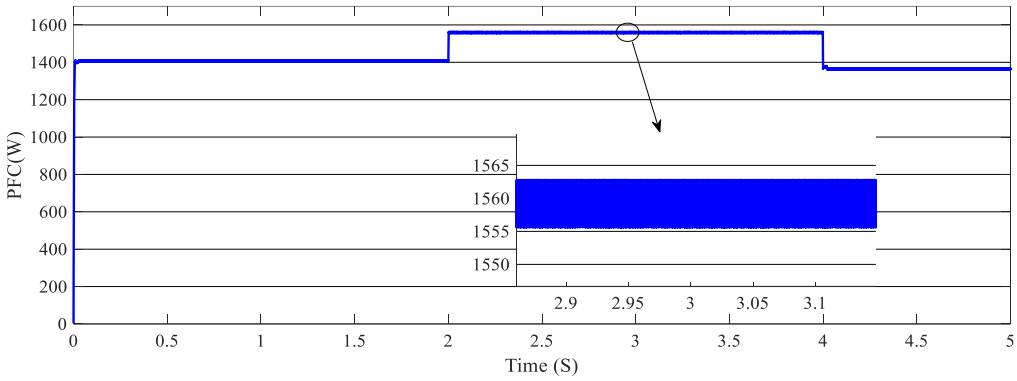

Figure 4. 21output voltage of PEMFC system.

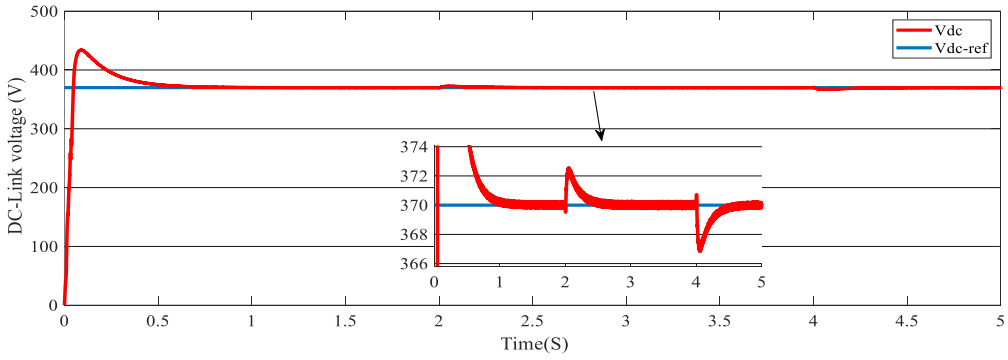

Figure 4. 22DC-link voltage with reference.

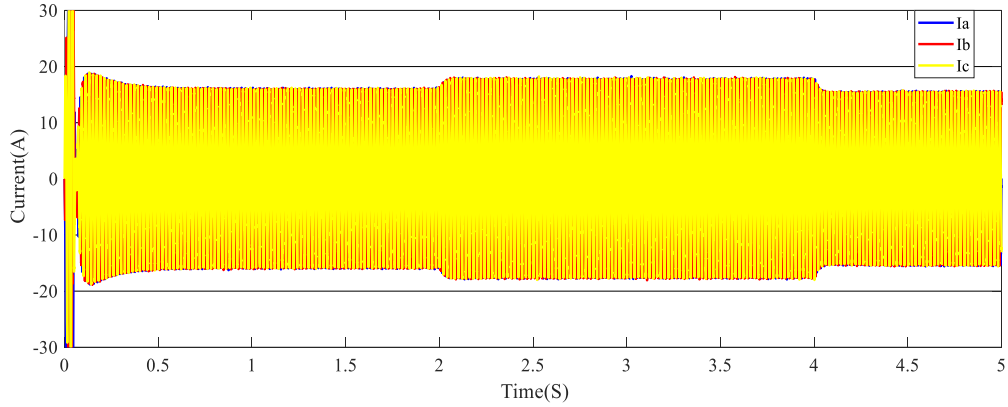

(a)

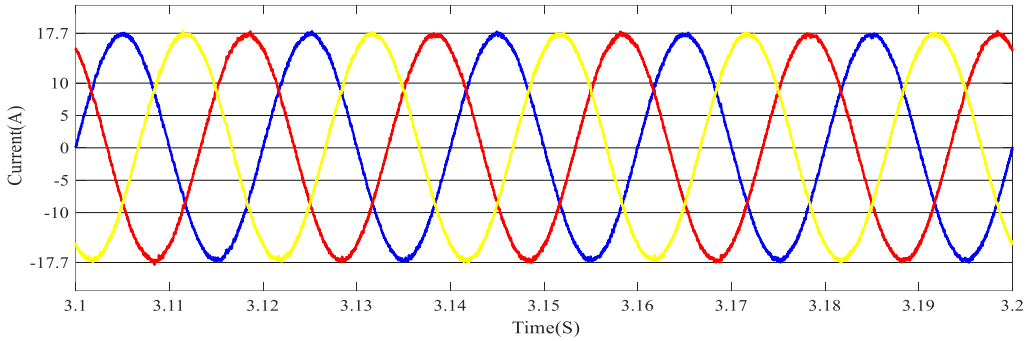

Figure 4. 23(a) grid current, (b) zoom grid current.

To calculate the THD in, we used the (FFT) to determine the harmonic magnitude of the three-phase and we obtained THD results of the PEMFC grid-connected system It is represented in the following values 1.39% for 305K, 1.29% for 355K, 1.36% for 325K.In scenario 2 THD% is represented in the following values 1.36% for 315K and Pa=Pc=2 atm, 1.30% for 355K and Pa=Pc=3.5 atm, 1.38% for 325K and Pa=Pc=2.5 atm, which is significantly much less than the maximum limit for the grid connection.

All the obtained values of THD% for the two scenarios are summarized in the table below:

Table 4. 6Obtained THD for all Cases

Scenario 1			
Tempuratuer	305K	355K	325K
THD%	1.39%	1.29%	1.36%
Scenario 2			
Tempuratuer	315K	345K	305K
Pressure	2atm	3.5 atm	2.5 atm
THD%	1.36%	1.30%	1.38%

4.9.3 FCS-MPCC for Grid-Connected PEMFC using three-Level single phase F-Type-Inverter:

The proposed system was simulated utilizing MATLAB/Simulink and Simpower system packages. The settings for PEMFC, boost converter, and the Rg, Lg filter were presented in Table 4.7.The evaluation of system performance is conducted under specific conditions.

Table 4. 7proposed system paramatres.

PEMFC prametres	
A	$70cm^2$
S	87
δ_1	0.994
δ_2	0.00354
δ_3	$7x10^{-8}$
δ_4	$1.96x10^{-4}$
λ	12
J_{max}	$1.7cm^{-2}$
Bock-Boost converter electrical parameters	
Inductore L	0.2H
DC-link capasitors C_1=C_2	2200µF
Grid parameters	
Grid peak voltage	110V
Grid inductance L_f	10mH
Grid resistance R_g	0.1Ω
Grid frequency F_g	50HZ
Simulation parameters	
Sampling time T_s	10µs

The efficacy of the suggested control scheme will be demonstrated through a demonstration of its improvement. The objective of this study is to demonstrate the efficacy of the suggested control technique utilizing FCS-MPCTS to improve DC-link capacitor voltage balancing, and grid current THD%.

The influence of temperature and change in impedance values, the outcomes illustrated in Figures 4.24 to 4.31 was investigated by means of computational modeling conducted using Matlab/Simulink and Simpower system software. The perfect system that was connected to the grid was equipped with a three-level single phase F-Type inverter and implemented a control strategy that relied on Finite Control Set Model Predictive Current Control (FCS-MPCC).

In the first scenario, the objective was to evaluate the Fuzzy Logic Control (FLC) and the proposed FCS-MPCC techniques. The partial pressures of Pa and Pc were kept constant, while the temperature of the Proton Exchange Membrane (PEM) fuel cell was varied.

The temperature profile figure 4.24 with different sudden shifts in temperature is used to test the system, The temperature step shift from 343.15K to 343.15K then to 323.15k.

As illustrated in Figure 4.24 a sudden decrease in PEMFC temperature from 343.15k to 313.15 k at a specific moment of 3 seconds. The fuzzy logic MPPT achieves the new maximum power point in an immediate way and with less fluctuation, without any deviation. Moreover, the previously mentioned change leads to a deficiency in voltage across the capacitor (Vdc) in comparison to its reference, accompanied by a brief increase in time, as illustrated in Figure 4.25 and 4.26. According to Figure 4.27, it can be observed that VC1 and VC2 maintained identical values throughout the simulation, indicating the ideal equilibrium of the DC-link through the proposed FSC-MPCC method. Figure 4.28 represents the direct current voltage difference between VC1 and VC2, given that they are in equilibrium within an error of ±0.1%. Figure 4.29 illustrates the simulated responses of the grid voltage and current. It is notable that the current flowing through the grid is in synchronization with the voltage across the grid.

The Fast Fourier Transform (FFT) analysis of the grid current depicted in Figure 4.30 indicates that a mere 1.53% of Total Harmonic Distortion (THD%) was detected upon implementation of the FSC-MPCC technique.

Figure 4.31 illustrates the current injected into the grid for varying inductance values, specifically 20 mF, 5 mF, and 15 mF, as depicted in subfigures (a), (b), and (c), respectively. The observation that the waveform maintained its sinusoidal form without any distortion for all values of inductance serves as evidence for the efficacy of the proposed algorithm across varying inductance values.

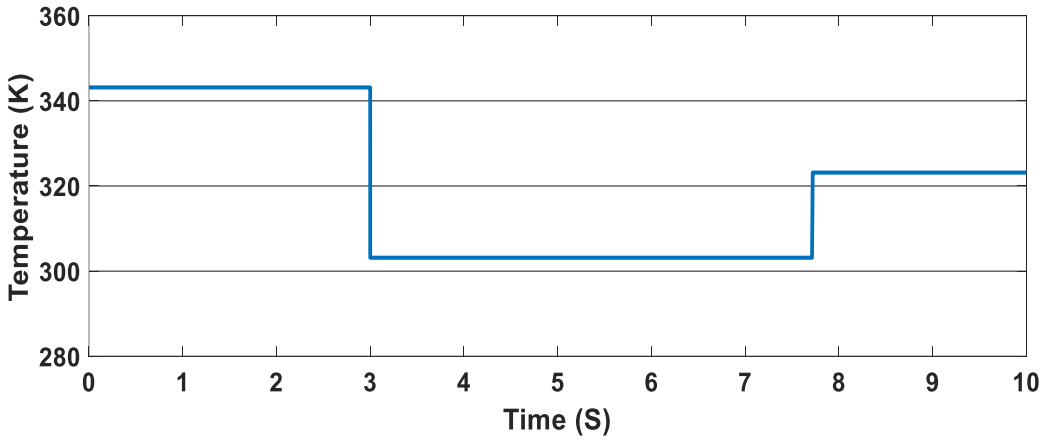

Figure 4. 24 Temperature profile.

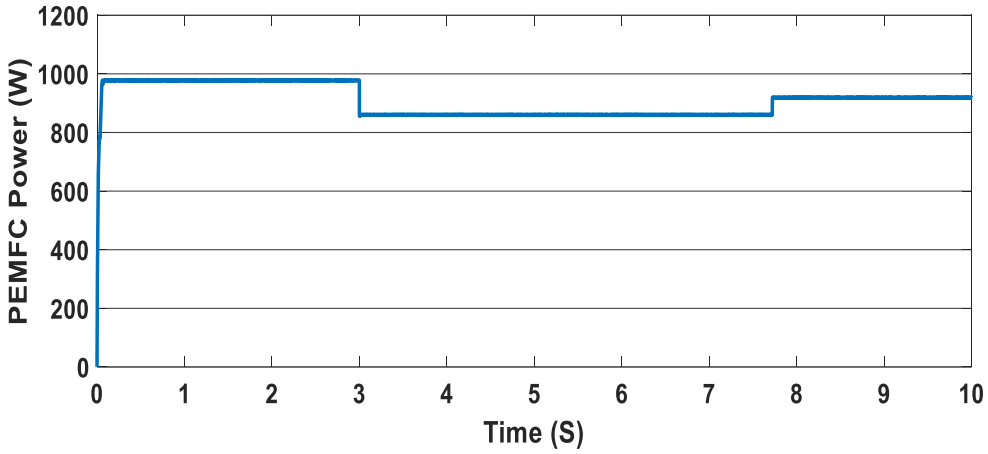

Figure 4. 25PEMFC ouput Power

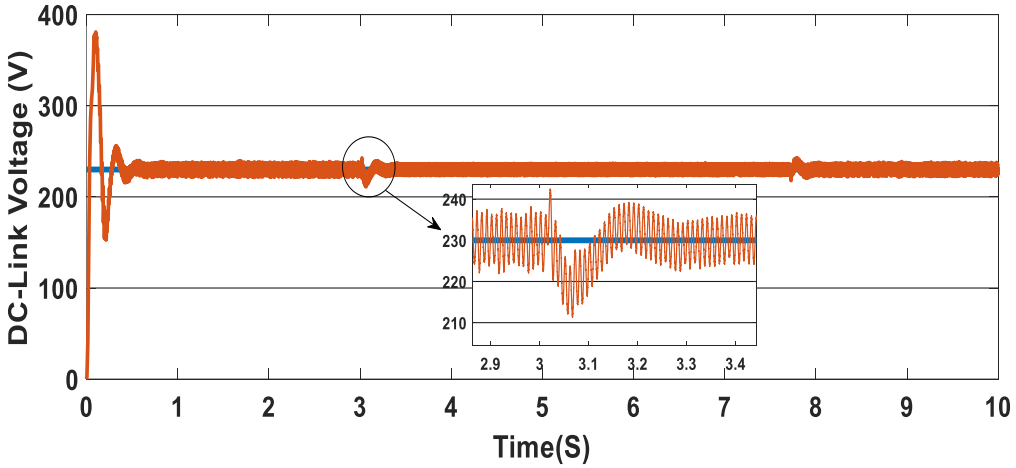

Figure 4. 26DC-link voltage.

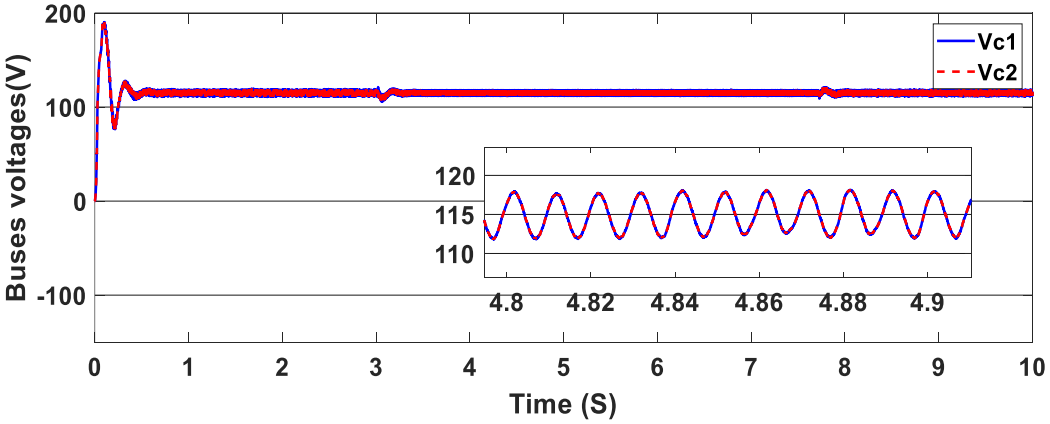

Figure 4. 27Capacitors voltages.

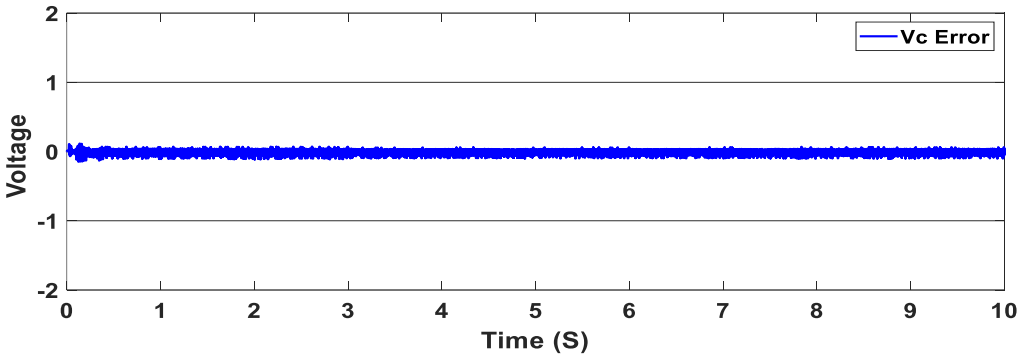

Figure 4. 28DC voltage error.

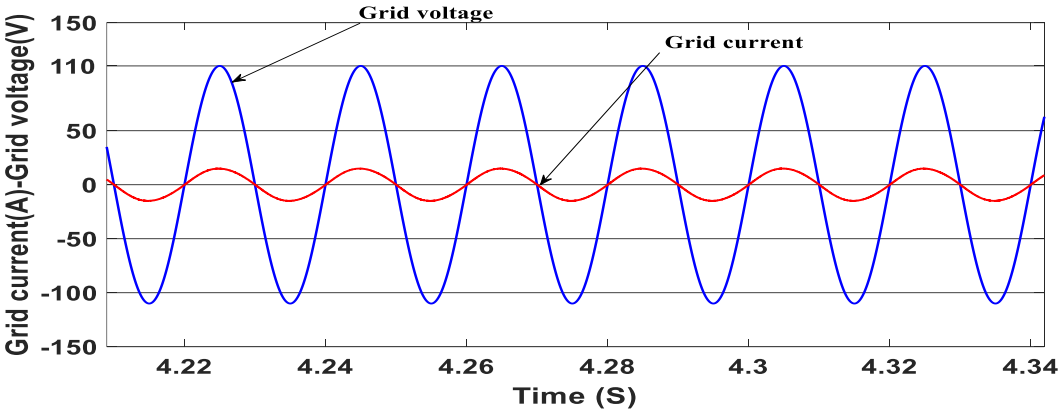

Figure 4. 29Grid voltage and grid current waveform.

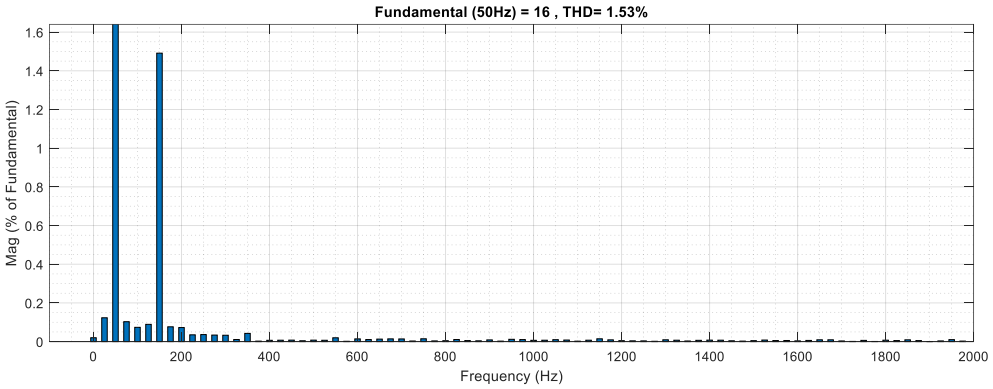

Figure 4. 30Total harmonic distortion.

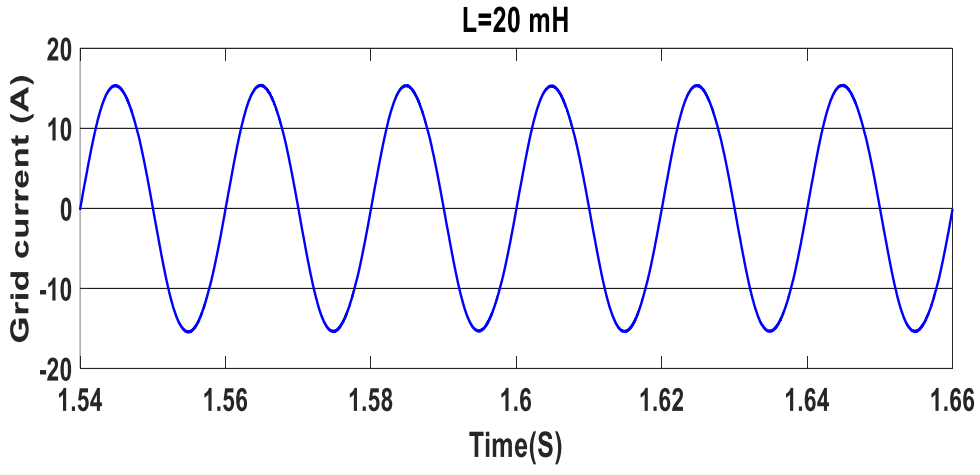

(a)

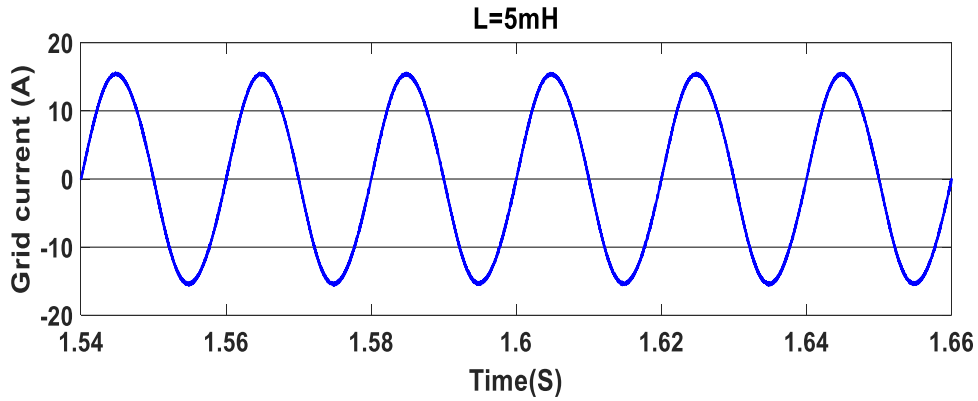

(b)

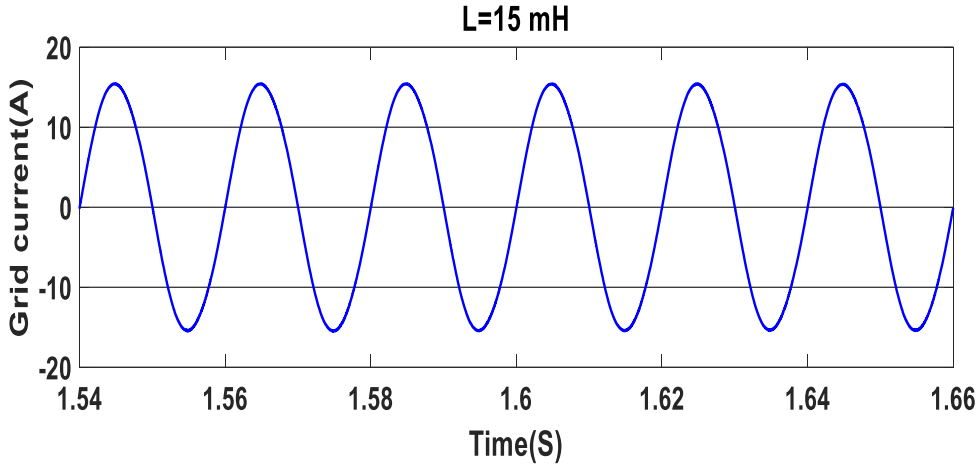

(c)

Figure 4. 31Grid current waveform with a different value of the inductance.

4.10 Conclusion:

This study proposes control schemes for grid-connected photovoltaic (PV) systems and proton exchange membrane fuel cell (PEMFC) systems utilizing a three-level neutral point clamped (NPC) inverter with a finite control set model predictive current two-step (FCS-MPCTS) controller. Additionally, the study explores grid-connected PEMFC systems utilizing a three-level single-phase F-Type inverter with an FCS-MPCC controller.The utilization of fuzzy logic in maximum power point tracking is a subject of interest in academic research. The application of buck-boost converter and boost converter is utilized to maximize the power extraction from the photovoltaic (PV) array and proton exchange membrane fuel cell (PEMFC).Furthermore, an FCS-MPCTS is suggested for controlling the three-level Neutral Point Clamped (NPC) inverter. Additionally, an FCS-MPCC is proposed for controlling a three-level single-phase F-type inverter.The primary objectives of this study are to rapidly and accurately track the maximum power point (MPP) in photovoltaic (PV) arrays under sudden shifts in irradiation, as well as in proton exchange membrane fuel cells (PEMFC) under sudden changes in temperature and pressure. This will be achieved by implementing a fuzzy

logic maximum power point tracking (MPPT) approach.The secondary objective is to design FCS-MPCTS and FCS-MPCC controllers that can effectively regulate the balance of the two DC-link capacitor voltages, regardless of the disparity between the extracted power from the PV system and PEMFC system, while ensuring high-quality current injection into the grid.

The simulation results demonstrate that the proposed control schemes have successfully achieved the stated objectives. The proposed Maximum Power Point Tracking (MPPT) technique exhibits higher tracking capabilities in relation to power oscillations, speed, and tracking precision.Furthermore, $ig\alpha$-β currents are tightly regulated, DC-link capacitor voltages are perfectly balanced and high grid current quality (THD%) has been provided during different irradiation for grid-tied PV systems using three-level NPC and different temperatures and pressure for grid-tied PEMFC systems using three-level NPC. Also, ig currents are tightly regulated, DC-link capacitor voltages are perfectly balanced, and high grid current quality (THD%) has been provided during temperatures and different values of inductance for grid-tied PEMFC systems using three-level F-Type inverter, by the proposed schemes.

Chapter 5 Energy management strategy based on state machine control for multi-source storage system

5.1 Introduction:

The world's usage of electrical energy has expanded significantly in recent years. In the current scientific studies, the first primary source of electricity has already been fossil fuels and their derivatives, which produce 78-80% of total energy[160], however, these sources are finite, these primary sources will end and do not meet our needs in the long terms[161]. Furthermore the necessity to electricity the transportation industry never has been more obvious or pressing. Based on the International Energy Agency (IEA), transportation consumes 72.1% of all petroleum products (IEA), when burnt, it usually causes anthropogenic climate change[162].moreover,with the tremendous increase in human population and energy consumption, the trend is toward new and sustainable renewable energy such as solar, wind, and hydrogen, this is due to they provide several benefits to both humans and the environment when compared to conventional energy sources like heavy oil, coal, and natural gas, these alternatives are more sustainable and emit less CO2[10]. the renewable energy resources (RES) will take on a greater role in energy production. form all renewable energy resources solar energy is the most promising existing RES technology since it is widespread, free, and ecologically good[163,164]. The Pv systems are becoming increasingly popular in both developing and developed nations. While those technology are improving in many ways, the negatives connected with them, such as their high investment cost, continue to be the major barriers to their use. Hydrogen is a sustainable energy carriers that may use sun electric energy generated by PV panels for water electrolysis while emitting no CO2[165].

In the present day the experts are considering clean hybrid renewable energy systems (CHRES), which will become highly interesting in the coming years to produce 100% renewable sources such as the hybrid photovoltaic-feul cell-storage system and solar-powered electricity generation[166], In addition the design of hybrid system it must consist two renewable sources or more and renewable energy sources generally thought as one of the most efficient power producing systems. However, because renewable energy are dependent on weather conditions and are intermittent, therefore don't really deliver steady electricity. Furthermore, combining numerous renewable energy sources, like wind and solar systems results in large output power[167]. Following a lengthy development period, a growing number of academic research works and demonstration blueprint on PV/Battery DC microgrids and PV/Wind/Battery DC microgrids have been completed, nevertheless, the power generated of PV and wind generators varies greatly depending on the climatic condution[168,169]. Since the battery performance and size limitations, this type of DC

microgrid is incapable to meet long-term energy needs[170,171]. To address the difficulty, the fuel cell is gaining popularity owing to its capability for long-term generating systems. At the same time, the photovoltaic panels serve as a main source and the battery pack as a short-term energy storage system and the hybrid dc microgrid comprising PV generation, fuel cell systems, a battery system, and domestic loads, on the other hand, getting more interested by researcher[172].The primary advantage of a HES system is its ability to be self-sufficient during varying climatic circumstances because it is not dependent on a single source.HES can sometimes be linked to the power grid or operated as a stand-alone microgrid[173].furthermore the advantage of the combination for more than one renewable source than a conventional hybrid system(CHS) like diesel generator with batteries is largely to save fossil fuels while also reducing their influence on the environment. But the CHSare costly to run and maintain, particularly in rural places. Furthermore, they have a negative influence on the planet.in contrast HES systems, whom are more ecologically benign and sustainable,this is the cause why hybrid energy systems based on renewable sources have garnered a significant amount of attention in the last few years.

With an increase in the use of DC components a lot of academics are interested in developing energy management techniques, Many scholars have proposed strategies for energy management: we can clasived them in two types : Management strategies based on rules and management strategies based on optimization [174,175].There are two types of rule-based management techniques : Filters control (FBC) is an example of a deterministic rule-based EMS,wavelet transform and state machine control (SMC)[176–178].The second form of EMS is fuzzy rule-based, which has standard fuzzy, adapting fuzzy, and Adaptive neuro-fuzzy inference[179–181].for fuel cell and hybrid power systems such as a photovoltaic-fuel cell production system with batteries is being investigated in ref [182].in ref [183] the author propose a experimental validation of hybrid power system consists photovoltaic/fuel cell/ electrolyzer/batteries.a new energy management strategy called a proportional grid connected for hybrid renewable energy sources consist PV/wind in ref [184] A hybrid energy management method is being used to improve the functioning of PV/FC/supercapacitor-battery renewable systems was discesd in ref [185].The suggested single DC/DC converter operates in one way for the three sources of power (PV and FC) but in 2 ways for the battery bank.despite the fact that the findings validated the suggested converter's strong performance at the transitory and stable state operation functioning of the loads and PV irradiation step change,Among the drawbacks of the approach is that if there is an issue with the converter, the system will fail and the same design has been discussed in the ref[186,187].in ref [188]they proposed an energy management system consisting of PV/fuel cell/battery validated

with Arduino. The authors in this ref [189] they proposed novel energy management in hybrid electric vehicle applications for a hybrid system consisting of fuel cell/battery and supercapacitor.

In this chapter paper we segested an energy management system for PV/fule cell/battery storag system depenting on the control objective of the SMC and the stability the DC bus and meet the rquarement of the load demmande, The proposed energy management strategy SMC is responsible for distributing net system power between the battery pack and the fuel cell system. The system's principal source is photovoltaic. a backup power supply that consists of a fuel cell and a secondary battery.Surplus power from PV used to store in a battery depends on the state of the power system. Also, the battery is promoted to deliver power to the load,and the fuel cell has two objectives the first one works as a backup system if the PV system and the battery do not generate enough power for the load, and the second one charges the battery when the state of charge is low.

5.2 hybrid system configuration:

The proposed system represented in figure(5-1) and divided in to four parts as follow:

- photovoltaic system consist a photovoltaic PV panels and DC/DC buck—boost converter controlled by fuzzy logic MPPT to track and maintain the maximum power point(MPPT) .
- Fule cell connected with DC/DC boost converter.
- Batteries connected with DC/DC bidirectional converter.
- A DC load .

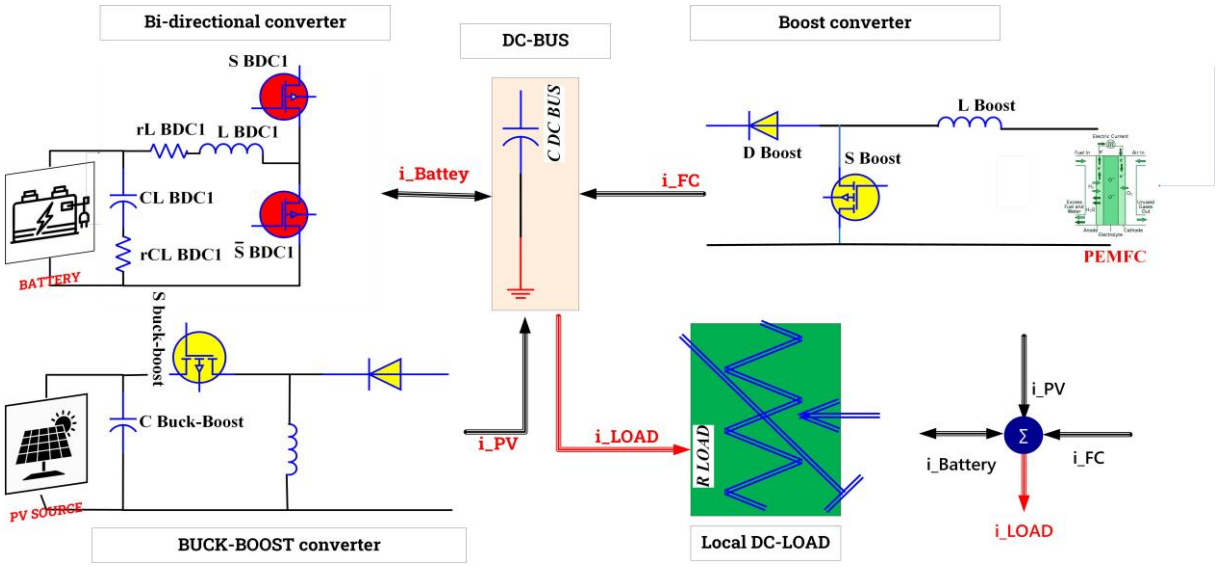

Figure 5. 1globle system configurations

5.2.1 PV modeling

Photovoltaic generation is a type of renewable energy production that transforms sunlight directly into electrical energy via the photovoltaic effect, with photovoltaic cells acting as the primary component.Since the characteristics P-V ,I-V of the PV array varies depending on the external circumstances, the PV array will be connected to the DC bus through a DC/DC converter,thus to reach the maximum power point, many researchers propose a lot of MPPT controller. In ref[190] the authors proposed and hardware implementation of FLC through SMC to extract the MPPT from the PV panel.a novel fuzzy regression MPPT proposed in ref [191], also the authors in ref[192] they proposed a modified INC to extracted the maximum power from the PV array. Several mathematical models of solar panels have been created to depict their nonlinear behavior resulting from the semiconductors junction at their implementation.The PV module is created by connecting a number of series and parallel cells; the same process used for modules produces a PV generator or array.

To make up a PV module we must connect many PV cells in series (N_s) and parallel (N_p),the PV module equation represents in the equation below:

$$I_{pv} = N_p I_{ph} - N_p I_{sd}\left(\exp\left(\frac{N_s V_{pv} + \left(N_s / N_p\right) R_s I_{pv}}{n N_s K T}\right) - 1\right) - \left(\frac{N_s V_{pv} + \left(N_s / N_p\right) R_s I_{pv}}{(N_s / N_P) R_{sh}}\right) \quad (5.1)$$

The photovoltaic generator (GPV) is linked to the DC bus via a buck-boost converter, allowing it to function at full power.The most common dc /dc converter is buck-boost, which incorporates the electrical characteristics of both a buck and a boost[183]. Figure(5.2) depicts the P-V and I-V characteristics of a PVmodule and under various sun irradiation conditions.As shown in figure.5.2 (a), as the outcome voltage Vpv increases, the PV module current Ipv varies little and when the voltage reaches a certain threshold, the PV module current Ipv decreases quickly as the output voltage Vpv still increases.As a result, near the highest power limit, the U-I characteristic shapes are non - linear.If the photovoltaic module voltage Vpv remains fixed, the current of the photovoltaic panel Ipv rises proportionately to the increased irradiation.Once the sunlight is constant, PV module power exhibits a non-monotonic tendency with the shift of its Vpv as shown in figure (5.2) (b).Once the PV voltage is insufficient, the power of the photovoltaic panel's Ppv rises as the output voltage Upv improves[193].Whenever the PV module voltage is higher, the Ppv of the photovoltaic module diminishes as the output voltage Vpv increases.The p-v characteristic graphs show a significant link between photovoltaic array production power and sunlight. The lower the voltage disturbance near the maximum power point, the larger the power adjustment.

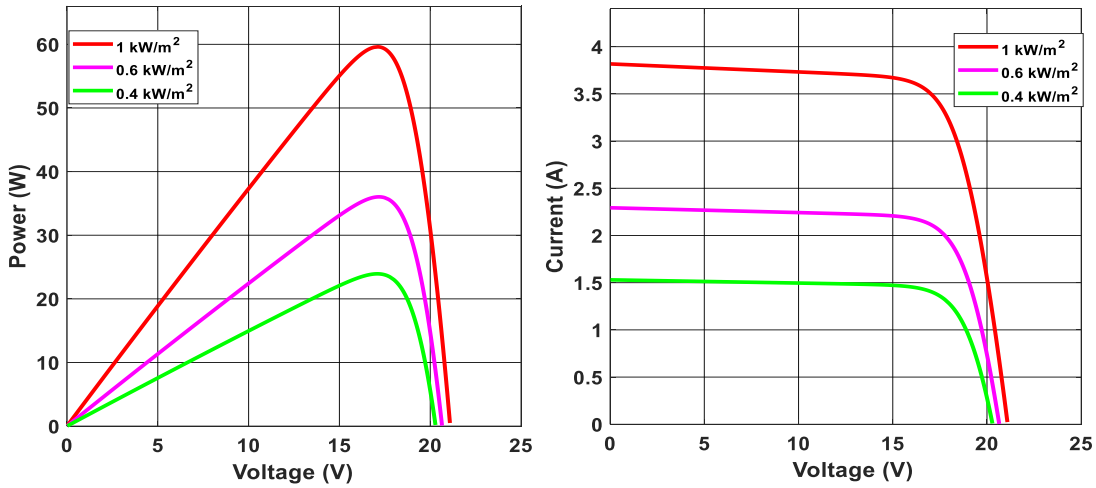

(a) (b)

Figure 5. 2P-V and I-V curves of photovoltaic panel

The command of the buck-boost converter is provided via the PWM signal.Fuzzy logic control is used for maximum power point tracking and membership functions of the inputs and the output are represented in fig.(5.3). the FLC has two inputs the error E and the change in the error DE and one output dD as shown in equation :

$$E(k)=\frac{P_{PV}(k)-P_{PV}(k-1)}{I_{PV}(k)-I_{PV}(k-1)}$$
$$dE(k)=E(k)-E(k-1) \qquad (5.2)$$

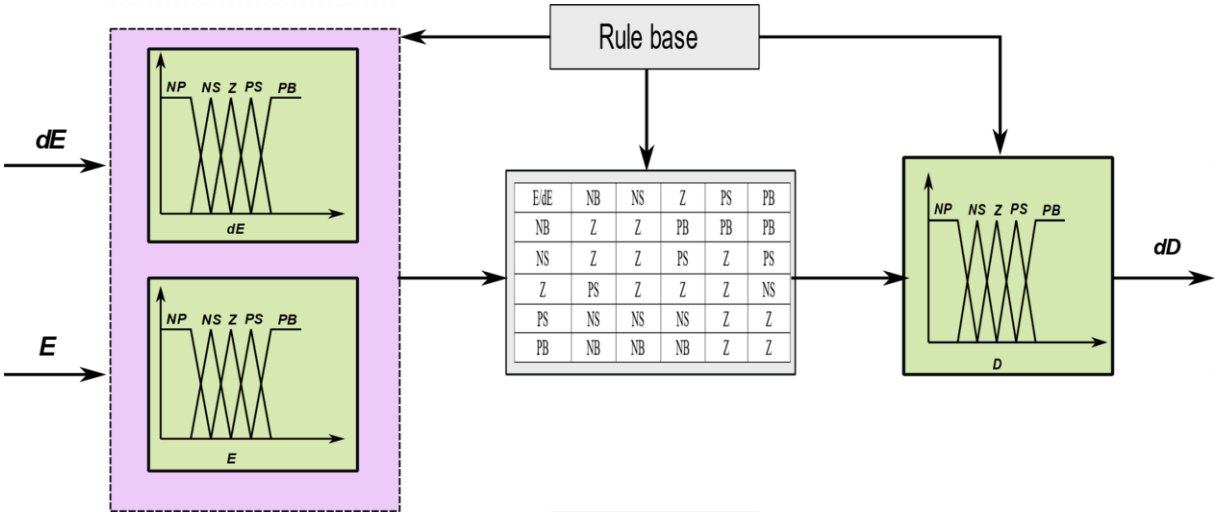

Figure 5. 3fuzzy logic membership: E, DE and dD

5.2.2 PEM fule cell modeling:

When compared to other kinds of FCs, the primary benefits of a Proton Exchange Membrane Fuel Cell (PEMFC) as a power source are: effective electrical power in steady-state, dependable power production, small size, minimal working noise, and ecofriendliness . PEMFC is made up of several fuel cells linked in series called stacks; additionally, the PEMFC curve is non-linear and is influenced by temperature, oxygen and hydrogen pressure, and so on. Figure(5.4) depicts the electrical model of the PEMFC. The PEM fuel cell stack output voltage is generally determined as follows:

$V_{out} = N.V_{fc}$ (5.3)

Where N_{fc} and are the number of PEMFC connected in series and the output voltage respectively.in general, the output voltage of the fuel cell represents as follows[194]:

$$V_{fc} = E_{nernst} - v_{act} - v_{conc} - v_{ohmic} \quad (5.4)$$

The output voltage of the fule cell mentioned abouve consiste of $E_{nersent}$ represent the , V_{act} ,V_{conv} and V_{ohmic} .

$$E_{nernst} = 1.229 - (0.85\times10^{-3})\times T_{FC} - 298.15) + (4.31\times10^{-5}\times T_{FC}\times\ln(p_{H_2})\times0.5\times\ln(p_{O_2})) \quad (5.5)$$

$$v_{act} = -\left[\delta_1 + \delta_2 T_{fc} + \delta_3 T_{fc}\ln(C_{O_2}) + \delta_4 T_{fc}\ln(I_{fc})\right] \quad (5.6)$$

$$v_{ohm} = I_{FC}(R_M + R_C) \quad (5.7)$$

$$v_{con} = -\beta\ln\left(1 - \frac{j}{j_{\max}}\right) \quad (5.8)$$

$E_{nersent}$ denotes the chemical reactions of output voltage, T_{fc} the temperature, and the P_{O2} and P_{H2} the oxygen and hydrogen levels, respectively. V_{act} represent the activation loss that consiste $\delta_{1,2,3,4}$ empirical coefficients and C_{o2} empirical coefficients.V_{ohm} represent the ohmic voltage that **consiste** R_M and R_c represent indicates electron flow resistance and proton resistance respectively.V_{con} donait the **c**oncentration overvoltage that consiste j, jmax, and b, that represent The maximal current, maximum current density, and concentration loss are represented.

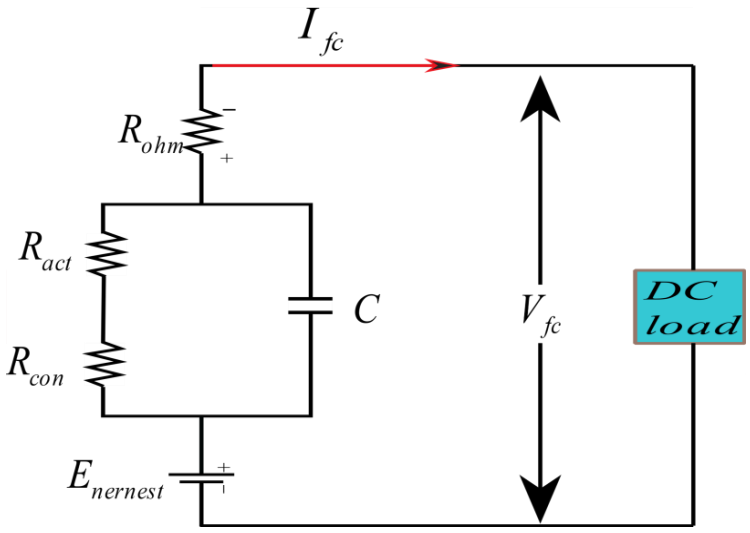

Figure 5. 4 Electrical model of PEM fuel cell

A PEMFC stack (P-V) and (I-V) properties are depicted in figure (5.5) below :

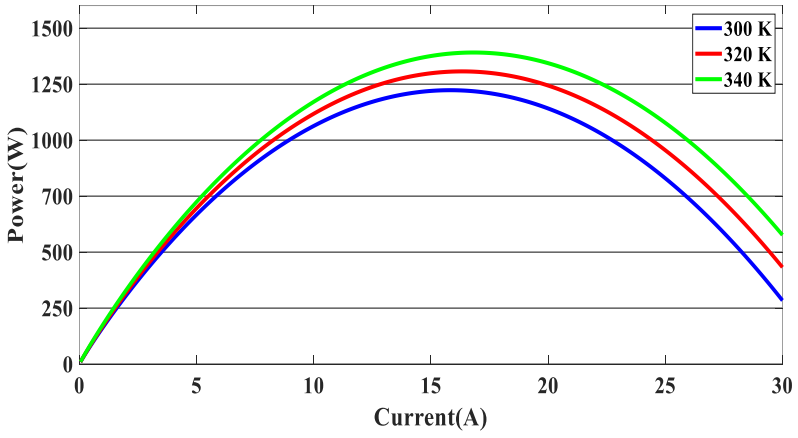

(a)

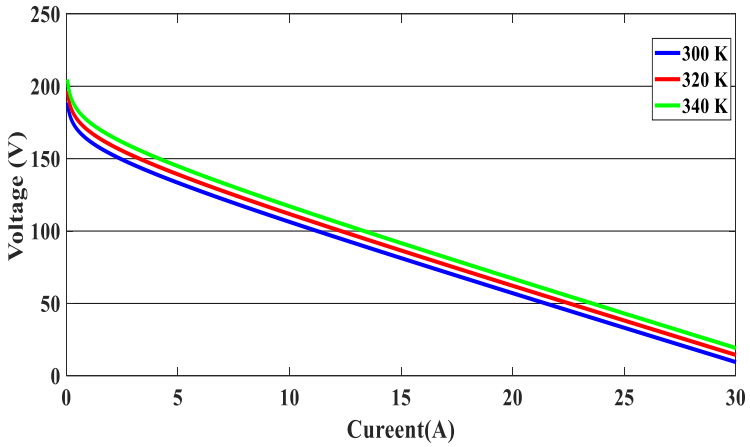

(b)

Figure 5. 5PEMFC characteristic (P-I) (a) and (V-I)(b).

P-I and V-I characteristic graphs of the PEMFC stack at various temperatures are shown. As illustrated in figure(5.5)(a), the increase in voltage and power of the fuel cell when the

temperature increases from 300 to 340 K is exceedingly tiny. The voltage steadily decreases as the fuel cell current rises in figure (5.5) (b)

5.2.3 Battery storage system

Because of the irregular, random, and unpredictability of renewable energy systems (RES) in loads, implementing a BES is critical to supporting energy output and dealing with RES breakdowns[195].This study applies Lithium Ion battery technology to a collection of DC-loads units.Lead-acid (LA) batteries are an established technology that is suited for static uses and has a cheap initial expenditure cost.Lithium batteries, on the opposite hand, have better energy and power densities, greater performance, an extended life span, as well as other technical advantages over competing kinds.As a result of their outstanding performance, such batteries are also suitable for stationary Solar systems, and continuous power supply (CPS)[196,197].To choose the best battery type, a number of technological factors are taken into account, including maturity, weight, size, discharge rate, temperature sensitivity, upkeep, and the effectiveness of costs[198,199].in this paper, we use the lithium-ion battery for the advantages mentioned above and semerized in table. 1-5 blow , and Appendix shows the statistics for the Li-Ion battery, the DC/DC boost converter, and the buck converter's specifications.

Table 5. 1comparison between lithium-ion and lead acid [190]

Lithium -ion	**Lead acid**
Effecency (%)	
85% – 95%	60%– 80%
Advantages	
Low upkeep, high effectiveness, lightweight, and low self-discharge.	Low capital cost, grown technology
Drawbacks:	
more susceptible to high temps, and is still regarded as a developing technology	The maintenance includes watering, and watching the 50% flow limit—inadequate effectiveness.

5.3 Power converter:

This study focuses on non-isolated DC-DC converters that connect the PV PEMFC battery to the load via a DC-coupled bus as illustrated in figure(5.1) .The buck-Boost converter, also known as a step-up/step-down converter, is a mono-directional device that guarantees - flowing Ipv that charges the battery, or shares the load via the local DC bus.The boost converter is a step-up converter that guarantees the PEMFC current is supplied to the load via the DC bus and also charges the battery if needed.A bi-directional converter (BDC) guarantees bi-directional current transferring from the battery to the load via the DC bus [200] .in figure (5.6) the power control of the proposed hybrid system, the DC-link voltage reference, the PEMFC reference current and the current battery reference, refer to V^*_{DC}, I^*_{fc} and I^*_{batt} respectevly.the PV power is tracked using a buck-boost converter and controlled

with fuzzy logic MPPT during variable conditions.Using a dual-loop construction, the BDC detects the DC-link voltage to adjust for unequal power via battery storage charge/discharge. the power of the load calculated in the flowning equation below :

$$p_{load} = V_{dc-bus}.I_{dc-bus} = V_{dc-bus}C_{dc-bus}.(V_{dc-bus}/dt) \quad (5.9)$$

It has been proposed that the DC link is a capacitor. Once all of the basic models were defined, we coupled the power sources according to the DC bus design. Direct current (DC) is provided by every supply source gathered on the bus.The calculation for the DC link current is as follows:

$$C_{dc-bus}\frac{dV_{dc-bus}}{dt} = I_{pv} + I_{fc} \pm I_{batt} \quad (5.10)$$

the efficiency of the global system (converters and the load) is represented by η and could be expressed in the equation below:

$$P_{load} = P_{pv}\eta_{buck-boost} + P_{fc}\eta_{boost} + P_{pv}\eta_{BDC} \quad (5.11)$$

$$\eta_{load} = (\eta_{pc} + \eta_{fc} + \eta_{BDC})/3 \quad (5.12)$$

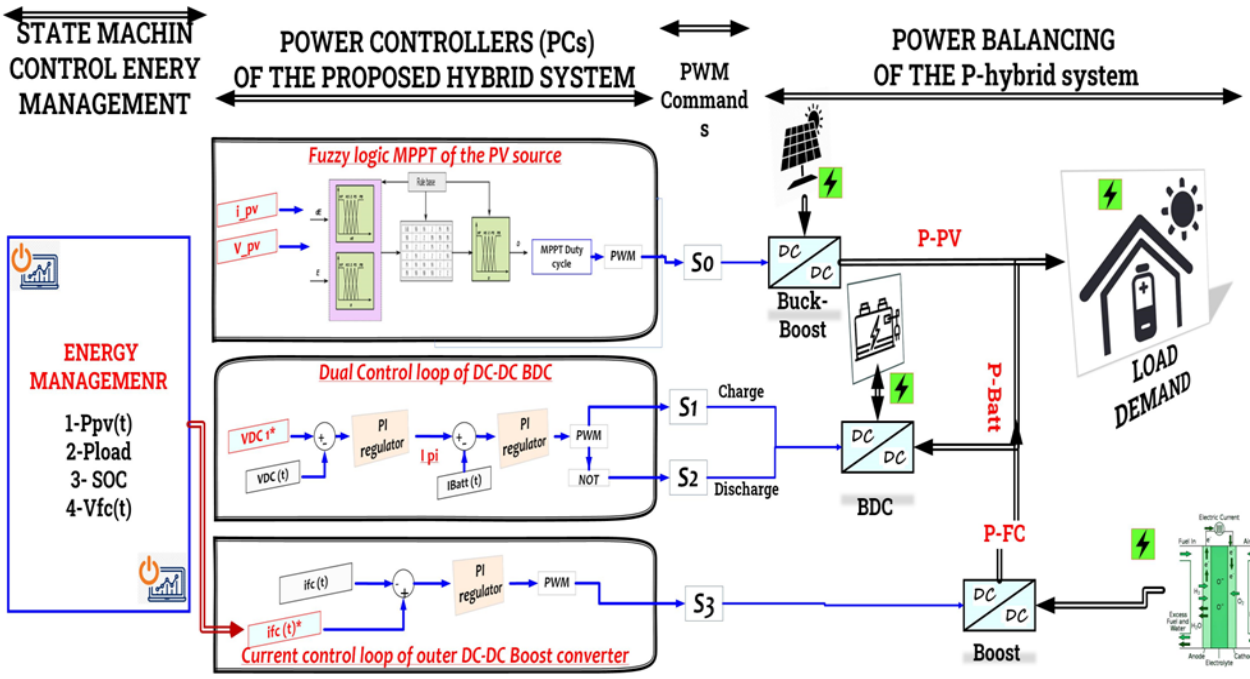

Figure 5. 6state machin energy management,power controller and power balancing of the proposed system.

5.4 Proposed energy management strategy :

Creation of a power control strategy for an integrated system is the primary focus of this section ,An innovative HEMS system was created and used to track and manage the efficacy of the suggested system.Variations in sun irradiation must be accommodated in the working

strategy that will be devised for the proposed system. The net power calculation of the proposed hybrid system can be expressed as :

$$P_{net} = P_{load} - P_{pv} \tag{5.13}$$

One of the rule-based control strategies for the microgrid's energy management system is the state machine control strategy. For this propose hybrid system.As shown in table 2-5, the state machine control method used comprises fivteen states under three SOC interval .The three different SoC interval are classified as High means that (SOC >SOC_{max}), Normal means that (SOC_{max}> SOC <SOC_{min}), and Low means that (SOC< SOC_{min}).The highest limit SOC_{max} and lower limit SOC_{min} of the SOC. It is clear that the battery SoC interval as well as the net power of the system $P_{net}$are used to calculate the PEMFC reference power and concurrently taken into consideration are the following limits: P_{pv} is the output power of the PV generation device, and P_{load} is the load requirement; The fuel cell system's minimal, optimal medium, and maximum output powers are designated as Pfc_{min}, Pfc_{opt}, P_{mid}, and Pfc_{max} respectively,the SOC_{max} and SOC_{min} the lower and the upper limits respectively.

Table 5. 2proposed state machine contro.l

state	SOC	Net power $P_{net}(t)$	$P^*_{fc}(t)$
1	**LOW**	p_{net} (t)< Pfc_{min}	$P^*_{fc} = Pfc_{opt}$
2		p_{net} (t) ∈ [Pfc_{min},Pfc_{opt}[	$P^*_{fc} = Pfc_{opt}$+ Pfc_{min}
3		p_{net} (t) ∈ [Pfc_{cop},Pf_{mid}[	$P^*_{fc} = P_{mid}$
4		p_{net} (t) ∈ [Pfc_{mid},Pfc_{max}[	$P^*_{fc} = Pfc_{mid}$+ Pfc_{opt}
5		p_{net} (t) >= Pfc_{max}	$P^*_{fc} = Pfc_{max}$
6	**MEDIUM**	p_{net} (t) < Pfc_{min}	$P^*_{fc} = Pfc_{min}$
7		p_{net} (t) ∈ [Pfc_{min},Pfc_{opt}[	$P^*_{fc} = Pfc_{min}$+ Pfc_{opt}
8		p_{net} (t) ∈ [Pfc_{cop},Pf_{mid}[	$P^*_{fc} = Pfc_{opt}$
9		p_{net} (t) ∈ [Pfc_{mid},Pfc_{max}[	$P^*_{fc} = P_{net}$
10		p_{net} (t) >= Pfc_{max}	$P^*_{fc} = Pfc_{mid}$+ Pfc_{min}
11	**HIGHT**	p_{net} (t)< Pfc_{min}	$P^*_{fc} = Pfc_{min}$
12		p_{net} (t) ∈ [Pfc_{min},Pfc_{opt}[	$P^*_{fc} = Pfc_{mid}$-Pfc_{opt}
13		p_{net} (t) ∈ [Pfc_{cop},Pf_{mid}[	$P^*_{fc} = Pfc_{opt}$
14		p_{net} (t) ∈ [Pfc_{mid},Pfc_{max}[	$P^*_{fc} = Pfc_{mid}$- Pfc_{min}
15		p_{net} (t) >= Pfc_{max}	$P^*_{fc} = Pfc_{mid}$

5.5 Results and discussions:

The following section shows the analysis of the proposed state machine control for the proposed hybrid system using the MATLAB/SIMILUN toolbox. the parameter of the global hybrid system is represented in the appendix. The findings focus of the scenarios study emphasize the impact of using variable irradiation for the PV source and the different SOCs of the battery on the system's ability to operate under load changes.

Table 5. 3global system parameters

PV module	**value**
Max power	60 w
Max voltage	17.1 V
Max current	3.5 A
Series modules	5
Parallel modules	3
PEMFC	**value**
A	$70cm^2$
$\varepsilon_1, \varepsilon_2\ \varepsilon_3\ \varepsilon_4$	$-0.944, 0.0354, 7.5 \times 10^{-8}, 1.96 \times 10^{-4}$
Rc	15×10^{-4}
Jmax	$1.7 A/cm^2$
BATTERY	**Value**
Number of series battery 12v	8
Nominal voltage	96 V
Rated capacity	14 Ah
Converters parameters	**Value**
C_{dc}	1100×10^{-6} F
Buck boost	
C_{in}	1×10^{-4} F
L	40×10^{-3} H
Boost	
L	0.05 H
Bi-directional	
C_{in}	1×10^{-4} F
L	1×10^{-2} H

The following results are presented in order: PV-PEMFC-battery powers and Load power waveforms, DC bus voltages, and SOCs of the battery, and finally Efficiency of the global system in different cases. In this scenario, the temperature is fixed at 25°C and the irradiation varies from 700W/m2 to 1000W/m2, we divide this scenario into three cases depending on the state of charge of the battery (SOC), first case SOC>SOCmin (LOW), second case SCOmin<SOC<SOCmax (medium) and third cas SOC>SOCmax (hight) and the load-interval of the load = [1000W-1900W]. Figure (5.7) shows the load demand profile, the maximum power of the load is 1900W and the minimum value equal to 1000W and it divided into time intervals as following:1000W ∈ [0 s-1.5s] 1500W∈ [1.5s -3s], 1200W∈ [3s-4.5], 1900w∈ [4.5s-6s] and 1700W∈ [6s-7.5s] illustrated in figure (5-7). As represented in figure (5-8) the irradiation profile is divided in the interval time as follows: 700W ∈ [0 s-1.5s] 800W∈ [1.5s -3s], 1000W∈ [3s-4.5s], 900w∈ [4.5s-6s] and 700W∈ [6s-7.5s].

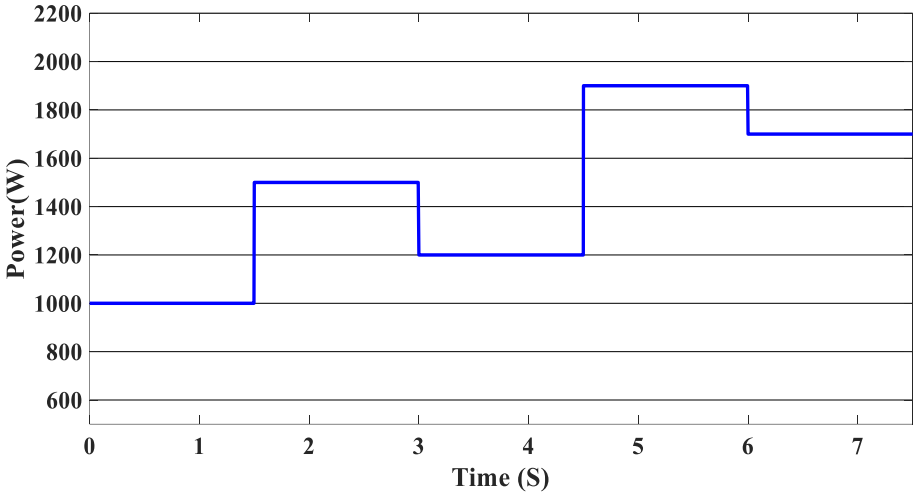

Figure 5. 7load demand profile

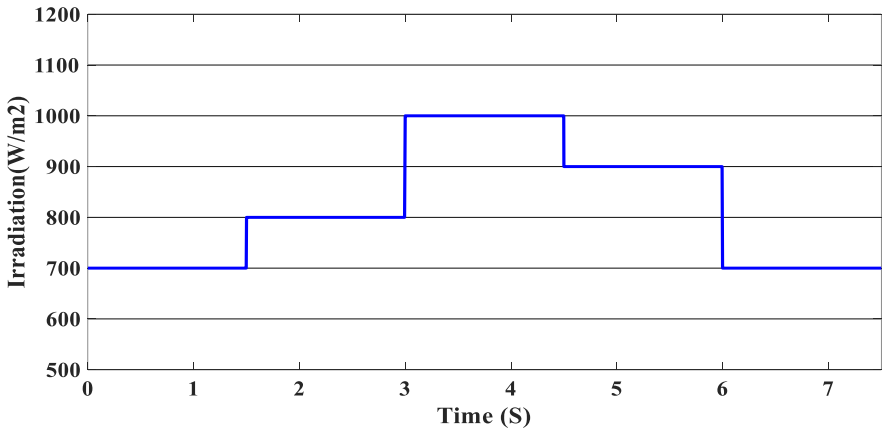

Figure 5. 8 Irradiation profile.

- **Case 1 :SOC<SOC$_{min}$:**

Figure (5.9) illustrates the changes in the power curves of the battery, PEMFC, and PV, as well as the load demand power of the hybrid generation systemThe highest power produced by the photovoltaic system is 903 W, and the maximum power produced by the PEMFC is 1.350 Kw.

At the time interval [0-1.5s] the PV irradiation equal to 800w/m2 and the maximum power is equal to 670 w which is less than the load demand, at the same time to reach 1000 w which is the load demand, the PEMFC system generated 646W to fulfill the need load demand and charge the battery at the same time because the SOC of the batteries is less than SOC$_{min}$ which equal to 20%. Next, the time interval is equal to [1.5s – 3 s] the load demand is equal to 1500W, to reach this value the PV system irradiation is equal to 800w/m2 and generates a power equal to 743W, this value is not enough to fulfill the load damande, in this case, the

PEMFC generate a power equal to 1.197Kw to fill the need of the load demand and charge the batteries.

From 3 s to 4.5 the power generated from the PV system = 903 W at the irradiation value equale to 1000W/m2, the request power higher than the PV power and equal to 1200W in this case the PEMFC generated a power = 646 W this power can fulfill the needed of the load power and the excess power charge the batteries. AT 4.5 s the demand power is high and equal to 1900 W which is higher than the PV system power equals = 832 W which means we need more power, the need for the power is generated from the PEMFC system = 832 W, and the excess power goes to the batteries directly to charge them. Finely in the time interval [6s – 7.5s] the load demand = 1700 W, it's higher than the PV system maximum power means the PEMFC generates a power equal to 1.197KW to fulfill the need of the power needed in the load and charges batteries. Figure (5.10) represents the load reference and load power generated by the hybrid system we can see that the power generated follows the reference load which means the efficiency of the proposed SM Control.

Figure (5.11) illustrates the DC link voltage, the reference value equal to 180W we noticed that the bus voltage tracks the reference efficiently, the picks in the 1.5s,3s,4.5s, and 6 s caused by the change in the load demand we see there is a deviation from the reference and return rapidly to tracks the reference value. Figure(5.12) represents the SOC of the batteries we notice that the batteries, in this case, are charging no matter what the value of the load demand, the power generated from the PEMFC system supplies the power to the load and charges the battery because the SOC of the batteries is less than the SOC_{min}. Figure (5.13) depicts the calculated efficiency of the globe hybrid (buck-boost converter, boost converter, and bi-directional DC/DC converter) during the change in irradiation. This is the case when the SOC is lower than the SOCmin, moreover, the average of power between the input and output sides of converters is used to generate the visualized figure of the global system's (PV source (Buck-Boost), PEMFC (BOOST), and batteries (Bi-directional)) efficiency. the efficiency of the hybrid system is summarized in table 5.4 below

Table 5. 4 Efficiency of the globle system (SOC<SOCmin)

Time	**Load demande (W)**	**Efficiency (%)**
[0s-1.5s]	1000W	95%
[1.5s-3s]	1500W	96%
[3s-4.5s]	1200W	95.5%
[4.5s-6s]	1900W	96%
[6s-7.5s]	1700W	96%

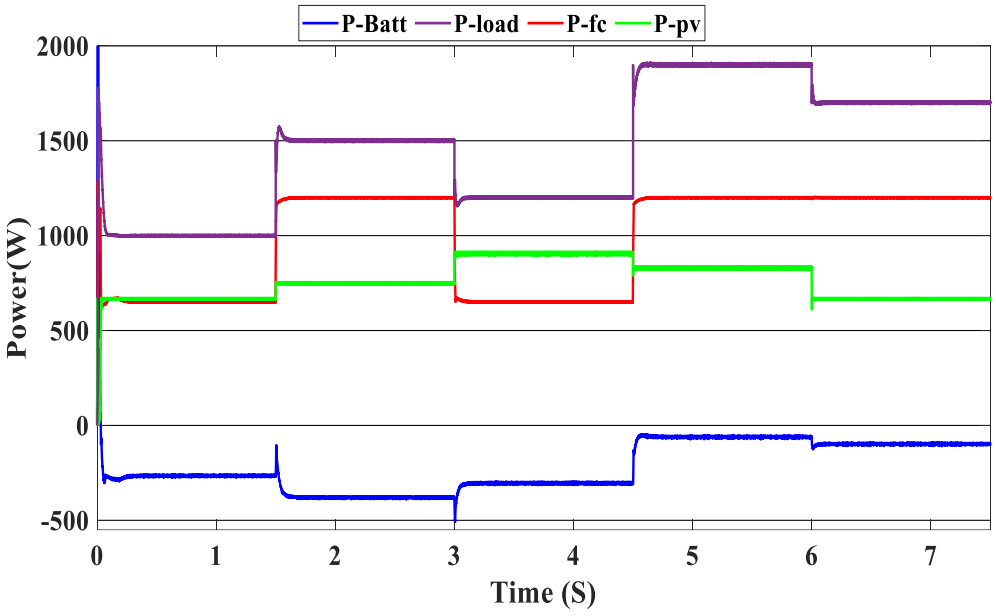

Figure 5. 9power generated by the hibryd system (SOC<SOCmin).

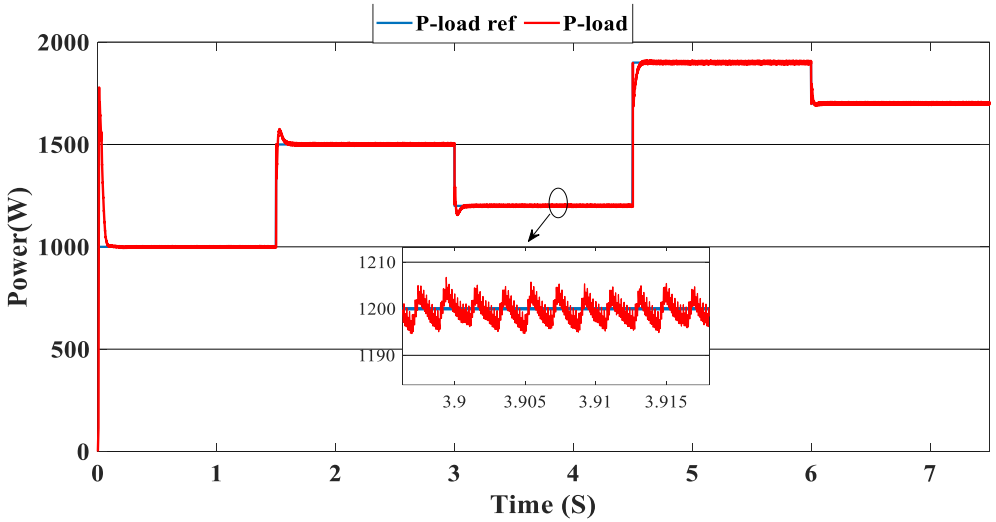

Figure 5. 10load power generated from the hybrid system (SOC<SOCmin).

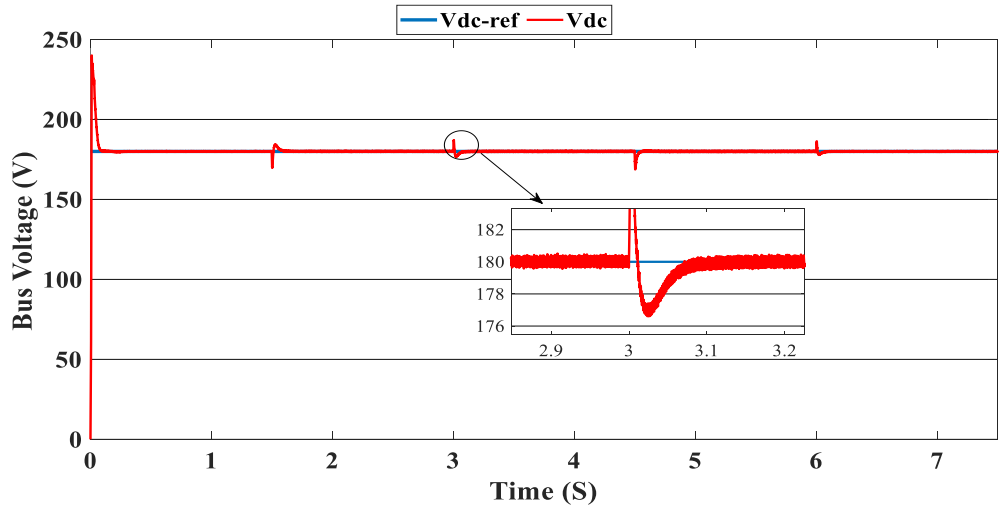

Figure 5. 11 DC bus voltage (SOC<SOCmin).

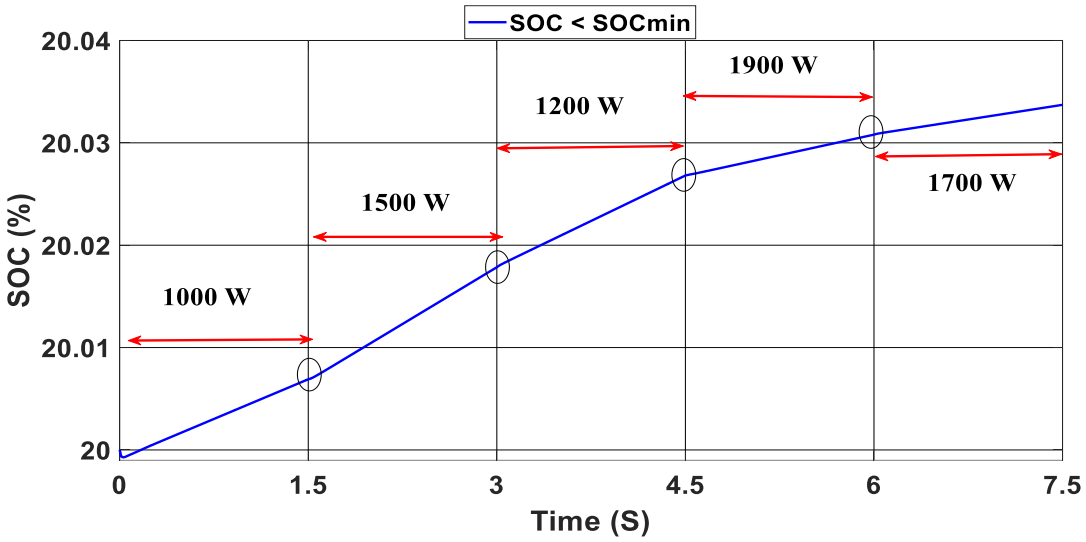

Figure 5. 12SOC of the batteries (SOC<SOCmin).

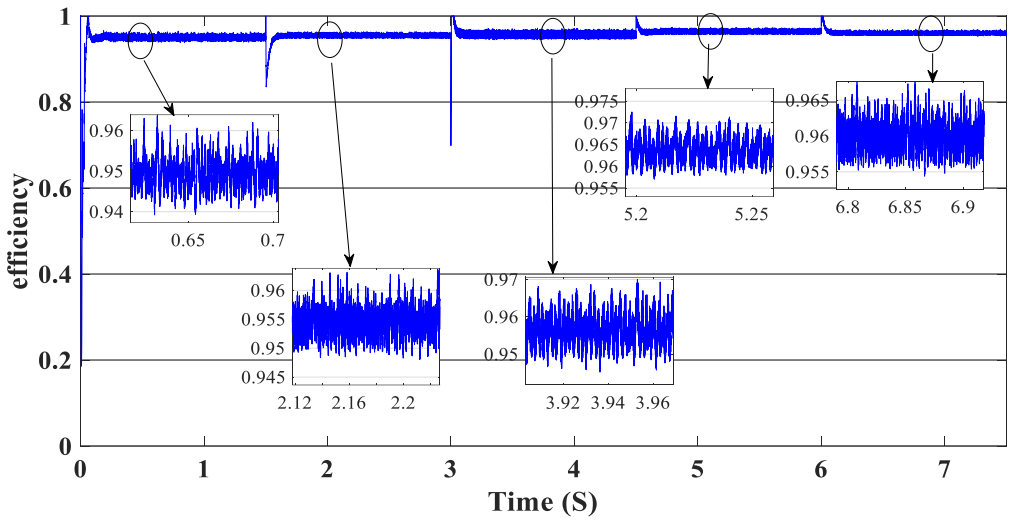

Figure 5. 13Efficiency of the globle hybrid system (SOC<SOCmin).

- **SOC_{min}< SOC <SOC_{max}**

In this case, we suppose the SOC =65% which means it's between SOC_{max} and $SOC_{min}$and the PV irradiance profile as we can see in Figure (5.8) starts from 700W/m2 to 1000W/m2 with a sudden change in 1.5s,3s,4.5, and 6s respectively. and the variation in load power demand mentioned in figure (5.7).

Figure(5.14) shows the electricity produced by the PV system, PEMFC system, and storage. Additionally, when the demand is 1000W and the PV system is producing 670W, This indicates that we need more power to carry out the load because this power is less than the load requirement.

In this instance, the PEMFC system produces a power of 646W, which is more than enough to carry out the load and fully charge the batteries.In the following time interval [1.5s-3s] the PV's irradiation changes from 700 watts per square meter to 800 watts per square meter, the

PV system produces more power equal to 754 watts, and at the same time the load demand increases to 1500 watts, the power is insufficient to meet the demand. In this case, the PEMFC and the batteries generate a power (740 watts from the PEMFC and 62 watts from the batteries).In the next time 3s, the power of the load decreased to 1200 w the PV generates power equal to 912 w/m2 while the irradiation is equal to 1000W, we need more energy to meet the load demand, in this case, the PEMFC generates power equal to 646 W and its enough and the exceed power go to charge the batteries.

The load demand increased to 1900W during the following time frame [4.5s to 6s], which indicates that neither the PV nor the PEMFC could meet the load's requirements. In this situation, the batteries produced enough power to meet the load's demand. The precise duration range is [6 s to 7.5s] The PV system cannot satisfy the requirements when the load is reduced to 1700W and the sunlight is equivalent to 700W/m2, so the PEMFC and batteries generate the necessary power as shown in the figure (5.14).

Figure (5.15) illustrates the required load. As can be seen, the power produced by the PV+PEMFC batteries tracks the reference load power, indicating that the suggested SMC operates effectively. next figure(5.16). shows the bus voltage, as can be seen, the bus voltage tracks the 180 V reference voltage. However, we also observed that the bus voltage deviates from the reference when the load demand changes and we quickly return to tracking the reference voltage with a small response time. next, figure(5.17) the state of charge of the batteries in the interval time[0-1.5s] the batteries charge because there is a exceeded power from the (PV+PEMFC), next from 1.5s to 3 s the batteries discharge because the PV+PEMFC can't satisfy the load demand so the battery gives a power,[3s-4.5]the batties charge finally in the interval time [4.5s-7.5] the batteries discharge no matter the load power value because we need the power to fulfill the needs of the load. the final figure, in this case, Figure(5-18) represents the efficiency of the global system, in this case, the SOC is belonged to the interval SOC_{min} and SOC_{max}, from the figure we can notice that the lowest efficiency = 95%, and the maximum effecency=97%, the table. 5.5 below summarized the figure founds.

Table 5. 5efficiency of the globle system (SOCmax<SOC<SOCmax)

Time	**Load demande (W)**	**Efficiency (%)**
[0s-1.5s]	1000W	95%
[1.5s-3s]	1500W	95.5%
[3s-4.5s]	1200W	95.5%
[4.5s-6s]	1900W	97%
[6s-7.5s]	1700W	96.5%

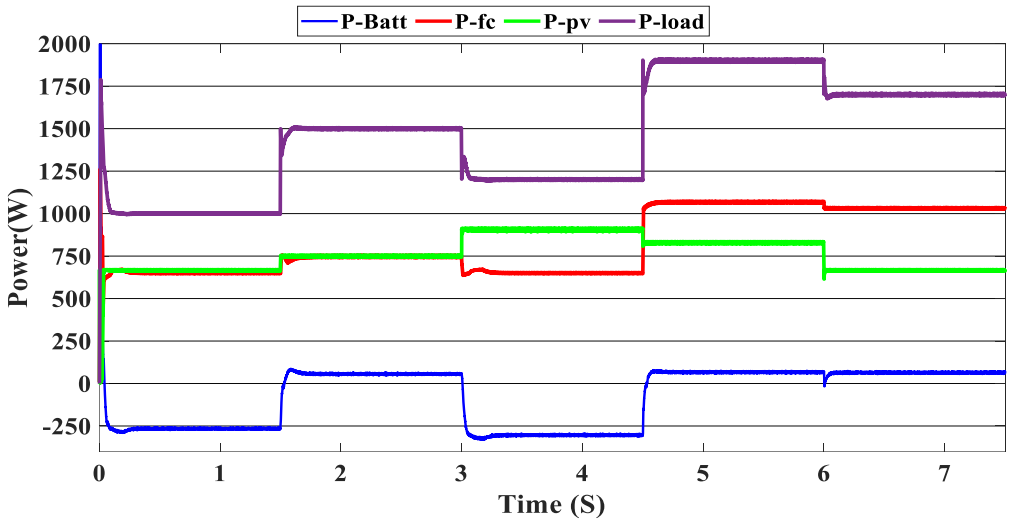

Figure 5. 14power generated by the hibryd system (SOCmin< SOC <SOCmax).

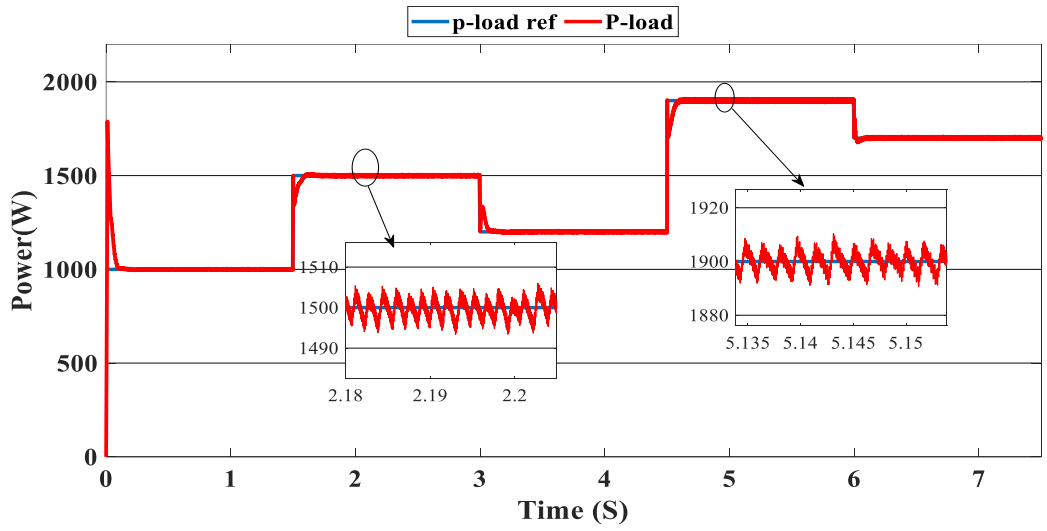

Figure 5. 15load demande power (SOCmin< SOC <SOCmax).

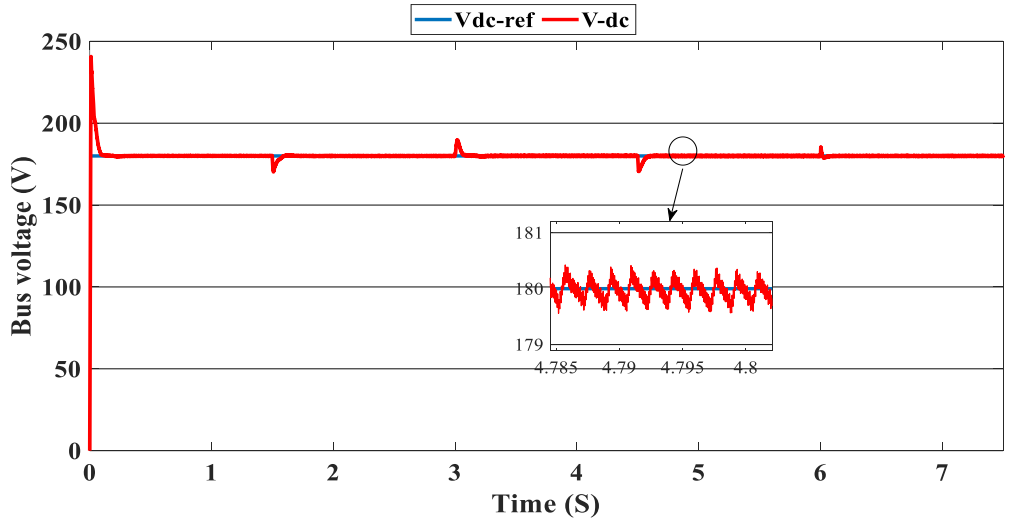

Figure 5. 16 DC-bus voltage (SOCmin< SOC <SOCmax).

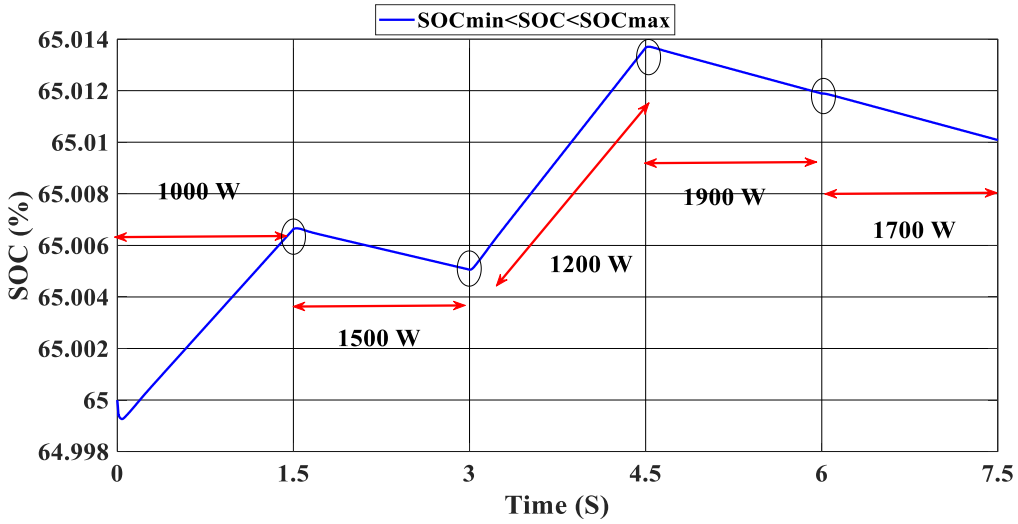

Figure 5. 17SOC of the batteries (SOCmin< SOC <SOCmax).

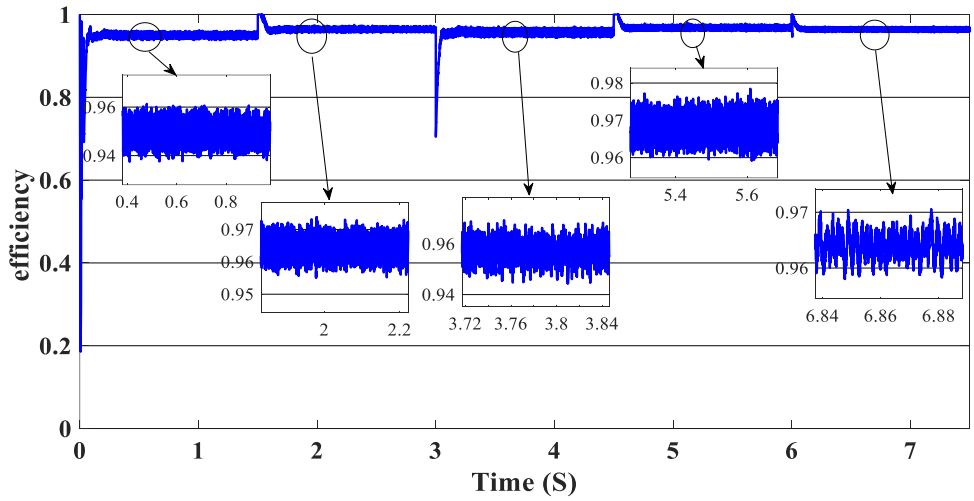

Figure 5. 18the efficiency of the hybrid system (SOCmin< SOC <SOCmax).

- **SOC>SOC$_{max}$:**

In this case, the state of the charger is higher than SOC max which is equal to 88% to test the objective of the global proposed system like the previous cases at the same irradiation profile and the load demand, figure(5.19) represents the power generated from the renewable hybrid source (PV,PEMFC and batteries) and the load power, the load power is always higher than the primary source (PV), in the first interval [0.1.5s] the PV system generates a power not enough the fulfill the load demand, in this case, the batteries generate power to meet the needs, and the PEMFC also generates a minimum power to support the batteries.

, next at 1.5s the irradiation change to 800W/m2 the power generated from the primary source(PV) is lower than the load demand this case like the previous one the Batteries still discharge and the PEMFC supports the needs of the power needs when the(PVand batteries) cant meets the need of the Load, now comes the interval time [3s-4.5s] in this time the load demand 1200w which means the PV, batteries and PEMFC) must generate power to fulfill

the load and that is what we can see from the figure, that the (Batteries and PV) generate a power to fulfill the Load and the PEMFC work in a lower value to support the needs. next, when the irradiation is equal = to 900W/m2 in the time interval [4.5-6s] the PV produces power, and the Batteries also discharge, and the need for the power to fulfill the load compensate by the PEMFC. Finely in when the interval time [6-7.5s] the power from the primary source (PV) produces low power in the previous state the batteries still discharging and the PEMFC gives the same value of the power to complete the (PV and batteries) to meet the load demand that equals to 1700W. Figure (5.20) represents the load demand as we can see that the load follows the reference load with a small time response when we change the Load value. Figure (5.21) depicts the DC link voltage. As can be seen, the DC bus voltage follows the standard (180V), with deviations occurring every 1.5s, 3s, 4.5s, and 6s. Figure (5.22) represents the SOC of the batteries with the initial value equal to 88% >SOCmax, in this case, the batteries must discharge Whatever the value of the load and the primary source this objective is fulfilled and the figure proves that. the final figure(5.23) represents the efficiency of the globe system, the efficiency of the global system for different load demand values is summarized in the table. 5.6 below.

Table 5. 6 Efficiency of the globle (SOC>SOCmax).

Time	Load demande (W)	Efficiency (%)
[0s-1.5s]	1000W	96%
[1.5s-3s]	1500W	96.5%
[3s-4.5s]	1200W	96.5%
[4.5s-6s]	1900W	97.5%
[6s-7.5s]	1700W	97%

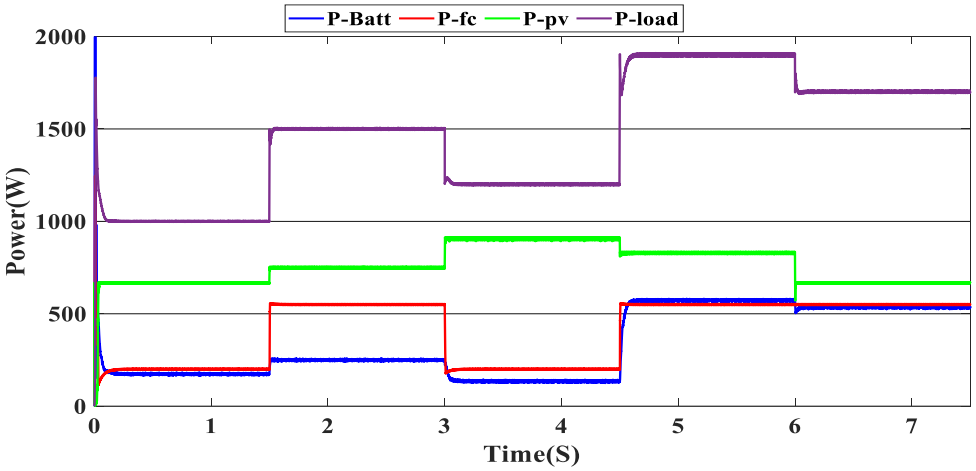

Figure 5. 19power generated by the hibryd system (SOC>SOCmax).

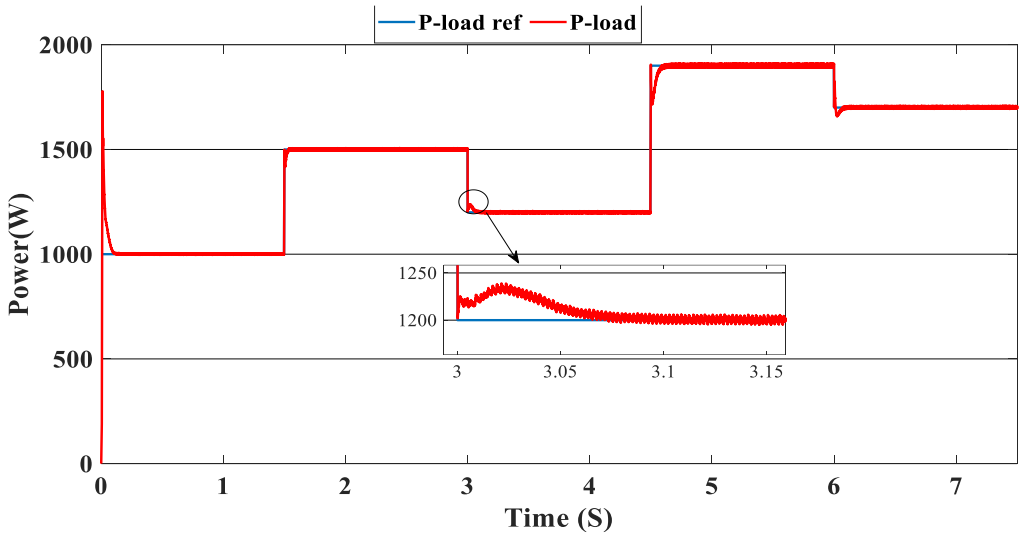

Figure 5. 20 Load demand (SOC>SOCmax).

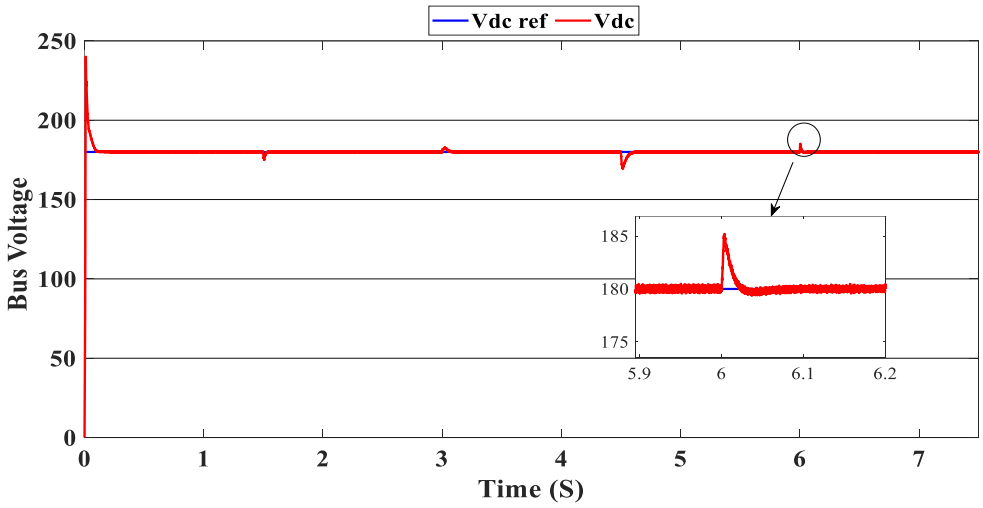

Figure 5. 21 DC link voltage (SOC>SOCmax).

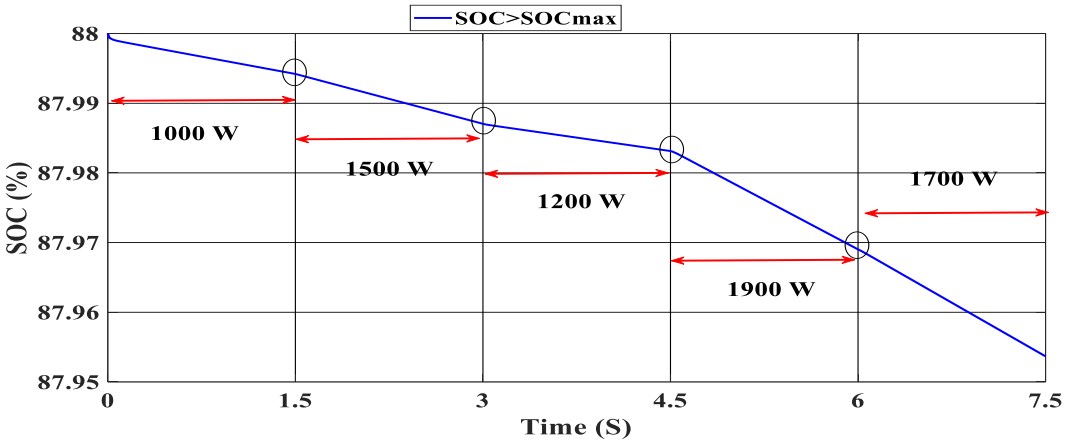

Figure 5. 22SOC of the batteries (SOC>SOCmax).

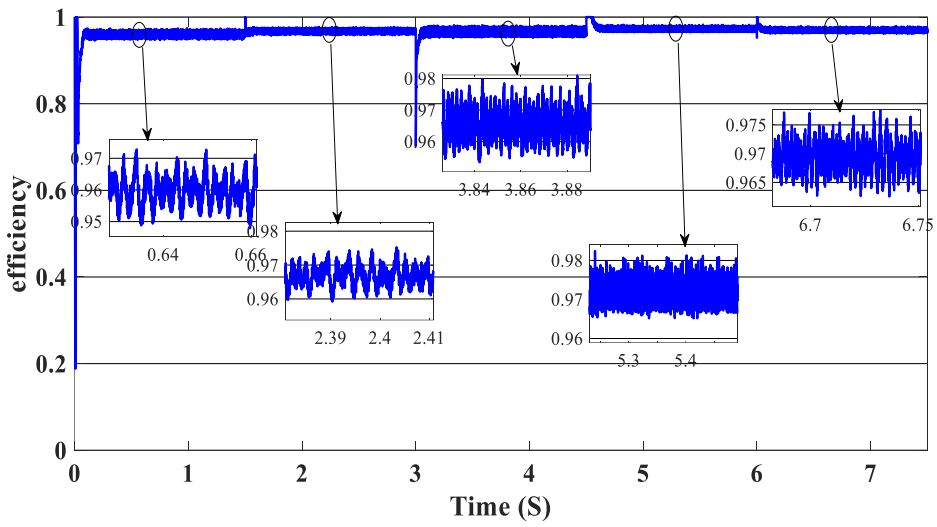

Figure 5. 23 Efficiency of the hybrid system (SOC>SOCmax).

5.6 Conclution

The primary goal of this work is to give a strategy for the multi-source green system's parts' energy management. The numerous simulated tests that are shown as examples support the decisions made regarding a stand-alone application. Power control and choosing the best components are important considerations when building MSRS.State machine control of MSRS, described in this article, is created up of a PV module, a fuel cell (PEMFC), and a pack of batteries.The solar panels serve as the main supply in this system, and the PEMFC serves as the principal reserve. (long-term supply). If necessary, a battery pack is used to meet load requirements.All energy sources are connected to a shared DC bus through power converters, which are regulated to accomplish appropriate energy management.Through the modeling and analysis of this paper, we can conclude that the proposed state machine control for the multi-source renewable system work successfully moreover the DC bus value is constant with divination when we change the load and PV irradiation, the PEMFC work in all proposed case as a long term supply back up, and charge the battery while the battery as a third back up when the sources don't meet the load needs. and for future work, its recommended to connect this system to the grid to inject the surplus power into the grid.

Chapter 6 Conclusions

6.1 General conclusion

In order to improve the energy harvesting from PV arrays and PEMFC and to inject the generated PV power and PEMFC into the grid with high grid current quality, grid-connected PV systems have been extensively researched in a number of research works.Additionally, a hybrid system energy management plan has been put out to provide DC loads The research studies given in this dissertation examined a number of appropriate conversion topologies and efficient control strategies for grid-connected PV systems and PEMFC systems.Grid-connected PV systems and PEMFC systems topologies have been investigated in this dissertation to obtain the best way to achieve a high energy harvesting capability and a high-performance operation as well as maintain the simplicity of the control design for these topologies. From these topologies, the dual-stage configuration has been considered in low-power grid . Furthermore, the advantages provided by dual-stage configuration have been combined with efficient grid-side multilevel converters in order to inject the produced PV power and PEMFC power with high-performance operation tha meas the the THD% must be less thean 5% , On the other hand, several controllers based on the Finite control set model predictive control for multilevel inverter and fuzzy logic for DC/DC side have been proposed for the presented topologies. The purposes of the controllers are: track the MPP rapidly and accurately under sudden irradiation changes for PV and pressures and temperature for PEMFC, regulate the DC-link voltage to its desired value, and guarantee the balance of DC-link voltage capacitors in case using multilevel NPC inverters, and F-type inverters and inject the produced PV current and PEMFC current into the grid with achieving a high grid current quality. The major weaknesses of the MPC (variable inherent switching frequency and computational burden) .The proposed control schemes for the investigated grid-connected PV topologies and PEMFC topologies have been validated through MATLAB simulations The research results presented in this dissertation promote the proposed control schemes based on FCS-MPC as a simple, efficient, and high-performance control tool for low, medium, power grid-connected PV systems and PEMFC. The topologies and control schemes presented in this dissertation can be employed in other power electronics and energy system applications

In the second part of this dissertation Hybrid renewable energy systems (HRES) need to be properly planned with appropriate integration of different types of renewable energy and energy storing techniques.To detect, watch, and handle the behavior of the mixed energy sources, an energy management system built on a control strategy is required.Battery state of charge (SOC), Photovoltaic power and load demand are used as inputs to construct the energy management strategy in green multi-source power systems (solar system fuel cells and

batteries)to maximize cost savings and battery lifespan extensions, these factors are crucial.This dissertation offers a PV-PEMFC-Batteries energy management strategy (EMS) that aims to meet the following goals: keep the DC link steady at the standard value; increase battery lifespan; and meet power demand.The suggested multi-source renewable system (MSRS) is made to meet load demand while using extra power to fill batteries.The MSRS depends on the photovoltaic as a primary source, it is controlled by Fuzzy logic MPPT to ensure that the PV work at its maximum power during different irradiation condition.The fuel cell (PEMFC) we consider it as a secondary source and has an objective: to support the needs of the load and charge the batteries of the SOC is lower than the minimum value and the third one are the batteries are working when the PV-PEMFC can't fulfill the load demand.the proposed stat machine control (SMC) has fifteen states, moreover, the SMC gives the priority to the PEMFC to work as a secondary source and charge the battery when we have an exceeded power and the SOC is low.The MSRS is made achievable by carefully orchestrated control and electricity management. Results from simulations using the MATLAB/Simulink software tools are used to confirm the accuracy and veracity of the modeling and management technique.

6.2 Author's contribution

The main contributions of this dissertation can be summed up as follows:

1. **A comprehensive analysis of control strategies for dual-stage grid-connected photovoltaic and dual-stage grid-connected proton exchange membrane fuel cell (PEMFC) systems:**

This text briefly discusses and compares a range of conventional and advanced Maximum Power Point Tracking (MPPT) techniques, DC-link voltage regulators, and grid power/current control techniques.

2. **Examination of three-level NPC inverters in photovoltaic (PV) systems and proton exchange membrane fuel cell (PEMFC) systems that are connected to the power grid:**

The utilization of the characteristics of three-level Neutral Point Clamped (NPC) inverters has been employed to facilitate the injection of photovoltaic (PV) power and Proton Exchange Membrane Fuel Cell (PEMFC) power with the highest efficiency.

3. **Three-level single phase F-type inverters are investigated in grid-connected PEMFC system:**

The features of Three-level single phase F-type invertershave been exploited in order to inject the mediumproduced PEMFC power with high performance operation.

4. **Finite set model predictive control for two-step is proposed to control grid-connected three-level NPC inverters for PV/PEMFC system application:**

The utilization of a Fuzzy Logic Maximum Power Point Tracking (FL-MPPT) technique has been implemented in both the buck-boost converter for the purpose of maximizing the power output generated by the photovoltaic (PV) array, as well as in the boost converter to maximize the power output produced by the proton exchange membrane fuel cell (PEMFC). Furthermore an FCS-MPCTS is proposed to control the three-level NPC inverter.The suggested controllers serve multiple objectives, including the rapid and precise tracking of the maximum power point (MPP) for photovoltaic (PV) systems in response to sudden changes in irradiation, as well as for proton exchange membrane fuel cells (PEMFC) in response to sudden changes in temperature and pressure. Additionally, these controllers ensure balance in the voltage of the two DC-Link capacitors, injecin jecte the current in tho grid and minimize switching frequency.The obtained results demonstrate that a significant enhancement by applying the proposed control .where the fuzzy logic MPPT technique offers superior tracking capabilities with respect to power oscillations, speed, and precise tracking during irradiation variation for PV and temperature and pressure variation for PEMFC.In addition, the regulation of $ig\alpha-\beta$ currents is achieved, ensuring that DC-Link capacitor voltages are precisely balanced and high-quality grid currents THD%.

5. **Finite set model predictive control Current control is proposed to control grid-connected three-level single phase F-Type inverters for PEMFC system application:**

an FCS-MPCC is proposed to control the three-level single-phase Ftype inverter. The suggested controllers serve two objectives. including the rapid and precise tracking of the maximum power point (MPP) for proton exchange membrane fuel cells (PEMFC) in response to sudden changes in temperature and pressure. Additionally, these controllers ensure balance in the voltage of the two DC-Link capacitors, injection of the current in the grid.where the fuzzy logic MPPT technique offers superior tracking capabilities with respect to power oscillations, speed, and precise tracking during temperature and pressure variation for

PEMFC. In addition, the regulation of $ig\alpha$−β currents is achieved, ensuring that DC-Link capacitor voltages are precisely balanced and high-quality grid currents THD%.

6. **A state machine energy management strategy for multi-source storage system:**

The aim of utilizing state machine control (SMC) is to exert comprehensive control over the power system and establish the current reference for various converters that regulate the power system components according to the energy balance of the system.The implementation of the proposed technique enhances the dynamic performance of multi-source storage systems that consist of a PV array , PEM fuel cell, and a pack of batteries in the face of severe transients resulting from variations in load demands and output power from solar photovoltaic array.The simulation results proposed SMC, fulfills the objective where the DC-linK is balanced and meets the load needs.

6.3 Future works

- Development of new MPPT algorithms that take into consideration the partially shaded condition
- Applying suggested control strategies with additional multilevel inverter topologies
- investigation of DC-DC multilevel converter topologies for grid-connected PV and PEMFC
- Development and energy management control for hybrid multi-source grid connected
- Investigation of LCL filters for the grid-connection with the design of an effective model predictive controller.
- Dvlopment an Intelligent energy management strategies for grid connection using a Multilevel inverter.

List of Publications

International Conference

Badreddine Kanouni, Abd Essalam badoud, and Saad. Mekhilef, "Predictive control and highly efficient of dual-stage Grid-connected PV System", International Conference on Innovative Applied Energy (Smart Exhibition) (DZENERGY 2021), 26 To 27 March 2021, Hassi Messaoud, Ouargla. ALGERIA.

Badreddine Kanouni, Abd Essalam badoud, and Saad. Mekhilef "Comparative study of fuzzy logic and P&O MPPT controllers for PEM Fuel Cell system", 1st International Conference on Sustainable Energy and Advanced Materials IC-SEAM'21 April 21-22, 2021, Ouargla, ALGERIA.

Rai N, Abbadi A, Hamidia F, **Kanouni B**, Kahlessenane A. A New Modified Incremental Conductance Algorithm Used for PV System BT - Artificial Intelligence and Heuristics for Smart Energy Efficiency in Smart Cities. In: Hatti M, editor., Cham: Springer International Publishing; 2022, p. 256–65.DOI: 10.1007/978-3-030-92038-8_26

Badoud AE, **Kanouni B,** Mekhilef S. FSC - MPC for single-stage grid connected PV system. 2022 19th International Multi-Conference on Systems, Signals & Devices (SSD), 2022, p. 768–72. https://doi.org/10.1109/SSD54932.2022.9955648.

Kanouni B, Badoud AE, Mekhilef S. Predictive current control two step of a single-phase inverter for grid connected PEMFC system. 2022 19th International Multi-Conference on Systems, Signals & Devices (SSD), 2022, p. 538–43. https://doi.org/10.1109/SSD54932

Kanouni B, Badoud AE, Mekhilef S. A SMC-Based MPPT Controller for Proton Exchange Membrane Fuel Cell System. 2022 19th International Multi-Conference on Systems, Signals & Devices (SSD), 2022, p. 527–31. https://doi.org/10.1109/SSD54932.2022.9955704.

- **Journal Papers**

Kanouni B, Badoud AE, Mekhilef S. A multi-objective model predictive current control with two-step horizon for double-stage grid-connected inverter PEMFC system. International Journal of Hydrogen Energy 2022;47:2685–707.

https://doi.org/https://doi.org/10.1016/j.ijhydene.2021.10.182. Impact Factor in january 2022:5.8)

KANOUNI B, BADOUD AE, MEKHILEF S. Fuzzy logic MPPT control algorithm for a Proton Exchange Membrane Fuel Cells System. Algerian Journal of Renewable Energy and Sustainable Development 2021;03:13–22. https://doi.org/10.46657/ajresd.2021.3.1.2.

Referance :

[1] Yimen N, Tchotang T, Kanmogne A, Abdelkhalikh Idriss I, Musa B, Aliyu A, et al. Optimal sizing and techno-economic analysis of hybrid renewable energy systems—A case study of a photovoltaic/wind/battery/diesel system in Fanisau, Northern Nigeria. Processes 2020;8:1381.

[2] Report GS. Renewables 2023 global status report. 2023.

[3] Lakhdara A, Bahi T, Moussaoui A. Study and Management of an Hybrid System Connected to The Network. Journal of Electrical Systems 2022;18:163–72.

[4] Kumar R, Gupta RA, Bansal AK. Economic analysis and power management of a stand-alone wind/photovoltaic hybrid energy system using biogeography based optimization algorithm. Swarm and Evolutionary Computation 2013;8:33–43.

[5] Sawle Y, Gupta SC, Bohre AK. Review of hybrid renewable energy systems with comparative analysis of off-grid hybrid system. Renewable and Sustainable Energy Reviews 2018;81:2217–35.

[6] Hansen CJ, Bower J. An economic evaluation of small-scale distributed electricity generation technologies. Oxford institute for energy studies; 2003.

[7] Arsad AZ, Hannan MA, Al-Shetwi AQ, Mansur M, Muttaqi KM, Dong ZY, et al. Hydrogen energy storage integrated hybrid renewable energy systems: A review analysis for future research directions. International Journal of Hydrogen Energy 2022;47:17285–312.

[8] Yaramasu V, Wu B, Chen J. Model-predictive control of grid-tied four-level diode-clamped inverters for high-power wind energy conversion systems. IEEE Transactions on Power Electronics 2013;29:2861–73.

[9] Yaramasu V. Predictive control of multilevel converters for megawatt wind energy conversion systems 2014.

[10] Abdelkareem MA, El Haj Assad M, Sayed ET, Soudan B. Recent progress in the use of renewable energy sources to power water desalination plants. Desalination 2018;435:97–113. https://doi.org/https://doi.org/10.1016/j.desal.2017.11.018.

[11] Kamel AA, Rezk H, Abdelkareem MA. Enhancing the operation of fuel cell-photovoltaic-battery-supercapacitor renewable system through a hybrid energy management strategy. International Journal of Hydrogen Energy 2021;46:6061–75. https://doi.org/10.1016/j.ijhydene.2020.06.052.

[12] Hariri MHM, Mat Desa MK, Masri S, Zainuri MAAM. Grid-connected PV generation system-components and challenges: A review. Energies 2020;13. https://doi.org/10.3390/en13174279.

[13] Vinod, Kumar R, Singh SK. Solar photovoltaic modeling and simulation: As a renewable energy solution. Energy Reports 2018;4:701–12. https://doi.org/10.1016/j.egyr.2018.09.008.

[14] Ebrahimi SM, Salahshour E, Malekzadeh M, Francisco Gordillo. Parameters identification of PV solar cells and modules using flexible particle swarm optimization algorithm. Energy 2019;179:358–72. https://doi.org/https://doi.org/10.1016/j.energy.2019.04.218.

[15] Diab AAZ, Sultan HM, Aljendy R, Al-Sumaiti AS, Shoyama M, Ali ZM. Tree growth based optimization algorithm for parameter extraction of different models of photovoltaic cells and modules. IEEE Access 2020;8:119668–87.

[16] Yang B, Wang J, Zhang X, Yu T, Yao W, Shu H, et al. Comprehensive overview of meta-heuristic algorithm applications on PV cell parameter identification. Energy Conversion and Management 2020;208:112595. https://doi.org/10.1016/j.enconman.2020.112595.

[17] Jariwala D, Howell SL, Chen KSK, Kang J, Sangwan VK, Filippone SA, et al. Integrated High-Performance Infrared Phototransistor Arrays Composed of Nonlayered PbS-MoS2 Heterostructures with Edge Contacts. Nano Letters 2016;16:1–9.

[18] Reddy KJ, Sudhakar N. ANFIS-MPPT control algorithm for a PEMFC system used in electric vehicle applications. International Journal of Hydrogen Energy 2019;44:15355–69. https://doi.org/10.1016/j.ijhydene.2019.04.054.

[19] Kinjyo Y, Asato B, Yona A, Senjyu T, Funabashi T, Kim C-H. Optimal Operation of Smart Grid with Fuel Cell in Isolated Islands. Journal of International Council on Electrical Engineering 2012;2:423–9. https://doi.org/10.5370/JICEE.2012.2.4.423.

[20] Kavousifard A. Impact of thermal recovery and hydrogen production of fuel cell power plants on distribution feeder

reconfiguration. IET Generation, Transmission & Distribution 2012;6:831-843(12).

[21] Stamatakis E, Yiotis A, Giannissi S, Tolias I, Stubos A. Modeling and simulation supporting the application of fuel cell & hydrogen technologies. Journal of Computational Science 2018;27:10–20. https://doi.org/https://doi.org/10.1016/j.jocs.2018.05.003.

[22] Pei P, Jia X, Xu H, Li P, Wu Z, Li Y, et al. The recovery mechanism of proton exchange membrane fuel cell in micro-current operation. Applied Energy 2018;226:1–9. https://doi.org/https://doi.org/10.1016/j.apenergy.2018.05.100.

[23] İnci M, Türksoy Ö. Review of fuel cells to grid interface: Configurations, technical challenges and trends. Journal of Cleaner Production 2019;213:1353–70. https://doi.org/10.1016/j.jclepro.2018.12.281.

[24] Wang C, Nehrir MH, Gao H. Control of PEM fuel cell distributed generation systems. IEEE Transactions on Energy Conversion 2006;21:586–95.

[25] Matheus B, … JF-2015 IP, 2015 undefined. Modeling and grid connection of a solid oxid fuel cell (SOFC) based on PQ theory for stationary loads. IeeexploreIeeeOrg n.d.

[26] Cox B, Treyer K. Environmental and economic assessment of a cracked ammonia fuelled alkaline fuel cell for off-grid power applications. Journal of Power Sources 2015;275:322–35. https://doi.org/10.1016/J.JPOWSOUR.2014.11.023.

[27] Sonnde C, Gruber M. Direct methanol fuel cell systems to supply small off-grid industrial equipment. INTELEC, International Telecommunications Energy Conference (Proceedings) 2005:357–60. https://doi.org/10.1109/INTLEC.2005.335119.

[28] Ro K, Rahman S. Two-loop controller for maximizing performance of a grid-connected photovoltaic-fuel cell hybrid power plant. IEEE Transactions on Energy Conversion 1998;13:276–81. https://doi.org/10.1109/60.707608.

[29] Hatziadoniu CJ, Lobo AA, Pourboghrat F, Daneshdoost M. A simplified dynamic model of grid-connected fuel-cell generators. IEEE Transactions on Power Delivery 2002;17:467–73. https://doi.org/10.1109/61.997919.

[30] Benyahia N, Denoun H, Zaouia M, Rekioua T, Benamrouche N. Power system simulation of fuel cell and supercapacitor based electric vehicle using an interleaving technique. International Journal of Hydrogen Energy 2015;40:15806–14. https://doi.org/https://doi.org/10.1016/j.ijhydene.2015.03.081.

[31] Derbeli M, Barambones O, Silaa MY, Napole C. Real-time implementation of a new MPPT control method for a DC-DC boost converter used in a PEM fuel cell power system. Actuators 2020;9:1–22. https://doi.org/10.3390/act9040105.

[32] Derbeli M, Farhat M, Barambones O, Sbita L. Control of PEM fuel cell power system using sliding mode and super-twisting algorithms. International Journal of Hydrogen Energy 2017;42:8833–44.

[33] Percin HB, Caliskan A. Whale optimization algorithm based MPPT control of a fuel cell system. International Journal of Hydrogen Energy 2023;48:23230–41. https://doi.org/10.1016/j.ijhydene.2023.03.180.

[34] Singh SN. Selection of non-isolated DC-DC converters for solar photovoltaic system. Renewable and Sustainable Energy Reviews 2017;76:1230–47.

[35] Gopi A, Saravanakumar R. High step-up isolated efficient single switch DC-DC converter for renewable energy source. Ain Shams Engineering Journal 2014;5:1115–27. https://doi.org/10.1016/j.asej.2014.05.001.

[36] Divya Navamani J, Vijayakumar K, Jegatheesan R. Non-isolated high gain DC-DC converter by quadratic boost converter and voltage multiplier cell. Ain Shams Engineering Journal 2018;9:1397–406. https://doi.org/10.1016/j.asej.2016.09.007.

[37] Mumtaz F, Zaihar N, Tanzim S, Singh B, Kannan R. Review on non-isolated DC-DC converters and their control techniques for renewable energy applications. Ain Shams Engineering Journal 2021;12:3747–63. https://doi.org/10.1016/j.asej.2021.03.022.

[38] Kummara VGR, Zeb K, Muthusamy A, Krishna TNV, Prabhudeva Kumar SVSV, Kim DH, et al. A comprehensive review of DC–DC converter topologies and modulation strategies with recent advances in solar photovoltaic systems. vol. 9. 2020. https://doi.org/10.3390/electronics9010031.

[39] Koski P, Pulkkinen V, Auvinen S, Ihonen J, Karimäki H, Keränen T, et al. Development of reformed ethanol fuel cell system for backup and off-grid applications—system design and integration. 2016 IEEE International Telecommunications Energy Conference (INTELEC), IEEE; 2016, p. 1–8.

[40] Rai R, Bhatia RS, Nijhawan P. Z-Source Inverter based DC-DC converter using SPWM technique for fuel cell application. 2016 IEEE 1st International Conference on Power Electronics, Intelligent Control and Energy Systems (ICPEICES), 2016, p. 1–4. https://doi.org/10.1109/ICPEICES.2016.7853565.

[41] Silva FA. Advanced DC\AC inverters: applications in renewable energy (Luo, FL and Ye, H.; 2013)[book news]. IEEE Industrial Electronics Magazine 2013;7:68–9.

[42] Hawke JT, Krishnamoorthy HS, Enjeti PN. A family of new multiport power-sharing converter topologies for large grid-connected fuel cells. IEEE Journal of Emerging and Selected Topics in Power Electronics 2014;2:962–71.

[43] Rashid MH. Power electronics handbook: devices, circuits, and applications/edited by Muhammad H. Rashid. 2011.

[44] Zorig A, Belkheiri M, Barkat S, Rabhi A. Control of three-level NPC inverter based grid connected PV system. 2015 3rd International Conference on Control, Engineering & Information Technology (CEIT), IEEE; 2015, p. 1–6.

[45] Poorfakhraei A, Narimani M, Emadi A. A Review of Multilevel Inverter Topologies in Electric Vehicles: Current Status and Future Trends. IEEE Open Journal of Power Electronics 2021;2:155–70. https://doi.org/10.1109/ojpel.2021.3063550.

[46] Batarseh MG, Za'ter ME. Hybrid maximum power point tracking techniques: A comparative survey, suggested classification and uninvestigated combinations. Solar Energy 2018;169:535–55. https://doi.org/10.1016/j.solener.2018.04.045.

[47] Baimel D, Shkoury R, Elbaz L, Tapuchi S, Baimel N. Novel optimized method for maximum power point tracking in PV systems using Fractional Open Circuit Voltage technique. 2016 International Symposium on Power Electronics, Electrical Drives, Automation and Motion (SPEEDAM), 2016, p. 889–94. https://doi.org/10.1109/SPEEDAM.2016.7525984.

[48] Saravanan S, Ramesh Babu N. Maximum power point tracking algorithms for photovoltaic system - A review. Renewable and Sustainable Energy Reviews 2016;57:192–204. https://doi.org/10.1016/j.rser.2015.12.105.

[49] Ahmadi S, Abdi S, Kakavand M. Maximum power point tracking of a proton exchange membrane fuel cell system using PSO-PID controller. International Journal of Hydrogen Energy 2017;42:20430–43. https://doi.org/https://doi.org/10.1016/j.ijhydene.2017.06.208.

[50] Li Z. UNIVERSIT E Doctor of the Aix-Marseille University 2014.

[51] Enrique JM, Andújar JM, Bohórquez MA. A reliable, fast and low cost maximum power point tracker for photovoltaic applications. Solar Energy 2010;84:79–89. https://doi.org/https://doi.org/10.1016/j.solener.2009.10.011.

[52] Rezk H, Fathy A. Performance improvement of PEM fuel cell using variable step-size incremental resistance MPPT technique. Sustainability (Switzerland) 2020;12. https://doi.org/10.3390/su12145601.

[53] Saravanan S, Babu NR. Performance analysis of boost & Cuk converter in MPPT based PV system. 2015 International Conference on Circuits, Power and Computing Technologies [ICCPCT-2015], IEEE; 2015, p. 1–6.

[54] Park S-H, Cha G-R, Jung Y-C, Won C-Y. Design and application for PV generation system using a soft-switching boost converter with SARC. IEEE Transactions on Industrial Electronics 2009;57:515–22.

[55] Silva FA. Power electronics and control techniques for maximum energy harvesting in photovoltaic systems (Femia, N. et al; 2013)[Book News]. IEEE Industrial Electronics Magazine 2013;7:66–7.

[56] Hussein KH, Muta I, Hoshino T, Osakada M. Maximum photovoltaic power tracking: an algorithm for rapidly changing atmospheric conditions. IEE Proceedings-Generation, Transmission and Distribution 1995;142:59–64.

[57] Liu F, Duan S, Liu F, Liu B, Kang Y. A variable step size INC MPPT method for PV systems. IEEE Transactions on Industrial Electronics 2008;55:2622–8.

[58] Tey KS, Mekhilef S. Modified incremental conductance MPPT algorithm to mitigate inaccurate responses under fast-changing solar irradiation level. Solar Energy 2014;101:333–42. https://doi.org/https://doi.org/10.1016/j.solener.2014.01.003.

[59] Li J, Wang H. A novel stand-alone PV generation system based on variable step size INC MPPT and SVPWM control. 2009 IEEE 6th International Power Electronics and Motion Control Conference, IEEE; 2009, p. 2155–60.

[60] Lee JH, Bae H, Cho BH. Advanced incremental conductance MPPT algorithm with a variable step size. 2006 12th International Power Electronics and Motion Control Conference, IEEE; 2006, p. 603–7.

[61] Hsieh G-C, Hsieh H-I, Tsai C-Y, Wang C-H. Photovoltaic power-increment-aided incremental-conductance MPPT with two-phased tracking. IEEE Transactions on Power Electronics 2012;28:2895–911.

[62] Zakzouk NE, Elsaharty MA, Abdelsalam AK, Helal AA, Williams BW. Improved performance low-cost incremental conductance PV MPPT technique. IET Renewable Power Generation 2016;10:561–74. https://doi.org/10.1049/iet-rpg.2015.0203.

[63] Liu Y-H, Huang J-W. A fast and low cost analog maximum power point tracking method for low power photovoltaic systems. Solar Energy 2011;85:2771–80.

[64] El Khateb A, Abd Rahim N, Selvaraj J, Uddin MN. Fuzzy-logic-controller-based SEPIC converter for maximum power point tracking. IEEE Transactions on Industry Applications 2014;50:2349–58.

[65] Leyva R, Olalla C, Zazo H, Cabal C, Cid-Pastor A, Queinnec I, et al. MPPT based on sinusoidal extremum-seeking control in

PV generation. International Journal of Photoenergy 2011;2012.

[66] Liu Y, Baktash C, Beene JR, Havener CC, Krause HF, Schultz DR, et al. Time profiles of ions produced in a hot-cavity resonant ionization laser ion source. Nuclear Instruments and Methods in Physics Research Section B: Beam Interactions with Materials and Atoms 2011;269:2771–80. https://doi.org/https://doi.org/10.1016/j.nimb.2011.08.009.

[67] Larbes C, Aït Cheikh SM, Obeidi T, Zerguerras A. Genetic algorithms optimized fuzzy logic control for the maximum power point tracking in photovoltaic system. Renewable Energy 2009;34:2093–100. https://doi.org/https://doi.org/10.1016/j.renene.2009.01.006.

[68] Bahgat ABG, Helwa NH, Ahmad GE, El Shenawy ET. Maximum power point traking controller for PV systems using neural networks. Renewable Energy 2005;30:1257–68. https://doi.org/https://doi.org/10.1016/j.renene.2004.09.011.

[69] Kottas TL, Boutalis YS, Karlis AD. New maximum power point tracker for PV arrays using fuzzy controller in close cooperation with fuzzy cognitive networks. IEEE Transactions on Energy Conversion 2006;21:793–803.

[70] Tarek B, Said D, Benbouzid MEH. Maximum power point tracking control for photovoltaic system using adaptive neuro-fuzzy "ANFIS." 2013 Eighth international conference and exhibition on ecological vehicles and renewable energies (EVER), IEEE; 2013, p. 1–7.

[71] Bounechba H, Bouzid A, Nabti K, Benalla H. Comparison of perturb & observe and fuzzy logic in maximum power point tracker for PV systems. Energy Procedia 2014;50:677–84.

[72] Hai T, Zhou J, Muranaka K. An efficient fuzzy-logic based MPPT controller for grid-connected PV systems by farmland fertility optimization algorithm. Optik 2022;267:169636.

[73] Hiyama T. Artificial neural network-polar coordinated fuzzy controller based maximum power point tracking control under partially shaded conditions. IET Renewable Power Generation 2009;3:239-253(14).

[74] Dzung PQ, Lee HH, Vu NTD. The new MPPT algorithm using ANN-based PV. International Forum on Strategic Technology 2010, IEEE; 2010, p. 402–7.

[75] Rai AK, Kaushika ND, Singh B, Agarwal N. Simulation model of ANN based maximum power point tracking controller for solar PV system. Solar Energy Materials and Solar Cells 2011;95:773–8. https://doi.org/https://doi.org/10.1016/j.solmat.2010.10.022.

[76] Anh HPH. Implementation of supervisory controller for solar PV microgrid system using adaptive neural model. International Journal of Electrical Power & Energy Systems 2014;63:1023–9.

[77] Messalti S. A new neural networks MPPT controller for PV systems. IREC2015 the sixth international renewable energy congress, IEEE; 2015, p. 1–6.

[78] Paul S, Thomas J. Comparison of MPPT using GA optimized ANN employing PI controller for solar PV system with MPPT using incremental conductance. 2014 International Conference on Power Signals Control and Computations (EPSCICON), IEEE; 2014, p. 1–5.

[79] Khanaki R, Radzi MAM, Marhaban MH. Comparison of ANN and P&O MPPT methods for PV applications under changing solar irradiation. 2013 IEEE Conference on Clean Energy and Technology (CEAT), IEEE; 2013, p. 287–92.

[80] Gaur P, Verma YP, Singh P. Maximum power point tracking algorithms for photovoltaic applications: A comparative study. 2015 2nd International Conference on Recent Advances in Engineering and Computational Sciences, RAECS 2015 2016. https://doi.org/10.1109/RAECS.2015.7453430.

[81] Yetayew TT, Jyothsna TR, Kusuma G. Evaluation of Incremental conductance and Firefly algorithm for PV MPPT application under partial shade condition. 2016 IEEE 6th International Conference on Power Systems (ICPS), 2016, p. 1–6. https://doi.org/10.1109/ICPES.2016.7584089.

[82] Windarko NA, Tjahjono A, Anggriawan DO, Purnomo MH. Maximum power point tracking of photovoltaic system using adaptive modified firefly algorithm. 2015 International Electronics Symposium (IES), 2015, p. 31–5. https://doi.org/10.1109/ELECSYM.2015.7380809.

[83] Nugraha SD, Wahjono E, Sunarno E, Anggriawan DO, Prasetyono E, Tjahjono A. Maximum power point tracking of photovoltaic module for battery charging based on modified firefly algorithm. 2016 International Electronics Symposium (IES), 2016, p. 238–43. https://doi.org/10.1109/ELECSYM.2016.7861009.

[84] Danandeh MA, Mousavi G. SM. Comparative and comprehensive review of maximum power point tracking methods for PV cells. Renewable and Sustainable Energy Reviews 2018;82:2743–67. https://doi.org/https://doi.org/10.1016/j.rser.2017.10.009.

[85] Phimmasone V, Kondo Y, Shiota N, Miyatake M. The effectiveness evaluation of the newly improved PSO-based MPPT controlling multiple PV arrays. 2013 1st International Future Energy Electronics Conference (IFEEC), 2013, p. 81–6. https://doi.org/10.1109/IFEEC.2013.6687483.

[86] Kandemir E, Cetin NS, Borekci S. A comprehensive overview of maximum power extraction methods for PV systems. Renewable and Sustainable Energy Reviews 2017;78:93–112. https://doi.org/https://doi.org/10.1016/j.rser.2017.04.090.

[87] Renaudineau H, Donatantonio F, Fontchastagner J, Petrone G, Spagnuolo G, Martin J-P, et al. A PSO-Based Global MPPT Technique for Distributed PV Power Generation. IEEE Transactions on Industrial Electronics 2015;62:1047–58. https://doi.org/10.1109/TIE.2014.2336600.

[88] Zheng Y, Wang W, Chen W, Li Q. Research on MPPT of photovoltaic system based on PSO under partial shading condition. 2016 35th Chinese Control Conference (CCC), 2016, p. 8654–9. https://doi.org/10.1109/ChiCC.2016.7554738.

[89] Tajuddin MFN, Ayob SM, Salam Z. Tracking of maximum power point in partial shading condition using differential evolution (DE). 2012 IEEE International Conference on Power and Energy (PECon), 2012, p. 384–9. https://doi.org/10.1109/PECon.2012.6450242.

[90] Mahamudul H, Saad M, Ibrahim Henk M. Photovoltaic system modeling with fuzzy logic based maximum power point tracking algorithm. International Journal of Photoenergy 2013;2013.

[91] George S, Sehgal N, Rana KPS, Kumar V. A comprehensive review on modelling and maximum power point tracking of PEMFC. Cleaner Energy Systems 2022;3:100031. https://doi.org/10.1016/j.cles.2022.100031.

[92] Rana KPS, Kumar V, Sehgal N, George S, Azar AT. Efficient maximum power point tracking in fuel cell using the fractional-order PID controller. Renewable Energy Systems, Elsevier; 2021, p. 111–32.

[93] Avanaki N, Sarvi M. A New Maximum Power Point Tracking Method for PEM Fuel Cell Based On Water Cycle Algorithm. Journal of Renewable Energy and Environment 2016;3:35–42.

[94] Gao D, Jin Z, Lu Q. Energy management strategy based on fuzzy logic for a fuel cell hybrid bus. Journal of Power Sources 2008;185:311–7.

[95] Harrag A, Messalti S. Variable Step Size IC MPPT Controller for PEMFC Power System Improving Static and Dynamic Performances. Fuel Cells 2017;17:816–24. https://doi.org/10.1002/fuce.201700047.

[96] Rezazadeh A, Sedighizadeh M, Karimi M. Proton Exchange Membrane Fuel Cell Control Using a Predictive Control Based on Neural Network. International Journal of Computer and Electrical Engineering 2010;2:81–5. https://doi.org/10.7763/ijcee.2010.v2.117.

[97] Hai T, Alazzawi AK, Zhou J, Farajian H. Performance improvement of PEM fuel cell power system using fuzzy logic controller-based MPPT technique to extract the maximum power under various conditions. International Journal of Hydrogen Energy 2023;48:4430–45. https://doi.org/https://doi.org/10.1016/j.ijhydene.2022.10.103.

[98] Soltani I, Sarvi M, Marefatjou H. An intelligent, fast and robust maximum power point tracking for proton exchange membrane fuel cell. World Appl Program 2013;3:264–81.

[99] Rana KPS, Kumar V, Sehgal N, George S. A Novel dPdI feedback based control scheme using GWO tuned PID controller for efficient MPPT of PEM fuel cell. ISA Transactions 2019;93:312–24. https://doi.org/10.1016/j.isatra.2019.02.038.

[100] Reddy BM, Samuel P. Modeling and Simulation of Proton Exchange Membrane Fuel Cell Hybrid Electric Vehicle BT - Intelligent Computing Techniques for Smart Energy Systems. In: Kalam A, Niazi KR, Soni A, Siddiqui SA, Mundra A, editors., Singapore: Springer Singapore; 2020, p. 281–91.

[101] Aung T, Naing TL. DC-link voltage control of DC-DC boost converter-inverter system with PI controller. International Journal of Electrical and Computer Engineering 2018;12:833–41.

[102] Tayebi SM, Hu H, Batarseh I. Advanced DC-link voltage regulation and capacitor optimization for three-phase microinverters. IEEE Transactions on Industrial Electronics 2018;66:307–17.

[103] Krama A, Zellouma L, Rabhi B. Anti-windup proportional integral strategy for shunt active power filter interfaced by photovoltaic system using technique of direct power control. Revue Roumaine Des Sciences Techniques Series Electrotechnique et Energetique 2017;62:252–7.

[104] Krama A, Zellouma L, Rabhi B, Laib A. Fuzzy logic controller for improving dc side of pv connected shunt active filter based on mppt sliding mode control. Artificial Intelligence in Renewable Energetic Systems: Smart Sustainable Energy Systems, Springer; 2018, p. 224–35.

[105] Chaya EC, Reddy K, Devaraju T. Implementation of ANFIS control for renewable interfacing inverter in distribution network. International Journal of Advanced Technology and Innovative Research 2015.

[106] Krama A, Zellouma L, Benaissa A, Rabhi B, Bouzidi M, Benkhoris MF. Design and experimental investigation of predictive direct power control of three-phase shunt active filter with space vector modulation using anti-windup PI controller optimized by PSO. Arabian Journal for Science and Engineering 2019;44:6741–55.

[107] Zellouma L, Rabhi B, Krama A, Benaissa A, Benkhoris MF. Simulation and real time implementation of three phase four wire shunt active power filter based on sliding mode controller. Rev Roum Des Sci Technol Ser Electrotech Energy 2018;63:77–82.

[108] Kihal A, Krim F, Talbi B, Laib A, Sahli A. A robust control of two-stage grid-tied PV systems employing integral sliding mode theory. Energies 2018;11:2791.

[109] Deshmukh N, Prabhakar S, Anand S. DC-link Voltage Feed Forward Controller for Buck Active Power Decoupling Circuit. 2020 IEEE International Conference on Power Electronics, Drives and Energy Systems (PEDES), 2020, p. 1–6. https://doi.org/10.1109/PEDES49360.2020.9379485.

[110] Nadiah A, Essalam BA, Merahi F, Laib A, Lazhar R. An improved DC-link control for dual-stage grid connected Photovoltaic system using three-level Neutral Point Climped inverter. 2022 19th International Multi-Conference on Systems, Signals & Devices (SSD), 2022, p. 810–5. https://doi.org/10.1109/SSD54932.2022.9955845.

[111] Mazouz F, Belkacem S, Colak I, Drid S, Harbouche Y. Adaptive direct power control for double fed induction generator used in wind turbine. International Journal of Electrical Power and Energy Systems 2020;114:105395. https://doi.org/10.1016/j.ijepes.2019.105395.

[112] Laggoun ZEZ, Khalile N, Benalla H. A Comparative study between DPC-SVM and PDPC-SVM. 2019 International Conference on Advanced Electrical Engineering (ICAEE), IEEE; 2019, p. 1–5.

[113] Chaoui A, Krim F, Gaubert JP, Rambault L. DPC controlled three-phase active filter for power quality improvement. International Journal of Electrical Power and Energy Systems 2008;30:476–85. https://doi.org/10.1016/j.ijepes.2008.04.009.

[114] Ouchen S, Steinhart H, Benbouzid M, Blaabjerg F. Robust DPC-SVM control strategy for shunt active power filter based on H∞ regulators. International Journal of Electrical Power and Energy Systems 2020;117:105699. https://doi.org/10.1016/j.ijepes.2019.105699.

[115] Al-Ogaili AS, Bin Aris I, Verayiah R, Ramasamy A, Marsadek M, Rahmat NA, et al. A three-level universal electric vehicle charger based on voltage-oriented control and pulse-width modulation. Energies 2019;12. https://doi.org/10.3390/en12122375.

[116] Teodorescu R, Liserre M, Rodriguez P. Grid converters for photovoltaic and wind power systems. vol. 29. John Wiley & Sons; 2011.

[117] Yang Y, Wen H, Li D. A Fast and Fixed Switching Frequency Model Predictive Control with Delay Compensation for Three-Phase Inverters. IEEE Access 2017;5:17904–13. https://doi.org/10.1109/ACCESS.2017.2751619.

[118] Donoso F, Mora A, Cardenas R, Angulo A, Saez D, Rivera M. Finite-Set Model-Predictive Control Strategies for a 3L-NPC Inverter Operating with Fixed Switching Frequency. IEEE Transactions on Industrial Electronics 2018;65:3954–65. https://doi.org/10.1109/TIE.2017.2760840.

[119] Yaramasu V, Wu B. Model predictive decoupled active and reactive power control for high-power grid-connected four-level diode-clamped inverters. IEEE Transactions on Industrial Electronics 2013;61:3407–16.

[120] Laib A, Krim F, Talbi B, Sahli A. A predictive control scheme for large-scale grid-connected PV system using high-level NPC inverter. Arabian Journal for Science and Engineering 2020;45:1685–701.

[121] Rodriguez J, Kazmierkowski MP, Espinoza JR, Zanchetta P, Abu-Rub H, Young HA, et al. State of the art of finite control set model predictive control in power electronics. IEEE Transactions on Industrial Informatics 2012;9:1003–16.

[122] Noguchi T, Tomiki H, Kondo S, Takahashi I. Direct power control of PWM converter without power-source voltage sensors. IEEE Transactions on Industry Applications 1998;34:473–9.

[123] Satti MB, Hasan A. Direct Model Predictive Control of Novel H-Bridge Multilevel Inverter Based Grid-Connected Photovoltaic System. IEEE Access 2019;7:62750–8. https://doi.org/10.1109/ACCESS.2019.2916195.

[124] Lal VN, Singh SN. Control and performance analysis of a single-stage utility-scale grid-connected PV system. IEEE Systems Journal 2015;11:1601–11.

[125] Bakeer A, Mohamed IS, Malidarreh PB, Hattabi I, Liu L. An Artificial Neural Network-Based Model Predictive Control for Three-Phase Flying Capacitor Multilevel Inverter. IEEE Access 2022;10:70305–16. https://doi.org/10.1109/ACCESS.2022.3187996.

[126] Rivera S, Kouro S, Wu B, Alepuz S, Malinowski M, Cortes P, et al. Multilevel direct power control—A generalized approach for grid-tied multilevel converter applications. IEEE Transactions on Power Electronics 2013;29:5592–604.

[127] Babaei E, Alilu S, Laali S. A new general topology for cascaded multilevel inverters with reduced number of components based on developed H-bridge. IEEE Transactions on Industrial Electronics 2013;61:3932–9.

[128] Elserougi AA, Abdelsalam I, Massoud A. Five-level F-type inverter with buck-boost converter-based equalization channels. Alexandria Engineering Journal 2023;64:155–71. https://doi.org/10.1016/j.aej.2022.08.029.

[129] Odeh C, Lewicki A, Morawiec M, Kondratenko D. Three-Level F-Type Inverter. IEEE Transactions on Power Electronics 2021;36:11265–75. https://doi.org/10.1109/TPEL.2021.3071359.

[130] Bhattacharyya S, P DSK, Samanta S, Mishra S. Steady Output and Fast Tracking MPPT (SOFT-MPPT) for P&O and InC Algorithms. IEEE Transactions on Sustainable Energy 2021;12:293–302. https://doi.org/10.1109/TSTE.2020.2991768.

[131] Azad ML, Sadhu PK, Das S. Comparative Study Between P&O and Incremental Conduction MPPT Techniques- A Review. 2020 International Conference on Intelligent Engineering and Management (ICIEM), 2020, p. 217–22. https://doi.org/10.1109/ICIEM48762.2020.9160316.

[132] Hsu T-W, Wu H-H, Tsai D-L, Wei C-L. Photovoltaic energy harvester with fractional open-circuit voltage based maximum power point tracking circuit. IEEE Transactions on Circuits and Systems II: Express Briefs 2018;66:257–61.

[133] KANOUNI B, BADOUD AE, MEKHILEF S. Fuzzy logic MPPT control algorithm for a Proton Exchange Membrane Fuel Cells System. Algerian Journal of Renewable Energy and Sustainable Development 2021;03:13–22. https://doi.org/10.46657/ajresd.2021.3.1.2.

[134] Elsheikh AH, Sharshir SW, Abd Elaziz M, Kabeel AE, Guilan W, Haiou Z. Modeling of solar energy systems using artificial neural network: A comprehensive review. Solar Energy 2019;180:622–39. https://doi.org/https://doi.org/10.1016/j.solener.2019.01.037.

[135] Nanadegani FS, Lay EN, Iranzo A, Salva JA, Sunden B. On neural network modeling to maximize the power output of PEMFCs. Electrochimica Acta 2020;348:136345. https://doi.org/10.1016/j.electacta.2020.136345.

[136] Espinoza-Trejo DR, Bárcenas-Bárcenas E, Campos-Delgado DU, De Angelo CH. Voltage-oriented input–output linearization controller as maximum power point tracking technique for photovoltaic systems. IEEE Transactions on Industrial Electronics 2014;62:3499–507.

[137] Talbi B, Krim F, Rekioua T, Laib A, Feroura H. Design and hardware validation of modified P&O algorithm by fuzzy logic approach based on model predictive control for MPPT of PV systems. Journal of Renewable and Sustainable Energy 2017;9:43503.

[138] Kollimalla SK, Mishra MK. A novel adaptive P&O MPPT algorithm considering sudden changes in the irradiance. IEEE Transactions on Energy Conversion 2014;29:602–10.

[139] Fam JY, Wong SY, Basri HBM, Abdullah MO, Lias KB, Mekhilef S. Predictive maximum power point tracking for proton exchange membrane fuel cell system. IEEE Access 2021;9:157384–97.

[140] Serpa LA, Barbosa PM, Steimer PK, Kolar JW. Five-level virtual-flux direct power control for the active neutral-point clamped multilevel inverter. 2008 IEEE Power Electronics Specialists Conference, IEEE; 2008, p. 1668–74.

[141] Eloy-Garcia J, Arnaltes S, Rodriguez-Amenedo JL. Extended direct power control for multilevel inverters including DC link middle point voltage control. IET Electric Power Applications 2007;1:571–80.

[142] Leon JI, Vazquez S, Franquelo LG. Multilevel converters: Control and modulation techniques for their operation and industrial applications. Proceedings of the IEEE 2017;105:2066–81.

[143] Portillo R, Vazquez S, Leon JI, Prats MM, Franquelo LG. Model based adaptive direct power control for three-level NPC converters. IEEE Transactions on Industrial Informatics 2012;9:1148–57.

[144] Laib A, Krim F, Talbi B, Feroura H, Kihal A. Decoupled active and reactive power control strategy of grid-connected six-level diode-clamped inverters based on finite set model predictive control for photovoltaic application. Revue Roumaine Des Sciences Techniques Serie Electrotechnique et Energetique 2019;64:51–6.

[145] Talbi B, Krim F, Laib A, Sahli A. Model predictive voltage control of a single-phase inverter with output LC filter for stand-alone renewable energy systems. Electrical Engineering 2020;102:1073–82. https://doi.org/10.1007/s00202-020-00936-5.

[146] Laib A, Krim F, Talbi B, Sahli A. A Predictive Control Scheme for Large-Scale Grid-Connected PV System Using High-Level NPC Inverter. Arabian Journal for Science and Engineering 2020;45:1685–701. https://doi.org/10.1007/s13369-019-04182-1.

[147] Ahmed M, Harbi I, Kennel R, Rodríguez J, Abdelrahem M. Maximum Power Point Tracking-Based Model Predictive Control for Photovoltaic Systems: Investigation and New Perspective. Sensors 2022;22:3069.

[148] Manoharan P, Subramaniam U, Babu TS, Padmanaban S, Holm-Nielsen JB, Mitolo M, et al. Improved perturb and observation maximum power point tracking technique for solar photovoltaic power generation systems. IEEE Systems Journal 2020;15:3024–35.

[149] Derbeli M, Charaabi A, Barambones O, Napole C. High-performance tracking for proton exchange membrane fuel cell system PEMFC using model predictive control. Mathematics 2021;9:1158.

[150] Kanouni B, Badoud AE, Mekhilef S. A multi-objective model predictive current control with two-step horizon for double-stage

grid-connected inverter PEMFC system. International Journal of Hydrogen Energy 2022;47:2685–707. https://doi.org/https://doi.org/10.1016/j.ijhydene.2021.10.182.

[151] Bouaouaou H, Lalili D, Boudjerda N. Model predictive control and ANN-based MPPT for a multi-level grid-connected photovoltaic inverter. Electrical Engineering 2022;104:1229–46.

[152] Bonala AK, Sandepudi SR, Muddineni VP. Model predictive current control with modified synchronous detection technique for three-phase 3L-NPC multi-functional solar photovoltaic system. 2016 IEEE International Conference on Power Electronics, Drives and Energy Systems (PEDES), IEEE; 2016, p. 1–6.

[153] Karami N. Control of a hybrid system based PEMFC and photovoltaic panels 2013.

[154] Rodríguez J, Pontt J, Cortés P, Vargas R. Predictive control of a three-phase neutral point clamped inverter. PESC Record - IEEE Annual Power Electronics Specialists Conference 2005;2005:1364–9. https://doi.org/10.1109/PESC.2005.1581807.

[155] Inverter N, Vargas R, Member S, Cortés P, Member S, Ammann U, et al. Predictive Control of a Three-Phase 2007;54:2697–705.

[156] Yaramasu V, Wu B, Chen J. Model-predictive control of grid-tied four-level diode-clamped inverters for high-power wind energy conversion systems. IEEE Transactions on Power Electronics 2014;29:2861–73. https://doi.org/10.1109/TPEL.2013.2276120.

[157] Priyadarshi N, Sanjeevikumar P, Bhaskar MS, Azam F, Taha IBM, Hussien MG. An adaptive TS-fuzzy model based RBF neural network learning for grid integrated photovoltaic applications. IET Renewable Power Generation 2022;16:3149–60.

[158] Harrag A, Messalti S. How fuzzy logic can improve PEM fuel cell MPPT performances? International Journal of Hydrogen Energy 2018;43:537–50. https://doi.org/https://doi.org/10.1016/j.ijhydene.2017.04.093.

[159] Ilyas A, Khan MR, Ayyub M. FPGA based real-time implementation of fuzzy logic controller for maximum power point tracking of solar photovoltaic system. Optik 2020;213:164668. https://doi.org/https://doi.org/10.1016/j.ijleo.2020.164668.

[160] Wu D, Nariman GS, Mohammed SQ, Shao Z, Rezvani A, Mohajeryami S. Modeling and simulation of novel dynamic control strategy for PV–wind hybrid power system using FGS− PID and RBFNSM methods. Soft Computing 2020;24:8403–25.

[161] Merahi F, Badoud AE, Mekhilef S. A novel power management strategies in PV-wind-based grid connected hybrid renewable energy system using proportional distribution algorithm. International Transactions on Electrical Energy Systems 2021;31. https://doi.org/10.1002/2050-7038.12931.

[162] Luca R, Whiteley M, Neville T, Shearing PR, Brett DJL. Comparative study of energy management systems for a hybrid fuel cell electric vehicle - A novel mutative fuzzy logic controller to prolong fuel cell lifetime. International Journal of Hydrogen Energy 2022;47:24042–58. https://doi.org/10.1016/j.ijhydene.2022.05.192.

[163] Kong L, Yu J, Cai G. Modeling, control and simulation of a photovoltaic /hydrogen/ supercapacitor hybrid power generation system for grid-connected applications. International Journal of Hydrogen Energy 2019;44:25129–44. https://doi.org/10.1016/j.ijhydene.2019.05.097.

[164] Mohammadi A, Mehrpooya M. A comprehensive review on coupling different types of electrolyzer to renewable energy sources. Energy 2018;158:632–55. https://doi.org/https://doi.org/10.1016/j.energy.2018.06.073.

[165] Kouro S, Leon JI, Vinnikov D, Franquelo LG. Grid-connected photovoltaic systems: An overview of recent research and emerging PV converter technology. IEEE Industrial Electronics Magazine 2015;9:47–61.

[166] Basaran K, Cetin NS, Borekci S. Energy management for on-grid and off-grid wind/PV and battery hybrid systems. IET Renewable Power Generation 2017;11:642–9.

[167] Baik M, Hammoudi M, Salhi Y, Kirati SK. Hydrogen production by hybrid system and its conversion by fuel cell in Algeria; Djanet. International Journal of Hydrogen Energy 2018;43:3466–74. https://doi.org/10.1016/j.ijhydene.2017.11.074.

[168] Gu Y, Xiang X, Li W, He X. Mode-adaptive decentralized control for renewable DC microgrid with enhanced reliability and flexibility. IEEE Transactions on Power Electronics 2013;29:5072–80.

[169] Sechilariu M, Wang BC, Locment F, Jouglet A. DC microgrid power flow optimization by multi-layer supervision control. Design and experimental validation. Energy Conversion and Management 2014;82:1–10. https://doi.org/https://doi.org/10.1016/j.enconman.2014.03.010.

[170] Liu J, Luo W, Yang X, Wu L. Robust model-based fault diagnosis for PEM fuel cell air-feed system. IEEE Transactions on Industrial Electronics 2016;63:3261–70.

[171] Han Y, Chen W, Li Q, Yang H, Zare F, Zheng Y. Two-level energy management strategy for PV-Fuel cell-battery-based DC microgrid. International Journal of Hydrogen Energy 2019:19395–404. https://doi.org/10.1016/j.ijhydene.2018.04.013.

[172] Han Y, Li Q, Wang T, Chen W, Ma L. Multisource Coordination Energy Management Strategy Based on SOC Consensus for a PEMFC–Battery–Supercapacitor Hybrid Tramway. IEEE Transactions on Vehicular Technology 2018;67:296–305. https://doi.org/10.1109/TVT.2017.2747135.

[173] LanreOlatomiwa S, Ismail MS, Moghavvemi M. â€ œEnergy management strategies in hybrid renewable energy systems: A reviewâ€. Renewable and Sustainable Energy Reviews n.d.;62:821â.

[174] Zhang Z, Guan C, Liu Z. Real-Time Optimization Energy Management Strategy for Fuel Cell Hybrid Ships Considering Power Sources Degradation. IEEE Access 2020;8:87046–59. https://doi.org/10.1109/ACCESS.2020.2991519.

[175] Qi W, Li Y, Li H, Wayne SW, Lin X. The development and numerical verification of a compromised real time optimal control algorithm for hybrid electric vehicle. Journal of Power Sources 2019;443:227272. https://doi.org/https://doi.org/10.1016/j.jpowsour.2019.227272.

[176] Snoussi J, Ben Elghali S, Benbouzid M, Mimouni MF. Auto-adaptive filtering-based energy management strategy for fuel cell hybrid electric vehicles. Energies 2018;11:2118.

[177] Zhang C, Shen Y, Wang Y-X. Wavelet Transform-Based Energy Management Strategy for Fuel Cell/Variable-Structure Super-capacitor Hybrid Power System. 2020 Asia Energy and Electrical Engineering Symposium (AEEES), 2020, p. 732–6. https://doi.org/10.1109/AEEES48850.2020.9121475.

[178] Konara KMSY, Kolhe ML, Sharma A. Power dispatching techniques as a finite state machine for a standalone photovoltaic system with a hybrid energy storage 2020.

[179] Corcau JI, Dinca L. Fuzzy energy management scheme for a hybrid power sources of high-altitude pseudosatellite. Modelling and Simulation in Engineering 2020;2020:1–13.

[180] Mohammadzadeh A, Rathinasamy S. Energy management in photovoltaic battery hybrid systems: A novel type-2 fuzzy control. International Journal of Hydrogen Energy 2020;45:20970–82. https://doi.org/https://doi.org/10.1016/j.ijhydene.2020.05.187.

[181] Tifour B, Boukhnifer M, Hafaifa A, Tanougast C. Monitoring and control of energy management system for fuel cell hybrid in electrical vehicle using fuzzy approach. Diagnostyka 2020;21.

[182] Zhang Z, Sato K, Nagasaki Y, Tsuda M, Miyagi D, Komagome T, et al. Continuous operation in an electric and hydrogen hybrid energy storage system for renewable power generation and autonomous emergency power supply. International Journal of Hydrogen Energy 2019;44:23384–95. https://doi.org/https://doi.org/10.1016/j.ijhydene.2019.07.028.

[183] Essalam A, Merahi F, Ould B. Bond graph modeling , design and experimental validation of a photovoltaic / fuel cell / electrolyzer / battery hybrid power system ScienceDirect Bond graph modeling , design and experimental validation of a photovoltaic / fuel cell / electrolyzer / batte. International Journal of Hydrogen Energy 2021. https://doi.org/10.1016/j.ijhydene.2021.05.016.

[184] Merahi F. A novel power management strategies in PV - wind - based grid connected A novel power management strategies in PV-wind-based grid connected hybrid renewable energy system using proportional distribution algorithm 2021. https://doi.org/10.1002/2050-7038.12931.

[185] Kamel AA, Rezk H, Ali M. ScienceDirect Enhancing the operation of fuel cell-photovoltaic- battery-supercapacitor renewable system through a hybrid energy management strategy. International Journal of Hydrogen Energy 2020. https://doi.org/10.1016/j.ijhydene.2020.06.052.

[186] Silva SB, Severino MM, de Oliveira MAG. A stand-alone hybrid photovoltaic, fuel cell and battery system: A case study of Tocantins, Brazil. Renewable Energy 2013;57:384–9. https://doi.org/https://doi.org/10.1016/j.renene.2013.02.004.

[187] Behzadi MS, Niasati M. Comparative performance analysis of a hybrid PV/FC/battery stand-alone system using different power management strategies and sizing approaches. International Journal of Hydrogen Energy 2015;40:538–48. https://doi.org/https://doi.org/10.1016/j.ijhydene.2014.10.097.

[188] Zghaibeh M, Okonkwo PC, Hasan NU, Farhani S, Bacha F. Energy Management System for Photovoltaic-Battery-Fuel Cell using Arduino Board and Matlab Simulink. 2022 IEEE Delhi Section Conference (DELCON), IEEE; 2022, p. 1–6.

[189] Mounica V, Obulesu YP. Hybrid power management strategy with fuel cell, battery, and supercapacitor for fuel economy in hybrid electric vehicle application. Energies 2022;15:4185.

[190] Laib A, Krim F, Talbi B, Feroura H, Belaout A. Hardware implementation of fuzzy maximum power point tracking through sliding mode current control for photovoltaic systems. Revue Roumaine Des Sciences Techniques Serie Electrotechnique et Energetique 2021;66:91–6.

[191] Bayarassou H, Megri AF. New approach based on a fuzzy regression model for a photovoltaic system. Electric Power Systems Research 2023;217:109091. https://doi.org/https://doi.org/10.1016/j.epsr.2022.109091.

[192] Rai N, Abbadi A, Hamidia F, Kanouni B, Kahlessenane A. A New Modified Incremental Conductance Algorithm Used for PV

System. Artificial Intelligence and Heuristics for Smart Energy Efficiency in Smart Cities: Case Study: Tipasa, Algeria, Springer; 2022, p. 256–65.

[193] Feroldi D, Degliuomini LN, Basualdo M. Chemical Engineering Research and Design Energy management of a hybrid system based on wind – solar power sources and bioethanol. Chemical Engineering Research and Design 2013;91:1440–55. https://doi.org/10.1016/j.cherd.2013.03.007.

[194] Kanouni B, Badoud AE, Mekhilef S. Predictive current control two step of a single-phase inverter for grid connected PEMFC system. 2022 19th International Multi-Conference on Systems, Signals & Devices (SSD), 2022, p. 538–43. https://doi.org/10.1109/SSD54932.2022.9955844.

[195] Hartani MA, Hamouda M, Abdelkhalek O, Mekhilef S. Impacts assessment of random solar irradiance and temperature on the cooperation of the energy management with power control of an isolated cluster of DC-Microgrids. Sustainable Energy Technologies and Assessments 2021;47:101484. https://doi.org/10.1016/j.seta.2021.101484.

[196] Zia MF, Benbouzid M, Elbouchikhi E, Muyeen SM, Techato K, Guerrero JM. Microgrid Transactive Energy: Review, Architectures, Distributed Ledger Technologies, and Market Analysis. IEEE Access 2020;8:19410–32. https://doi.org/10.1109/ACCESS.2020.2968402.

[197] Louzazni M, Cotfas DT, Cotfas PA. Management and performance control analysis of hybrid photovoltaic energy storage system under variable solar irradiation. Energies 2020;13. https://doi.org/10.3390/en13123043.

[198] Babu TS, Vasudevan KR, Ramachandaramurthy VK, Sani SB, Chemud S, Lajim RM. A Comprehensive Review of Hybrid Energy Storage Systems: Converter Topologies, Control Strategies and Future Prospects. IEEE Access 2020;8:148702–21. https://doi.org/10.1109/ACCESS.2020.3015919.

[199] Şahin ME, Blaabjerg F. A hybrid PV-battery/supercapacitor system and a basic active power control proposal in MATLAB/simulink. Electronics 2020;9:129.

[200] Li S, Li Y, Li T. An autonomous flexible power management for hybrid AC/DC microgrid with multiple subgrids under the asymmetric AC side faults. International Journal of Electrical Power & Energy Systems 2022;142:107985.

Contribution au contrôle et à la gestion de l'énergie des systèmes multi-sources connectés au réseau

Abstract :

This dissertation explores grid-connected photovoltaic (PV/PEMFC) topologies, and energy management strategies for stand-alone PV-PEFMC-Batteries storage systems. Moreover, various efficient control strategies have been suggested for these particular grid-connected topologies. The latter exhibits a number of limitations, including maximum power point tracking (MPPT), imprecise control over grid power, and low grid current quality. In order to address these limitations, a proposed approach involves the implementation of a model predictive control (MPC) strategy for the regulation of multi-level converters utilized in the grid-connected PV/PEMFC topologies.Firstly, a control strategy based on the predictive control strategy for a three-phase dual-stage grid-connected PV /PEMFC is proposed. A fuzzy logic MPPT is proposed and employed to control the DC-DC converter. An FSCTS model predictive control strategy is employed to control the DC-AC inverter. Subsequently, in grid-connected PV/PEMFC systems, The algorithm utilizes a three-level Neutral Point Clamped (NPC) inverter to facilitate the injection of current generated by the PV / PEMFC system while also ensuring the equilibrium of DC-link capacitor voltages. Similarly, F-type inverters are employed in grid-connected PEMFC systems to facilitate the injection of the current output into the grid while ensuring the best performance operation In contrast, this study presents a simple and effective algorithm, namely FSC-MPCC, designed for grid-connected PEMFC systems. The proposed method utilizes a three-level single-phase F-type inverter to effectively inject the current generated by the PEMFC system into the grid. Additionally, it ensures the equilibrium of DC-link capacitor voltages and achieves superior control performance. In the second part, a state machine energy management strategy is proposed for a multisource storage system consisting of PV, PEMFC, and batteries. A fuzzy logic MPPT is proposed and employed to control the DC-DC converter buck-boost converter, while state machine control is employed to control the boost converter that is connected to PEMFC. this study presents a simple and effective algorithm, and state machine control for the multisource storage system to facilitate meeting the load requirements. the simulation results validate the proposed control schemes for the investigated grid-connected PV topologies PEMFC topologies and the proposed stand-alone multi-source storage system.

Keywords:, grid-connected PV/PEMFC systems, multilevel inverters, maximum power point (MPPT), model Predictive Control, energy management.

Contribution au contrôle et à la gestion de énergie des systèmes multi-sources connectés au réseau

Résumé :

Cette thèse explore les topologies photovoltaïques connectées au réseau (PV/PEMFC) et les stratégies de gestion de l'énergie pour les systèmes de stockage autonomes PV-PEFMC-Batteries. De plus, diverses stratégies de contrôle efficaces ont été suggérées pour ces topologies particulières connectées au réseau. Ce dernier présente un certain nombre de limitations, notamment le suivi du point de puissance maximale (MPPT), un contrôle imprécis de l'alimentation du réseau et une faible qualité du courant du réseau. Afin de remédier à ces limitations, une approche proposée implique la mise en œuvre d'une stratégie de contrôle prédictif de modèle (MPC) pour la régulation des convertisseurs multi-niveaux utilisés dans les topologies PV/PEMFC connectées au réseau. Premièrement, une stratégie de contrôle basée sur la stratégie de contrôle prédictif pour un PV/PEMFC triphasé à deux étages connecté au réseau est proposée. Un MPPT à logique floue est proposé et utilisé pour contrôler le convertisseur DC-DC. Une stratégie de contrôle prédictif du modèle FSCTS est utilisée pour contrôler l'onduleur DC-AC. Par la suite, dans les systèmes PV/PEMFC connectés au réseau, l'algorithme utilise un onduleur à point neutre (NPC) à trois niveaux pour faciliter l'injection du courant généré par le système PV/PEMFC tout en assurant également l'équilibre des tensions des condensateurs du bus CC. De même, des onduleurs de type F sont utilisés dans les systèmes PEMFC connectés au réseau pour faciliter l'injection du courant de sortie dans le réseau tout en garantissant les meilleures performances de fonctionnement. En revanche, cette étude présente un algorithme simple et efficace, à savoir FSC-MPCC, conçu pour systèmes PEMFC connectés au réseau. La méthode proposée utilise un onduleur monophasé de type F à trois niveaux pour injecter efficacement le courant généré par le système PEMFC dans le réseau. De plus, il garantit l'équilibre des tensions des condensateurs du circuit intermédiaire et permet d'obtenir des performances de contrôle supérieures. Dans la deuxième partie, une stratégie de gestion de l'énergie d'une machine à états est proposée pour un système de stockage multisource composé de PV, de PEMFC et de batteries. Un MPPT à logique floue est proposé et utilisé pour contrôler le convertisseur abaisseur-élévateur du convertisseur DC-DC, tandis que le contrôle de la machine à états est utilisé pour contrôler le convertisseur élévateur connecté au PEMFC. cette étude présente un algorithme simple et efficace, ainsi qu'un contrôle de machine d'état pour le système de stockage multisource afin de faciliter la satisfaction des exigences de charge. les résultats de la simulation valident les schémas de contrôle proposés pour les topologies PV connectées au réseau étudiées, les topologies PEMFC et le système de stockage multi-source autonome proposé.***Mots-clés :,***systèmes PV/PEMFC connectés au réseau, onduleurs multiniveaux, point de puissance maximale (MPPT), La commande prédictive., gestion de l'énergie.

المساهمة في التحكم وإدارة الطاقة للنظام متعدد المصادر المتصل بالشبكة

ملخص:

تستكشف هذه الأطروحة طبولوجيا الخلايا الكهروضوئية المتصلة بالشبكة (PV/PEMFC)، واستراتيجيات إدارة الطاقة لأنظمة تخزين البطاريات الكهروضوئية-PEFMC المستقلة. علاوة على ذلك، تم اقتراح العديد من استراتيجيات التحكم الفعالة لهذه الطبولوجيا المتصلة بالشبكة. يُظهر الأخير عددًا من القيود، بما في ذلك الحد الأقصى لتتبع نقطة الطاقة (MPPT)، والتحكم غير الدقيق في طاقة الشبكة، وانخفاض جودة الشبكة الحالية. من أجل معالجة هذه القيود، يتضمن النهج المقترح تنفيذ استراتيجية نموذجية للتحكم التنبؤي (MPC) لتنظيم المحولات متعددة المستويات المستخدمة في طوبولوجيا PV/PEMFC المتصلة بالشبكة. أولاً، تم اقتراح استراتيجية تحكم تعتمد على استراتيجية التحكم التنبؤية لأنظمة الطاقة الكهروضوئية / PEMFC ثلاثية المراحل والمتصلة بالشبكة. تم اقتراح المنطق الضبابي MPPT واستخدامه للتحكم في محول DC-DC. تم استخدام استراتيجية التحكم التنبؤية لنموذج FSCTS للتحكم في عاكس DC-AC. بعد ذلك، في الأنظمة الكهروضوئية/PEMFC المتصلة بالشبكة، تستخدم الخوارزمية عاكسًا ثلاثي المستويات مثبت بنقطة محايدة (NPC) لتسهيل حقن التيار الناتج عن نظام PV/PEMFC مع ضمان توازن جهود مكثف وصلة التيار المستمر. وبالمثل، يتم استخدام محولات من النوع F في أنظمة PEMFC المتصلة بالشبكة لتسهيل حقن الإخراج الحالي في الشبكة مع ضمان أفضل أداء. في المقابل، تقدم هذه الدراسة خوارزمية بسيطة وفعالة، وهي FSC-MPCC، المصممة لـ أنظمة PEMFC المتصلة بالشبكة. تستخدم الطريقة المقترحة عاكسًا ثلاثي المستوى من النوع F أحادي الطور لحقن التيار الناتج عن نظام PEMFC بشكل فعال في الشبكة. بالإضافة إلى ذلك، فهو يضمن توازن جهود مكثف وصلة التيار المستمر ويحقق أداء تحكم فائق. في الجزء الثاني، تم اقتراح استراتيجية إدارة طاقة الآلة لنظام تخزين متعدد المصادر يتكون من الخلايا الكهروضوئية، وPEMFC، والبطاريات. يتم اقتراح منطق غامض MPPT واستخدامه للتحكم في محول دفعة باك لمحول DC-DC، بينما يتم استخدام التحكم في آلة الحالة للتحكم في محول التعزيز المتصل بـ PEMFC. تقدم هذه الدراسة خوارزمية بسيطة وفعالة، والتحكم في آلة الحالة لنظام التخزين متعدد المصادر لتسهيل تلبية متطلبات التحميل. تتحقق نتائج المحاكاة من صحة مخططات التحكم المقترحة للطبولوجيا الكهروضوئية المتصلة بالشبكة التي تم فحصها وطوبولوجيا PEMFC ونظام التخزين المستقل متعدد المصادر المقترح.

الكلمات المفتاحية : أنظمة **PV / PEMFC** المتصلة بالشبكة ، محولات متعددة المستويات ، نقطة طاقة قصوى (**MPPT**) ، تحكم تنبؤي ، إدارة الطاقة.